Supporting Information for the article

Revealing the Unusual Role of Bases in Activation/Deactivation of Catalytic Systems: O-NHC Coupling in M/NHC Catalysis

Victor M. Chernyshev,[†] Oleg V. Khazipov,[†] Maxim A. Shevchenko,[†] Andrey Yu. Chernenko,[†] Alexander V. Astakhov,[†] Dmitry B. Eremin,[‡] Dmitry V. Pasyukov,[†] Alexey S. Kashin,[‡] Valentine P. Ananikov[*,†,‡]

[†]Platov South-Russian State Polytechnic University (NPI), Prosveschenya 132, Novocherkassk, 346428, Russia

[‡]Zelinsky Institute of Organic Chemistry, Russian Academy of Sciences, Leninsky Prospect 47, Moscow, 119991, Russia

Table of contents

S1. Additional data, tables, schemes

Table S1. Reaction of M-NHC complexes with oxygen bases[a]

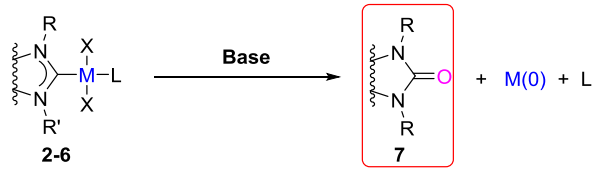

M = Ni, Pd, Pt; L = pyridine, 3-chloropyridine, NHC; X = halogen; **Base** = KOH, NaOH, *t*-BuOK, *t*-BuONa, K_2CO_3, Na_2CO_3, Cs_2CO_3

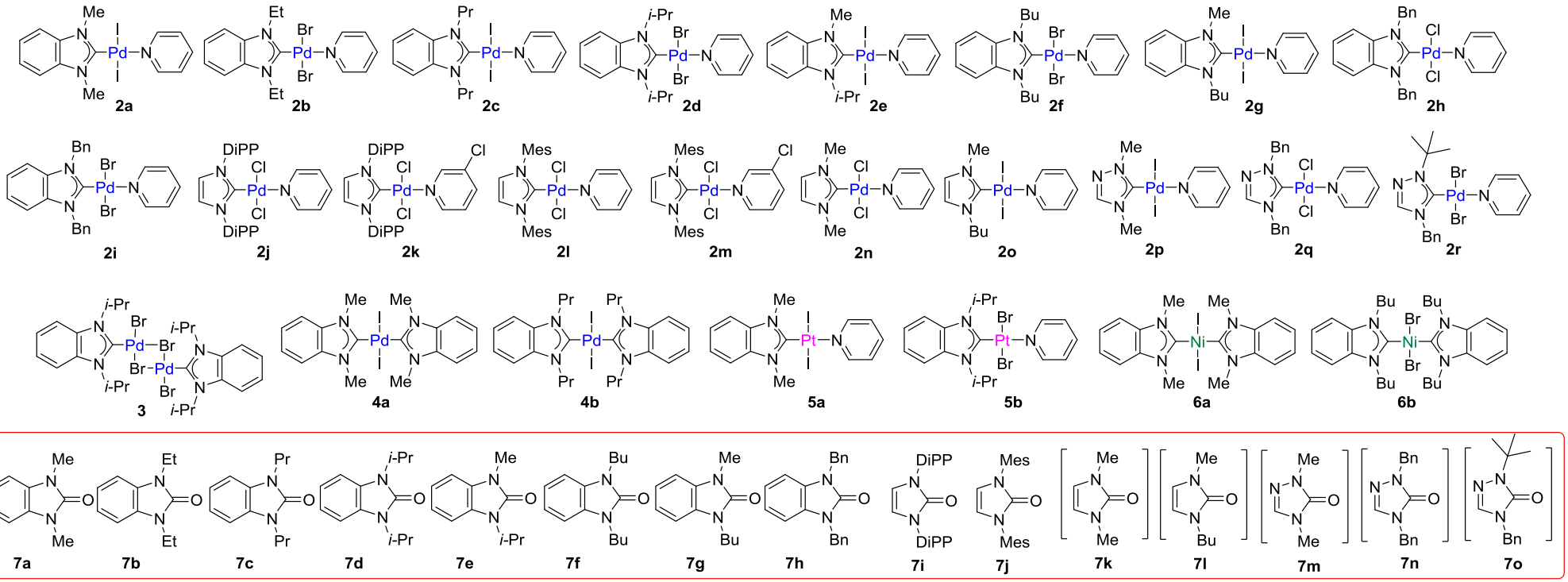

N	Starting M-NHC complex	Solvent (ml)	Base (mol : mol of M-NHC)	Reaction temperature, °C	Reaction time, h	Products	(HPLC or GC)/isolated yield of azolone **7**, %
1	**2a**	pyridine (4) + H_2O (1)	KOH[b] (10 : 1)	100	24	**7a**	96/72
2	**2a**	pyridine (4) + H_2O (1)	NaOH[b] (10 : 1)	100	24	**7a**	89
3	**2a**	1,4-dioxane (5)	*t*-BuOK (10 : 1)	100	3	**7a**	91/61
4	**2a**	1,4-dioxane (5)	*t*-BuONa (10 : 1)	100	3	**7a**	84
5	**2a**	1,4-dioxane (5)	*t*-BuONa (10 : 1)	100	24	**7a**	94
6	**2a**	1,4-dioxane (5)	Na_2CO_3 (10 : 1)	100	3	**7a**	trace

N	Starting M-NHC complex	Solvent (ml)	Base (mol : mol of M-NHC)	Reaction temperature, °C	Reaction time, h	Products	(HPLC or GC)/isolated yield of azolone **7**, %
7	**2a**	1,4-dioxane (5)	Na_2CO_3 (10 : 1)	100	24	**7a**	trace
8	**2a**	1,4-dioxane (5)	K_2CO_3 (10 : 1)	100	3	**7a**	trace
9	**2a**	1,4-dioxane (5)	K_2CO_3 (10 : 1)	100	24	**7a**	trace
10	**2a**	1,4-dioxane (5)	Cs_2CO_3 (10 : 1)	100	3	**7a**	24
11	**2a**	1,4-dioxane (5)	Cs_2CO_3 (10 : 1)	100	24	**7a**	57
12	**2a**	DMF (5)	*t*-BuOK (10 : 1)	100	24	**7a**	58
13	**2a**	DMF (5)	*t*-BuONa (10 : 1)	100	24	**7a**	43
14	**2a**	pyridine (5)	*t*-BuOK (10 : 1)	100	24	**7a**	95
15	**2a**	pyridine (5)	*t*-BuONa (10 : 1)	100	24	**7a**	96
16	**2a**	*i*-PrOH (5)	*t*-BuOK (10 : 1)	100	3	**7a**	62
17	**2b**	1,4-dioxane (5)	*t*-BuOK (10 : 1)	100	3	**7b**	97/79
18	**2b**	1,4-dioxane (4) + H_2O (1)	KOH[b] (10 : 1)	100	24	**7b**	56/48
19	**2b**	THF (4) + H_2O (1)	KOH[b] (10 : 1)	100	24	**7b**	60/51
20	**2c**	1,4-dioxane (5)	*t*-BuOK (10 : 1)	100	3	**7c**	87/79
21	**2d**	pyridine (4) + H_2O (1)	KOH[b] (10 : 1)	100	24	**7d**	85/42
22	**2d**	1,4-dioxane (5)	*t*-BuOK (10 : 1)	100	3	**7d**	87/72
23	**2e**	1,4-dioxane (5)	*t*-BuOK (10 : 1)	100	3	**7e**	89/78
24	**2f**	1,4-dioxane (5)	*t*-BuOK (10 : 1)	100	3	**7f**	89/76
25	**2g**	1,4-dioxane (5)	*t*-BuOK (10 : 1)	100	3	**7g**	91/68
26	**2h**	pyridine (4) + H_2O (1)	KOH[b] (10 : 1)	100	24	**7h**	90/74
27	**2i**	1,4-dioxane (4) + H_2O (1)	KOH[b] (10 : 1)	100	24	**7h**	76/62
28	**2i**	pyridine (4) + H_2O (1)	KOH[b] (10 : 1)	100	24	**7h**	94
29	**2i**	DMF (5)	K_2CO_3 (10 : 1)	140	24	**7h**	16
30	**2i**	DMF (4) + H_2O (1)	K_2CO_3 (10 : 1)	140	24	**7h**	47
31	**2j**	1,4-dioxane (5)	*t*-BuOK (10 : 1)	100	3	**7i**	65/40
32	**2k**	1,4-dioxane (5)	*t*-BuOK (10 : 1)	100	3	**7i**	42/28
33	**2l**	1,4-dioxane (5)	*t*-BuOK (10 : 1)	100	3	**7j**	46/35
34	**2m**	1,4-dioxane (5)	*t*-BuOK (10 : 1)	100	3	**7j**	29/17
35	**2n**	1,4-dioxane (4) + H_2O (1)	KOH[b] (3 : 1)	100	24	**7k**	trace
36	**2o**	1,4-dioxane (5)	*t*-BuOK (10 : 1)	100	3	**7l**	trace
37	**2o**	1,4-dioxane (4) + H_2O (1)	KOH[b] (3 : 1)	100	24	**7l**	2
38	**2p**	1,4-dioxane (4) + H_2O (1)	KOH[b] (3 : 1)	100	24	**7m**	trace
39	**2q**	1,4-dioxane (5)	*t*-BuOK (10 : 1)	100	3	**7n**	trace
40	**2q**	1,4-dioxane (4) + H_2O (1)	KOH[b] (3 : 1)	100	24	**7n**	trace
41	**2q**	1,4-dioxane (4) + H_2O (1)	KOH[b] (3 : 1)	100	1	**7n**	3
42	**2r**	1,4-dioxane (4) + H_2O (1)	KOH[b] (3 : 1)	100	24	**7o**	trace
43	**3**	1,4-dioxane (5)	*t*-BuOK (10 : 1)	100	3	**7d**	77/51
44	**4a**	pyridine (4) + H_2O (1)	KOH[b] (10 : 1)	100	24	**7a**	99/71

N	Starting M-NHC complex	Solvent (ml)	Base (mol : mol of M-NHC)	Reaction temperature, °C	Reaction time, h	Products	(HPLC or GC)/isolated yield of azolone **7**, %
45	**4a**	1,4-dioxane (5)	*t*-BuOK (10 : 1)	100	3	**7a**	86/58
46	**4b**	1,4-dioxane (5)	*t*-BuOK (10 : 1)	100	3	**7c**	87/79
47	**5a**	1,4-dioxane (4) + H_2O (1)	KOH[b] (10 : 1)	100	20	**7a**	trace
48	**5a**	1,4-dioxane (5)	*t*-BuOK (10 : 1)	100	20	**7a**	42/37
49	**5b**	1,4-dioxane (4) + H_2O (1)	KOH[b] (10 : 1)	100	20	**7d**	2
50	**5b**	1,4-dioxane (5)	*t*-BuOK (10 : 1)	100	20	**7d**	65/50
51	**6a**	1,4-dioxane (5)	*t*-BuOK (10 : 1)	100	48	**7a**	87/49
52	**6b**	1,4-dioxane (5)	*t*-BuOK (10 : 1)	100	48	**7f**	87/79

[a]A mixture of the complex **2-6** (0.3 mmol), solvent (5 mL) and base (0.9-3 mmol) was vigorously stirred in a teflon screw cap tube at 100 °C within 1-48 h, then neutralized with 20% HCl aqueous solution to pH ~9 under argon atmosphere. The resulted mixture was centrifuged and analyzed by HPLC and GC-MS. If necessary, the products **7** were isolated as described in the Experimental Section of the manuscript. [b]3M aqueous solution.

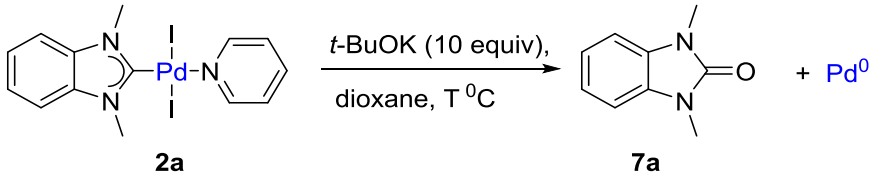

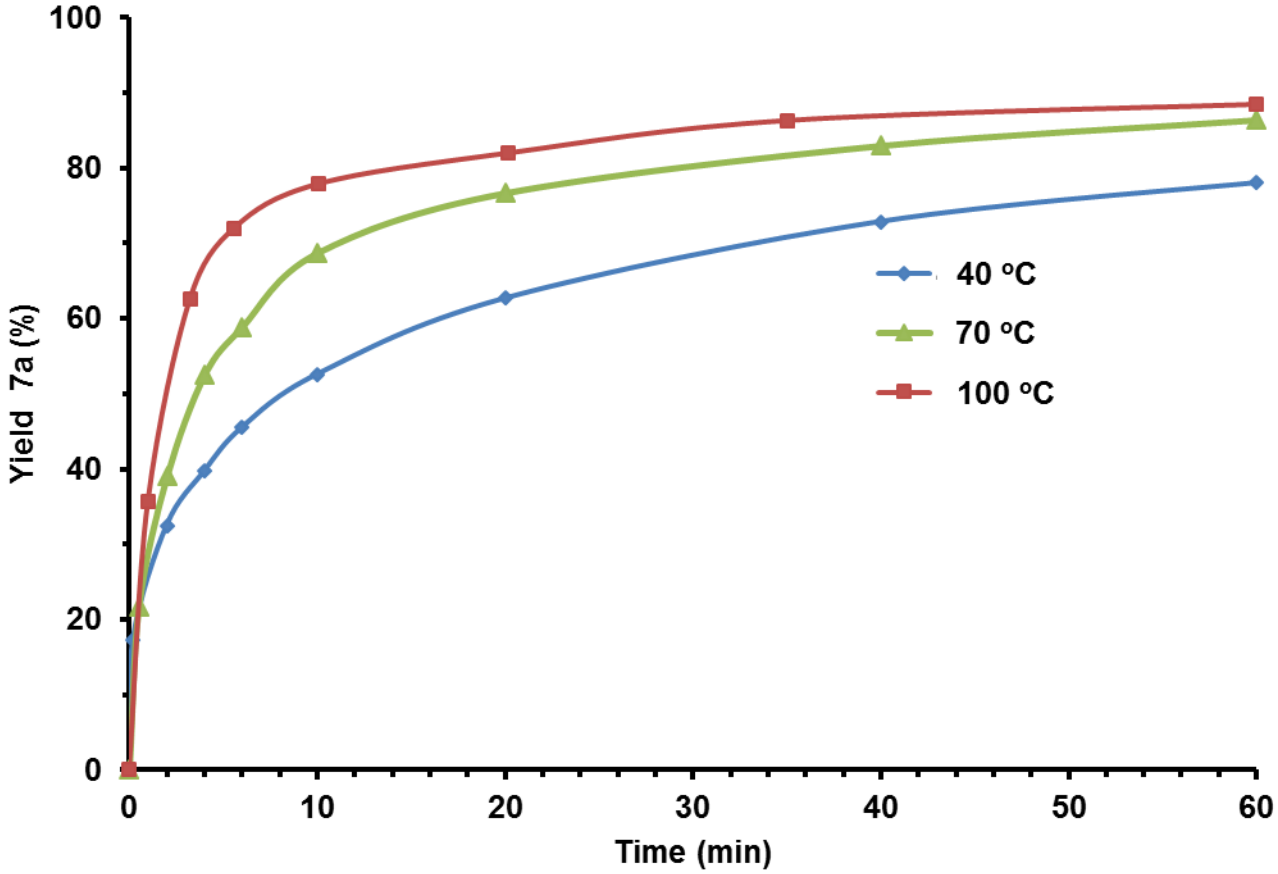

Figure S1. Variable temperature study for the formation of azolone **7a** in the reaction between the compound **2a** (0.1 mmol) and *t*-BuOK (1 mmol) in 1,4-dioxane at 40 °C, 70 °C, and 100 °C.

Table S2. Stability of azolones 7 in the presence of KOH and *t*-BuOK[a]

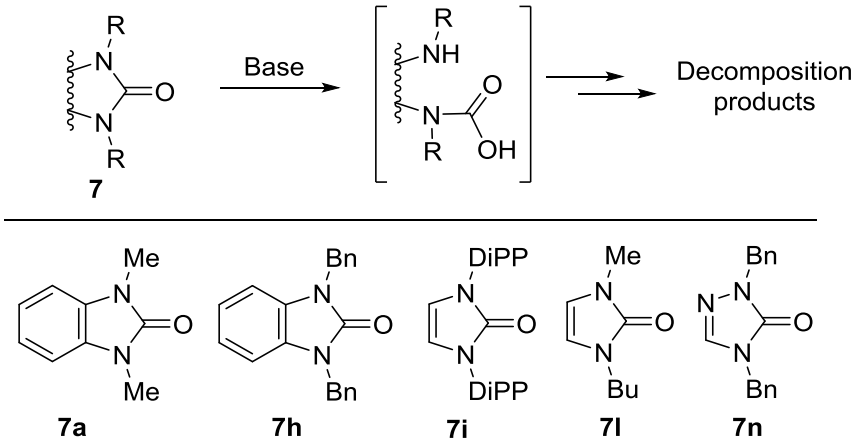

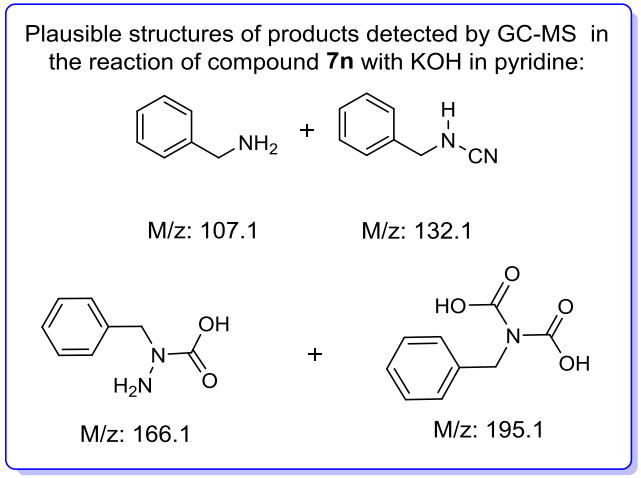

N	Starting azolone **7**	Solvent (ml)	Base (mol: mol of azolone **7**)	Reaction temperature, °C	Reaction time, h	Conversion of azolone **7**, %[c]
1	**7a**	pyridine (0.4) + H_2O (0.1)	KOH[b] (10 : 1)	100	24	~0
2	**7a**	pyridine (0.5)	*t*-BuOK (10 : 1)	100	24	~0
3	**7h**	pyridine (0.4) + H_2O (0.1)	KOH[b] (10 : 1)	100	24	~0
4	**7i**	pyridine (0.4) + H_2O (0.1)	KOH[b] (10 : 1)	100	24	4
5	**7i**	pyridine (0.4) + H_2O (0.1)	KOH[b] (10 : 1)	100	90	10
6	**7l**	pyridine (0.4) + H_2O (0.1)	KOH[b] (10 : 1)	100	24	99
7	**7l**	pyridine (0.5)	*t*-BuOK (10 : 1)	100	24	99
8	**7n**	pyridine (0.4) + H_2O (0.1)	KOH[b] (10 : 1)	100	24	99
9	**7n**	pyridine (0.5)	*t*-BuOK (10 : 1)	100	24	99

[a]A mixture of the compounds **7** (30 μmol), solvent and base (0.3 mmol) was vigorously stirred in a teflon screw cap tube at the corresponding temperature within 24-90 h, then analyzed by HPLC and GC-MS. [b]3M aqueous solution of KOH. [c]Determined by HPLC and GC-MS.

Scheme S1. Reactions of benzimidazolium salts 1 with strong oxygen bases.[1]

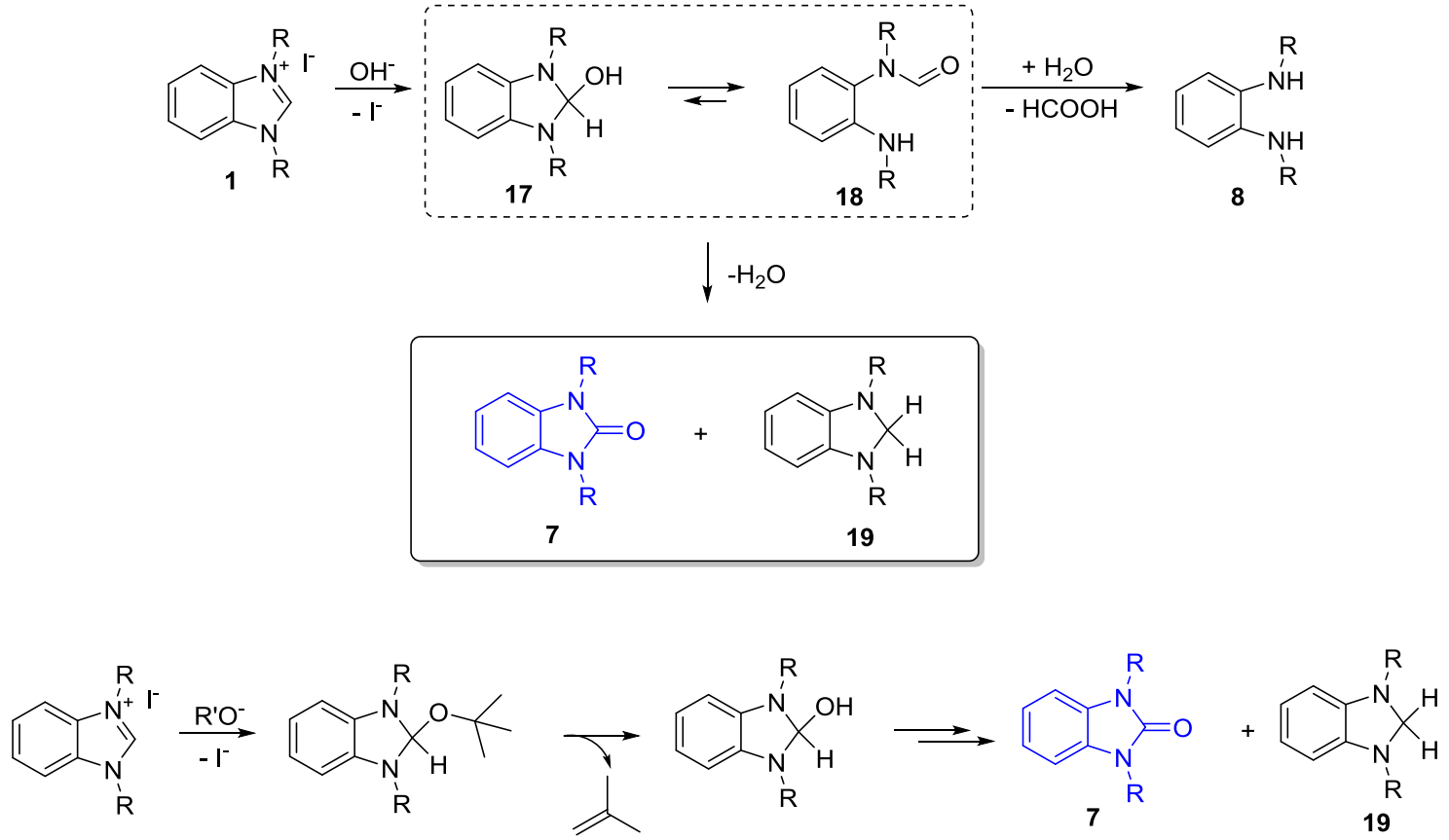

1,3-Dialkylated azolium salts are hydrolyzed by strong bases like KOH to give *N*,*N*-dialkylbenzene-1,2-diames **8**.[1] Hydrolysis usually accompanied by the disproportionation of "pseudobases" **17** and **18** to give azolones **7** and azolines **19**.[1] The azolines **19**, apparently, are unstable in the conditions of the Table S1. However, trace amounts of compounds with m/z corresponding to the [M^+] of azolines **19** were observed in GC-MS spectra of the reaction mixtures. Analogous reactions proceed under the action of alcoholates. Indeed, the HPLC yield of azolone **7a** in the reaction mixture after heating compound **1a** with *t*-BuOK in 1,4-dioxane at 100 °C within 20 h amounted ~ 10% (see Experimental Section for details).

(1) (a) Konstantinchenko, A. A.; Morkovnik, A. S.; Pozharskii, A. F.; Tertov, B. A. *Chem. Heterocycl. Compd.* **1985,** *21*, 1398-1399; (b) Korotkikh, N. I.; Shvaika, O. P.; Rayenko, G. F.; Kiselyov, A. V.; Knishevitsky, A. V.; Cowley, A. H.; Jones, J. N.; Macdonald, C. L. B. *Arkivoc* **2005,** *2005*, 10-46.

Scheme S2. Plausible stoichiometry's for the reactions of complexes 2-6 with KOH and *t*-BuOK[a]

Reactions of Type 1

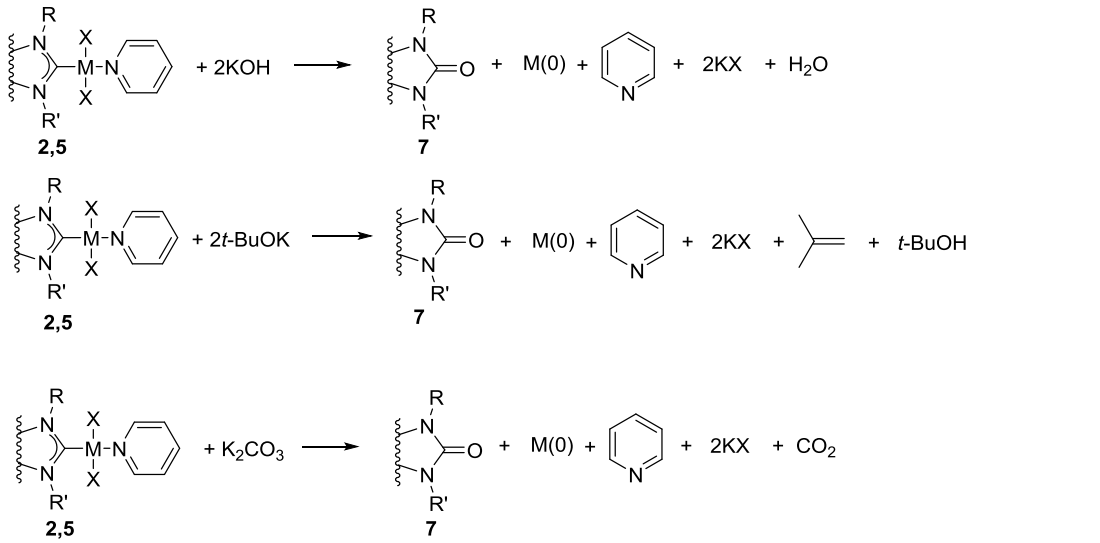

Reactions of Type 2

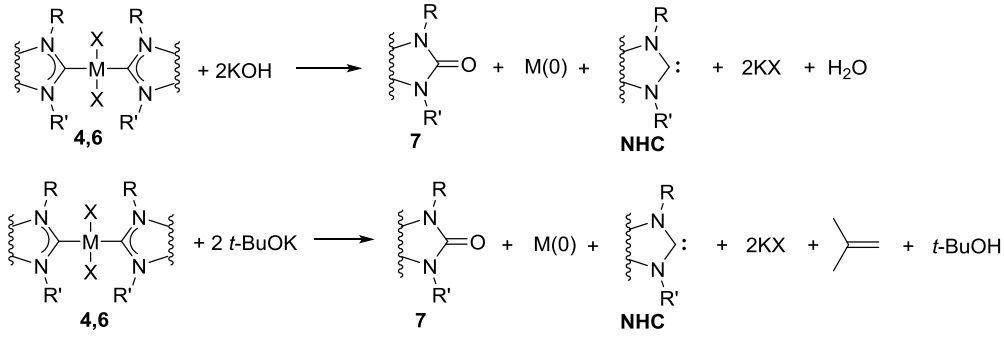

M = Pd, Ni; X = Cl, Br, I

Reactions of Type 3

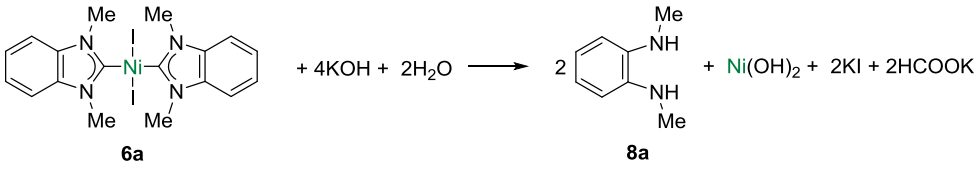

[a] For clarity, only 2-methylpropene and *t*-BuOH are shown as the products derived from *t*-BuOK, while another products like di-*t*-butyl ether may also be formed. For other alkaline metal bases (Na, Cs), stoichiometry's are similar.

S2. ESI-MS monitoring of Azolones formation

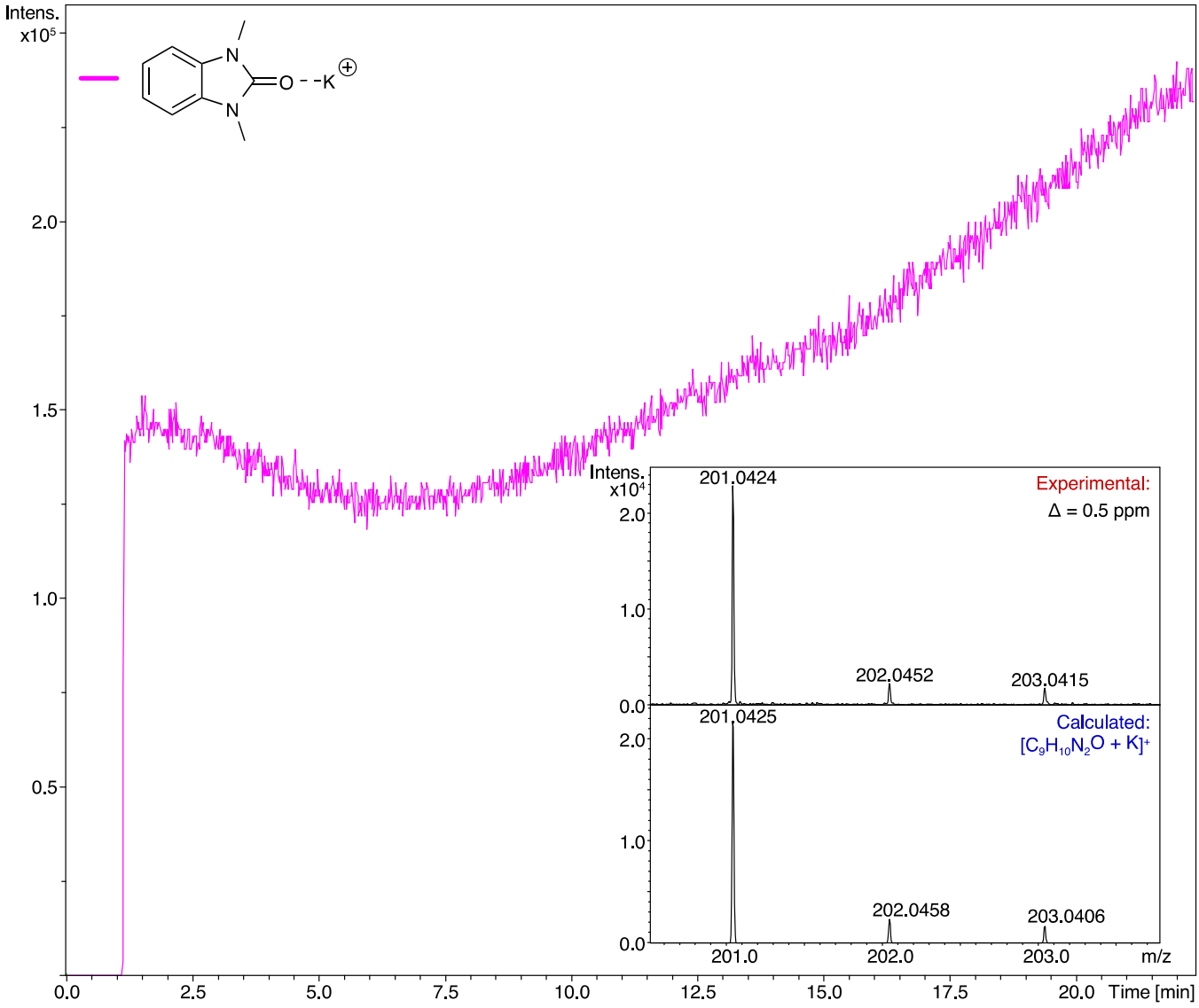

Figure S2. Real-time abundance of **7a** (in ionic $[M + K]^+$ form) in the reaction between the complex **2a** and KOH_{aq} in THF at 100 ºC. Solution of KOH in H_2O was added after 1.0 min. Insert shows the ESI-(+)MS spectrum of the reaction mixture, expanded to the $[M + K]^+$ region.

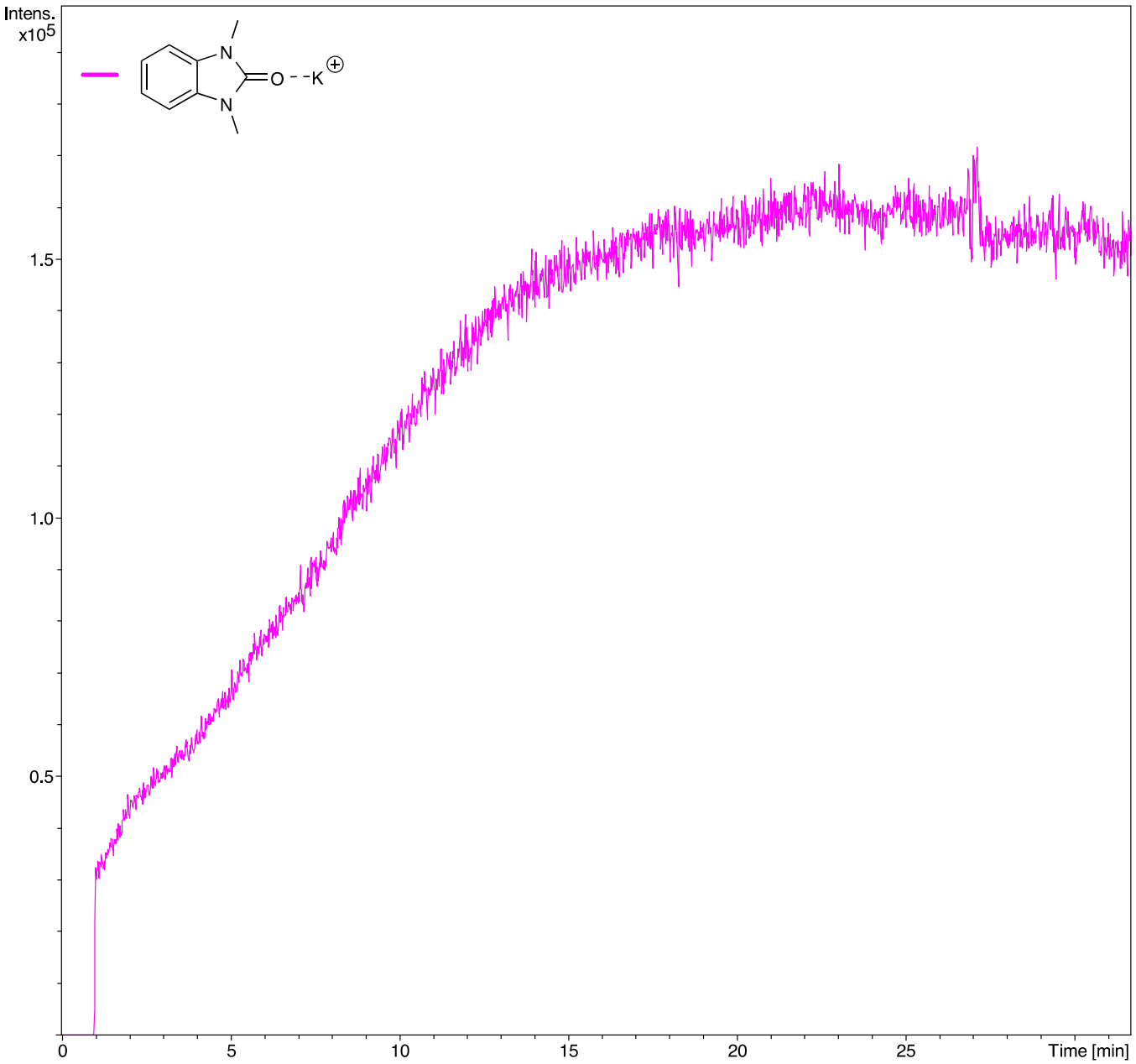

Figure S3. Real-time abundance of **7a** (in ionic $[M + K]^+$ form) in the reaction between the complex **4a** and KOH_{aq} in THF at 100 ºC. Solution of KOH in H_2O was added after 1.0 min.

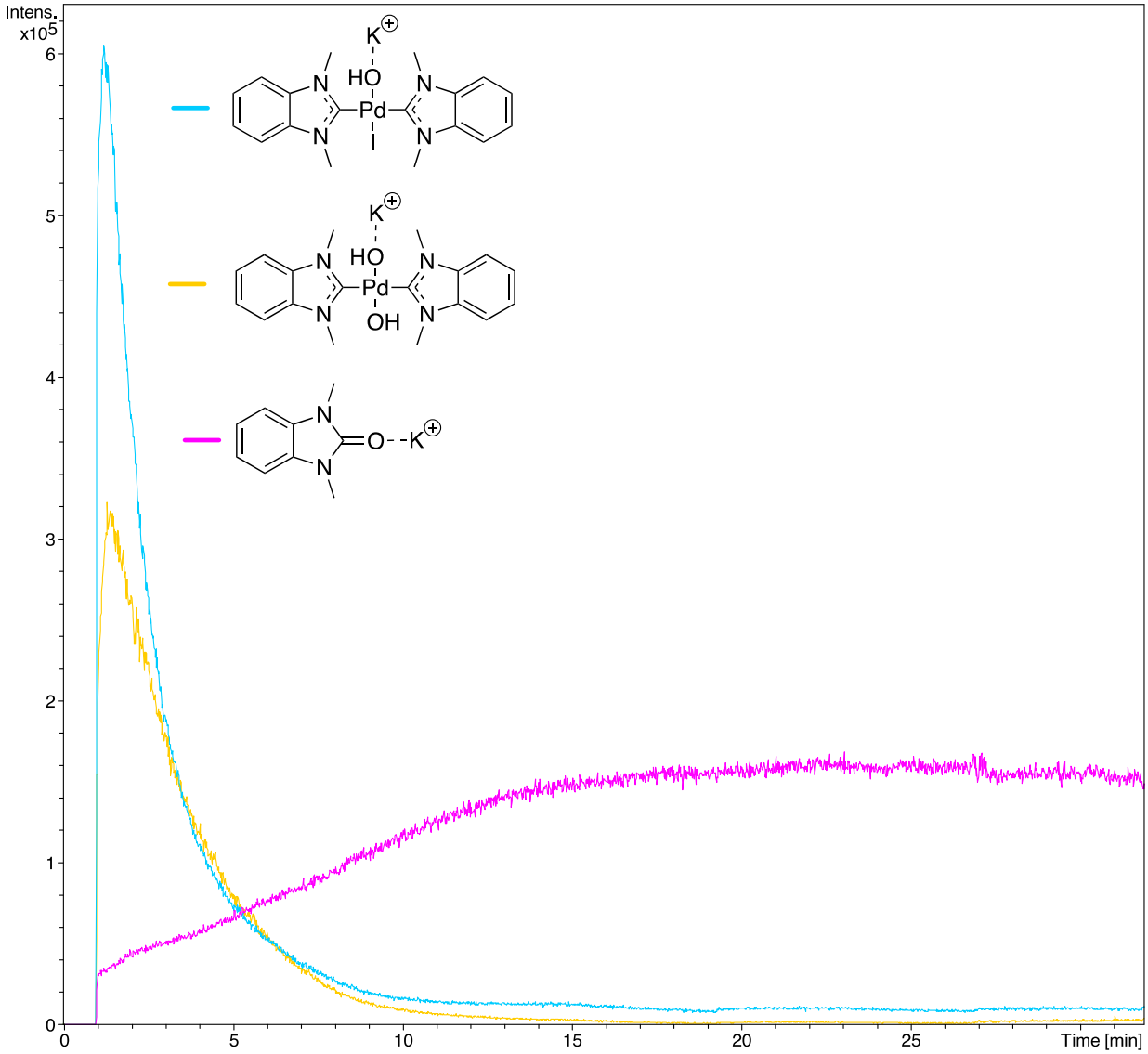

Figure S4. Real-time abundances (in ionic $[M + K]^+$ form) of **7a** (purple line) and intermediate hydroxy-complexes (blue and yellow lines) in the reaction between the complex **4a** and KOH_{aq} in THF at 100 ºC. Solution of KOH in H_2O was added after 1.0 min.

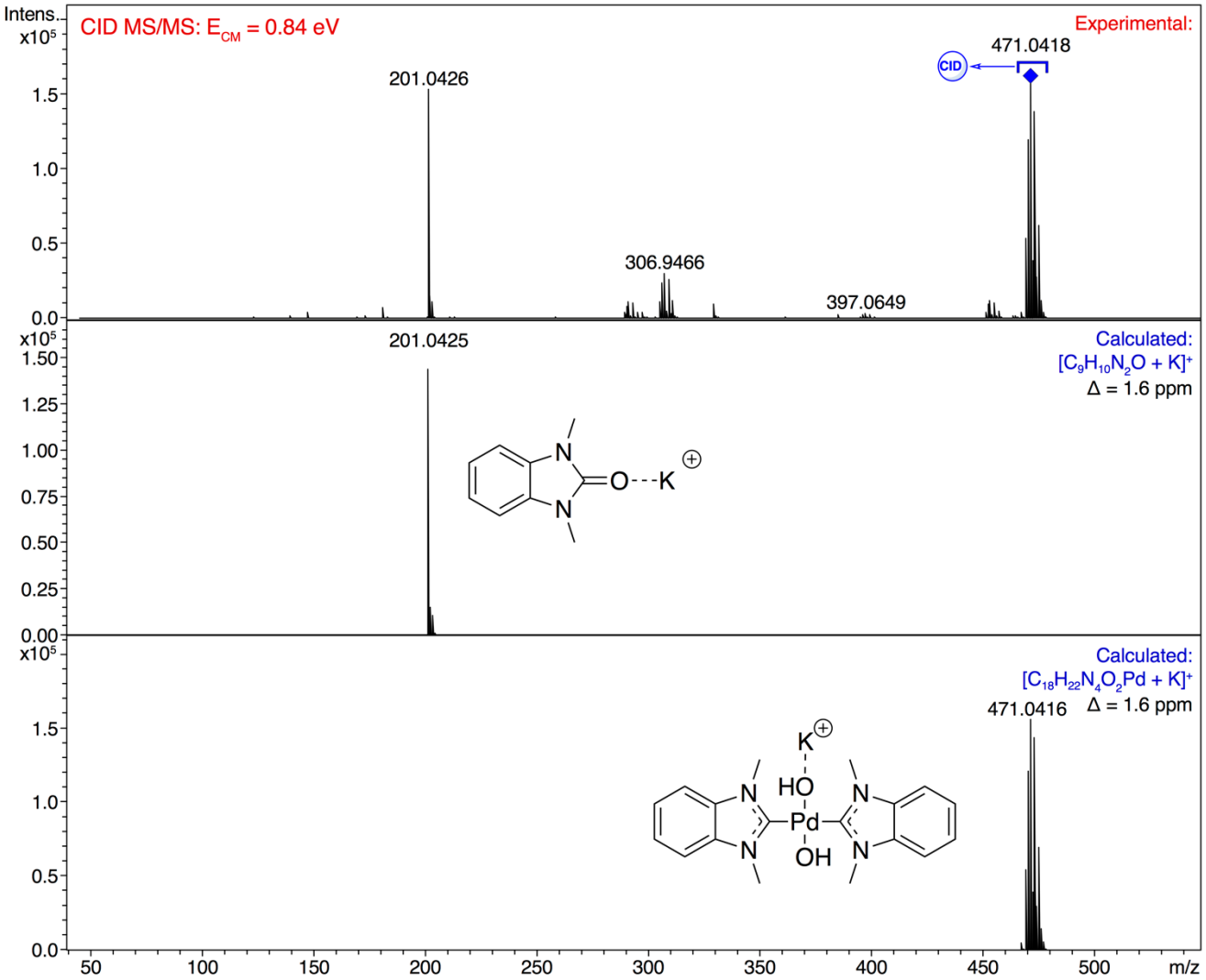

Figure S5. Collision induced dissociation tandem mass spectrometry experiment demonstrating the formation of **7a** (in ionic $[M + K]^+$ form) from the intermediate hydroxy-complex **9** (in a $[C_{18}H_{22}N_4O_2Pd + K]^+$ form) during the reaction between the complex **4a** and KOH_{aq} in THF at 100 ºC.

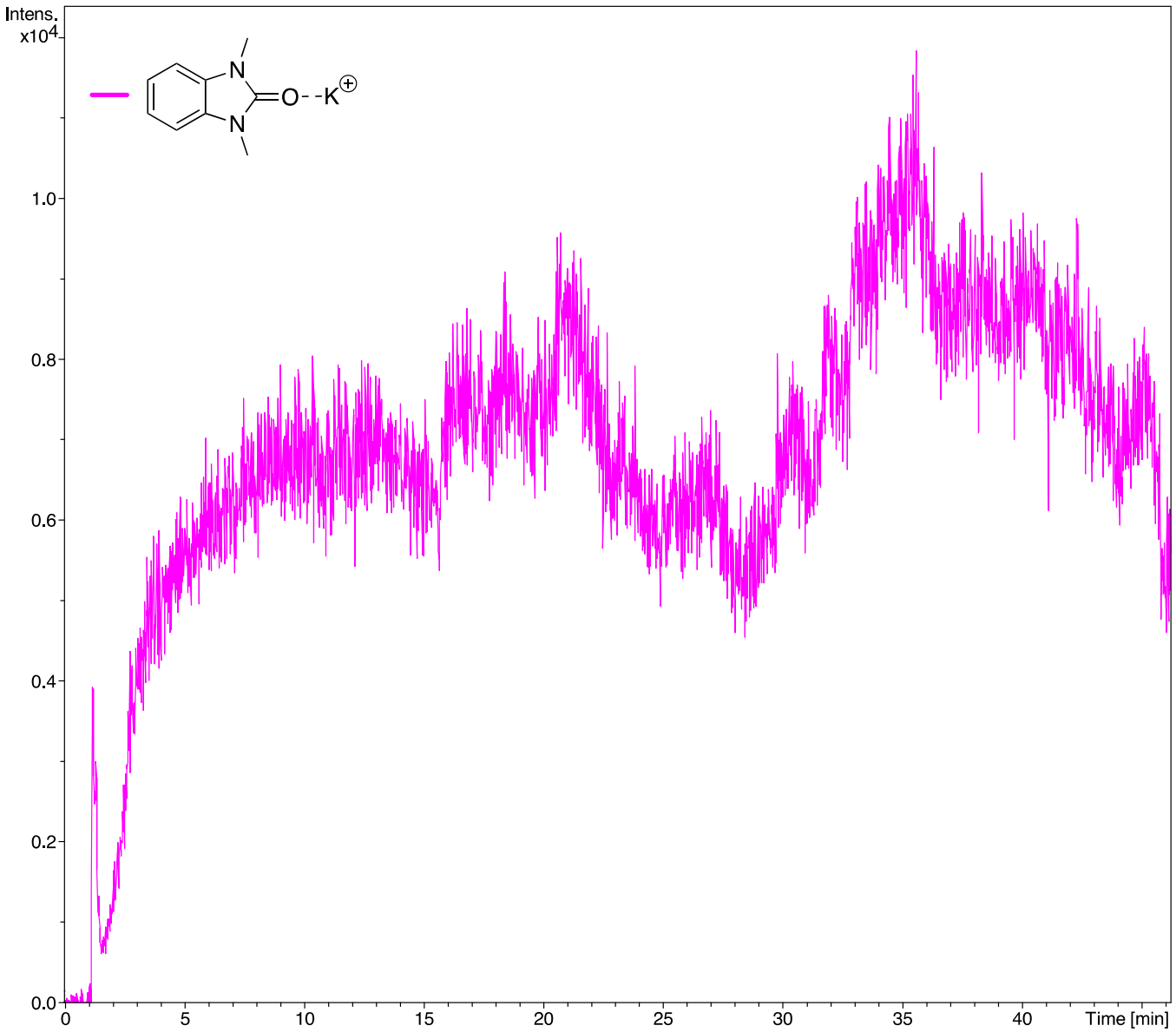

Figure S6. Real-time abundance of **7a** (in ionic $[M + K]^+$ form) in the reaction between the complex **2a** and *tert*-BuOK in THF at 100 ºC. Suspension of *tert*-BuOK in THF was added after 1.0 min.

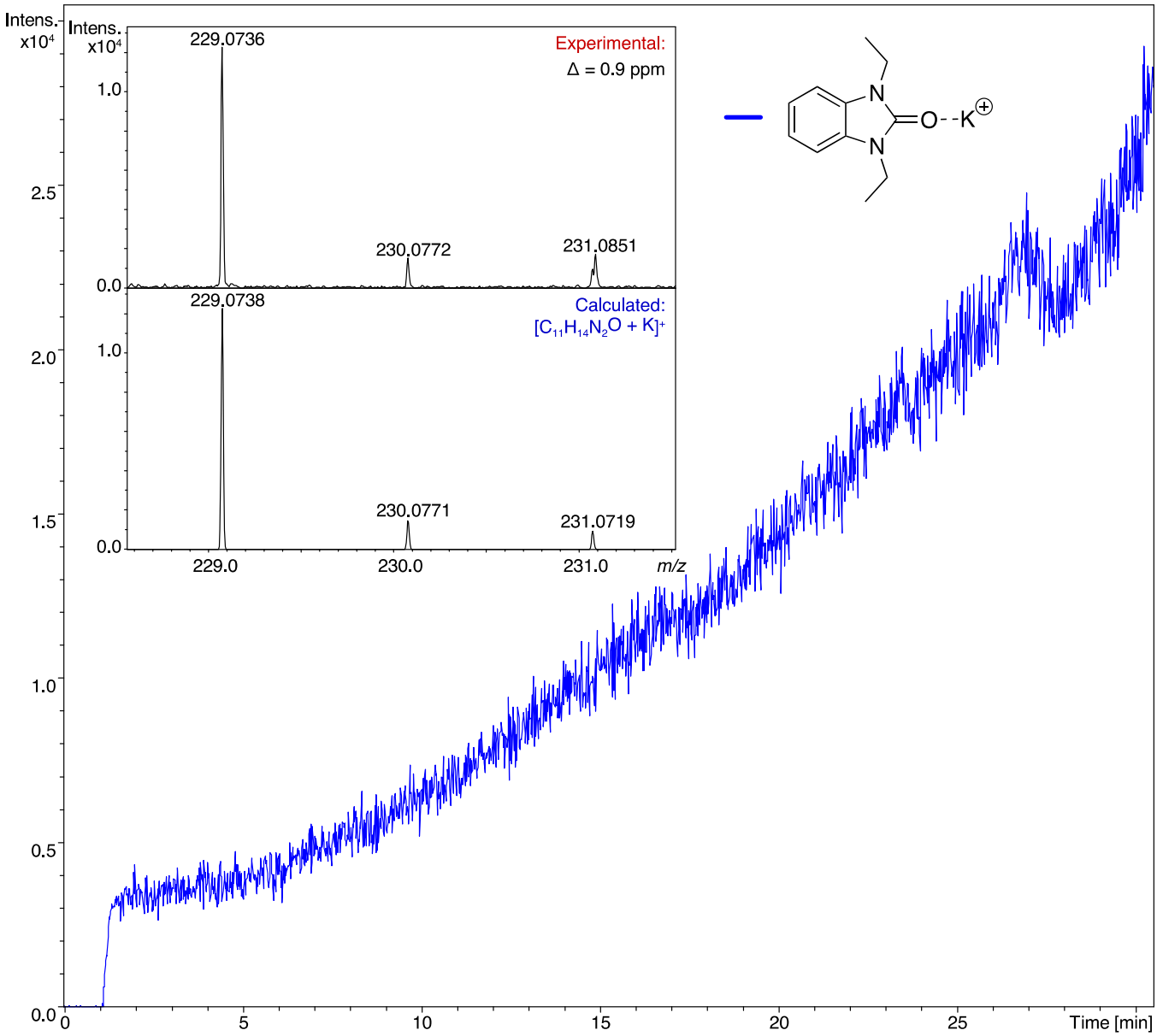

Figure S7. Real-time abundance of **7b** (in ionic $[M + K]^+$ form) in the reaction between the complex **2b** and KOH_{aq} in THF at 100 ºC. Solution of KOH in H_2O was added after 1.0 min. Insert shows ESI-(+)MS spectrum of the reaction mixture, expanded to the $[M + K]^+$ region.

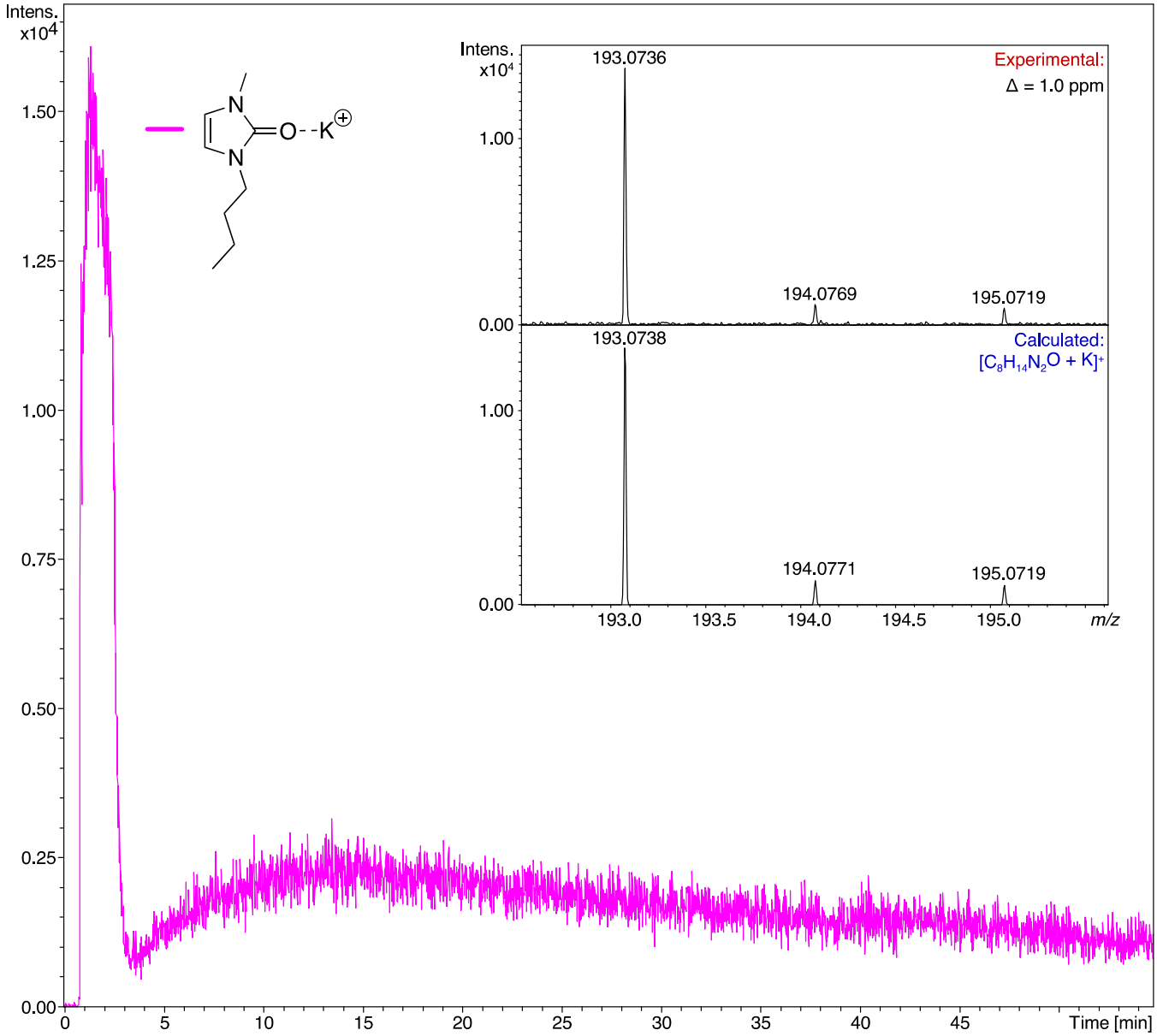

Figure S8. Real-time abundance of **7l** (in ionic $[M + K]^+$ form) in the reaction between the complex **2o** and KOH_{aq} in THF at 100 ºC. Solution of KOH in H_2O was added after 1.0 min. Insert shows ESI-(+)MS spectrum of the reaction mixture, expanded to the $[M + K]^+$ region. At the beginning of the reaction one of the products (apparently, potassium bromide) rapidly covered the shield in the MS interface that significantly dropped all the signals down in intensity because of changes in field potentials.

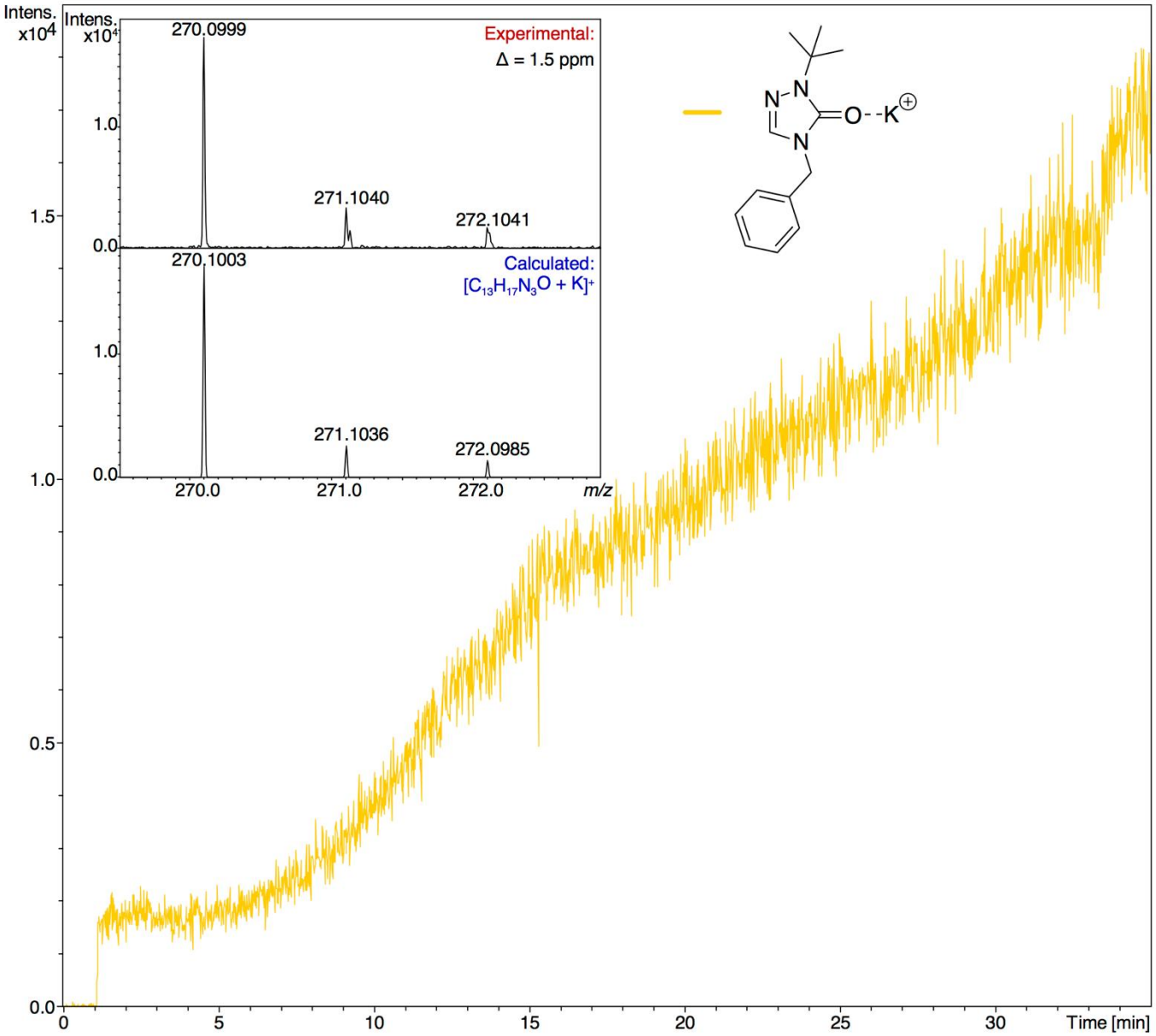

Figure S9. Real-time abundance of **7o** (in ionic $[M + K]^+$ form) in the reaction between the complex **2r** and KOH_{aq} in THF at 100 ºC. Solution of KOH in H_2O was added after 1.0 min. Insert shows ESI-(+)MS spectrum of the reaction mixture, expanded to the $[M + K]^+$ region.

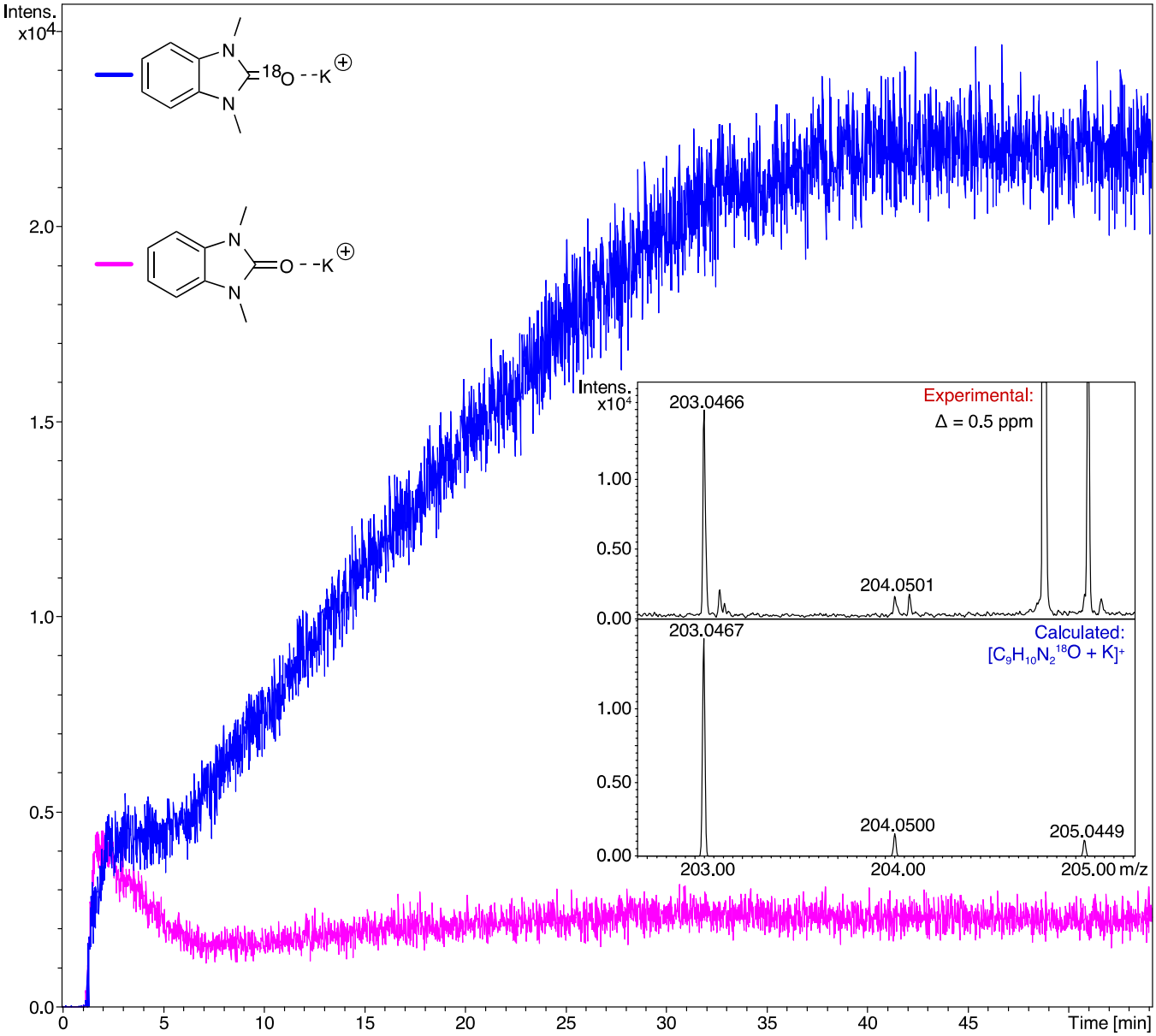

Figure S10. Real-time abundances of **7a-[**^{18}O] and **7a**-[^{16}O] (in ionic [M + K]$^+$ forms) in the reaction between the complex **2a** and K^{18}OH$_{aq}$ in THF at 100 ºC. Solution of KOH in $H_2{}^{18}O$ was added after 1.0 min. Insert shows ESI-(+)MS spectrum of the reaction mixture, expanded to the [(^{18}O)-M + K]$^+$ region.

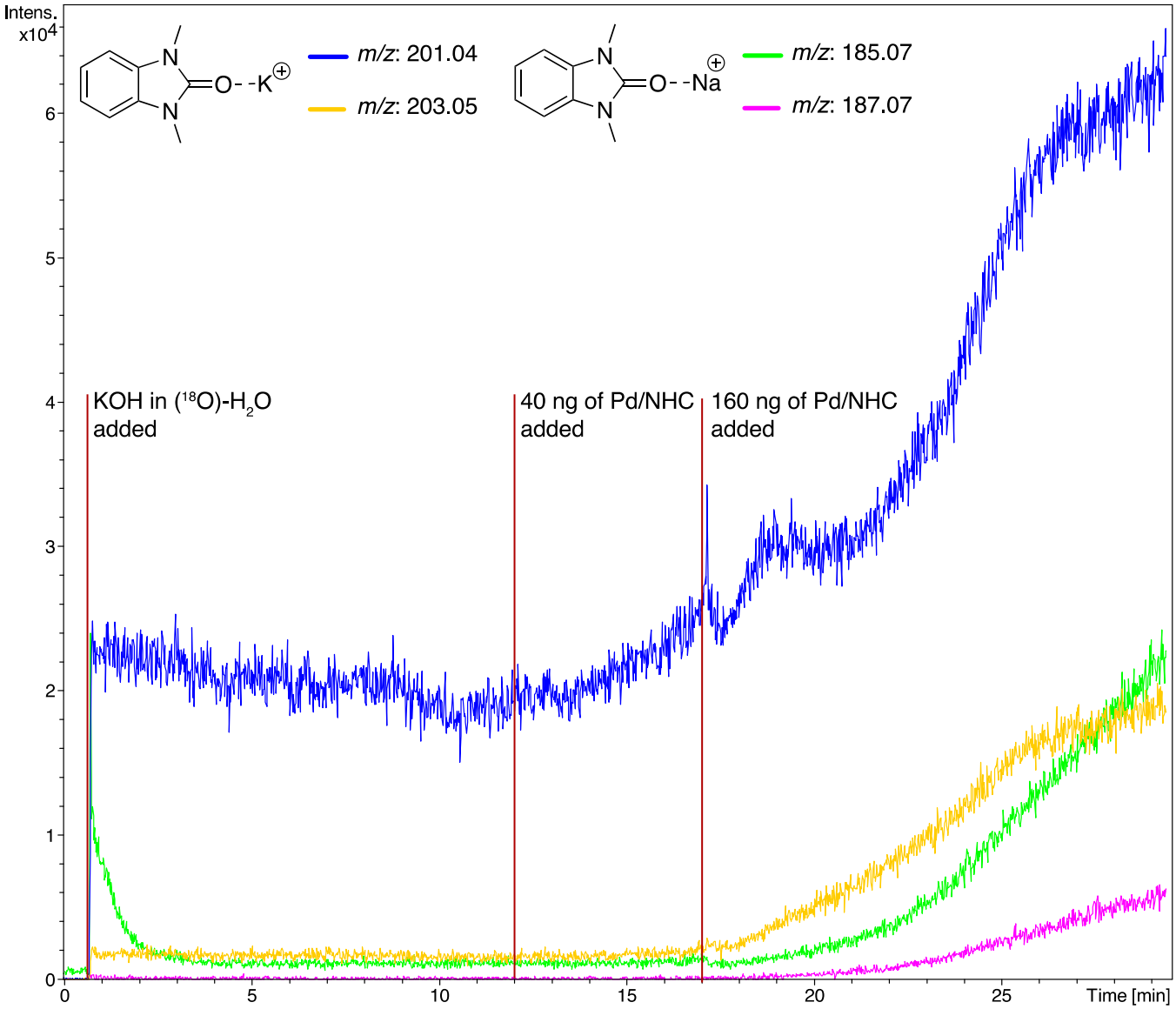

Figure S11. Real-time abundances of ions (in $[M + Na]^+$ and $[M + K]^+$ forms) confirming no isotope exchange between **7a**-[^{16}O] and KOH solution in $H_2{}^{18}O$.

In the first time region (up to ~ 0.8 min), a solution of non-labeled **7a**-[^{16}O] in THF was squeezed into the MS instrument. After the addition of a potassium hydroxide solution in $H_2{}^{18}O$ (at ~0.8 min), an $[M + K]^+$ ion of the non-labeled **7a**-[^{16}O] jumped in the intensity, but no **7a**-[^{18}O] isotopomer was formed according to the ion traces in the second time region (0.8-12 min). After the addition of a small amount (40 ng; added as solution see Exp. part) of **2a** (at 12 min), only a slight increase in the intensity of both **7a** isotopomers was detected. Only after the addition of the significant amount (160 ng; added as solution see Exp. part) of **2a** (17 min), a stable increase of the intensity of the **7a**-[^{18}O] isotopomer signal (purple line) was observed. These results corroborate the formation of the **7a**-[^{18}O] isotopomer from the reaction between the complex **2a** and $^{18}OH^-$ rather than through the isotope exchange between **7a**-[^{16}O] and KOH-$H_2{}^{18}O$ solution.

S3. FE-SEM/EDS data

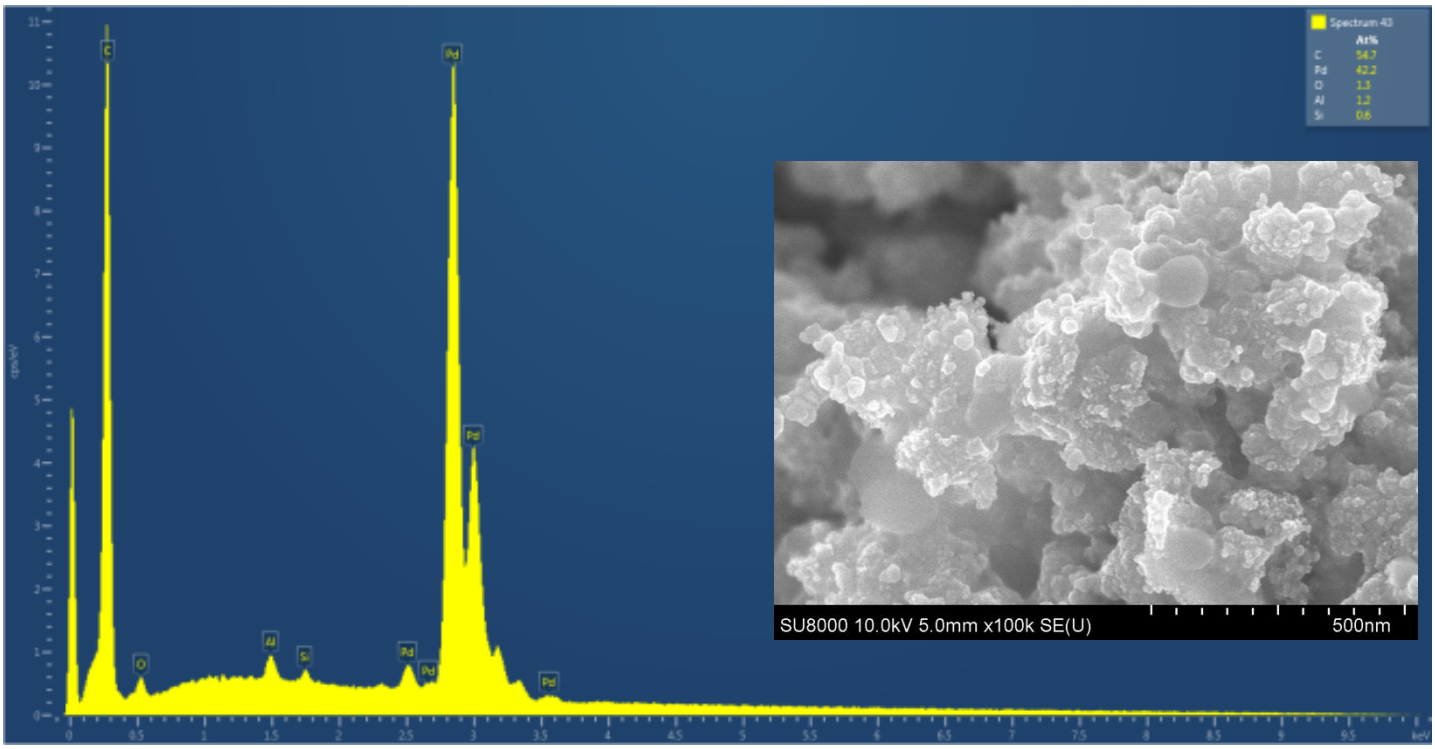

Figure S12. FE-SEM image and EDS spectrum of Pd black isolated from the reaction mixture after heating compound **2a** with KOH in pyridine at 100 ºC within 24 h.

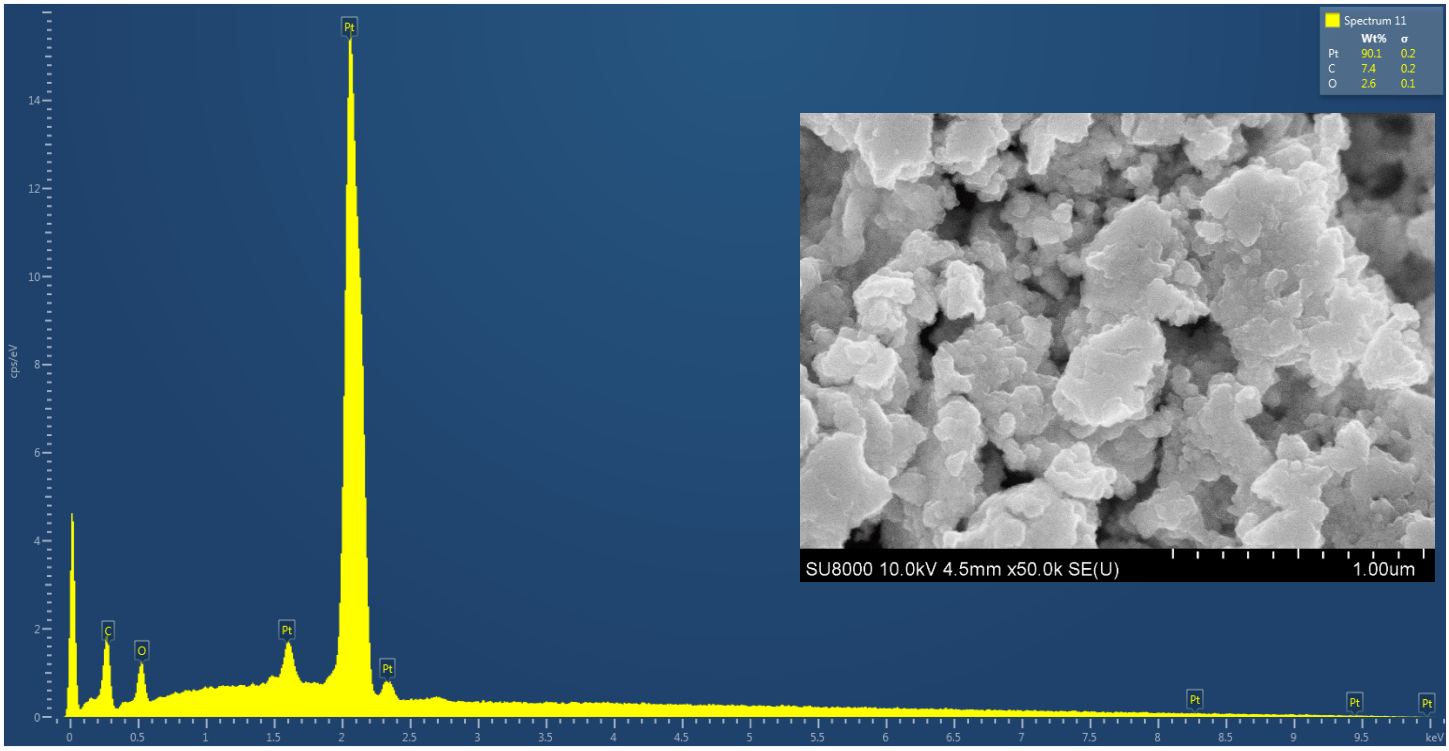

Figure S13. TEM image and EDS spectrum of Pt black isolated from the reaction mixture after heating compound **5a** with *t*-BuOK in 1,4-dioxane at 100 ºC within 20 h.

S4. Raman spectra

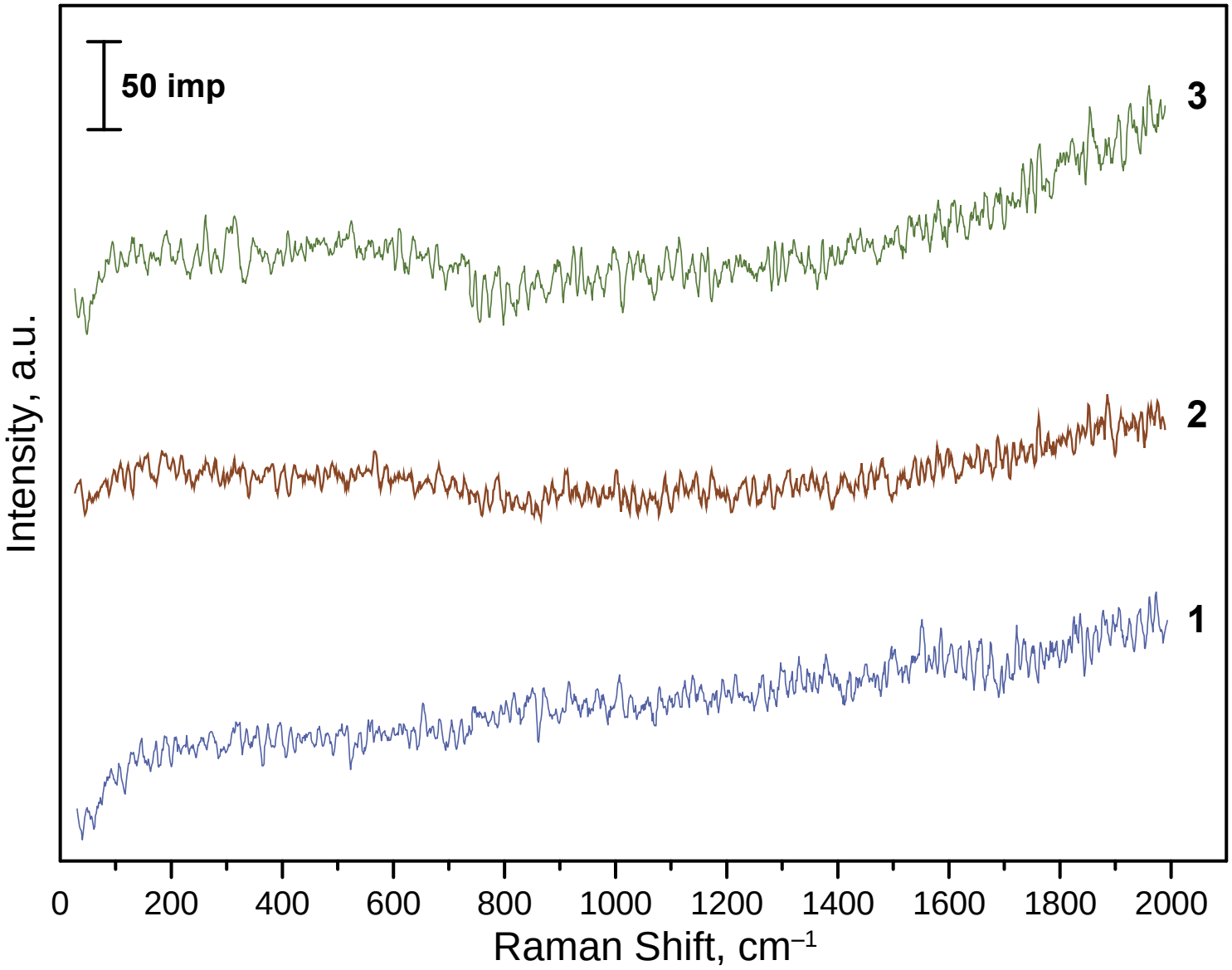

Figure S14. Raman spectra of palladium black isolated from the reaction mixtures: 1 - heating compound **2a** with 3M aqueous KOH solution in pyridine within 24 h; 2 – heating **2a** with *t*-BuOK in 1,4-dioxane at 100 ºC within 3 h; 3 – heating **4a** with 3M aqueous KOH solution in pyridine within 24 h.

The metal precipitates isolated from the reaction mixtures were identified as Pd(0) nanoparticles (Figure S12). The absence of strong enough Raman signals from the obtained samples of palladium black confirmed the absence of any Pd oxides or complexes in the analytic sample.

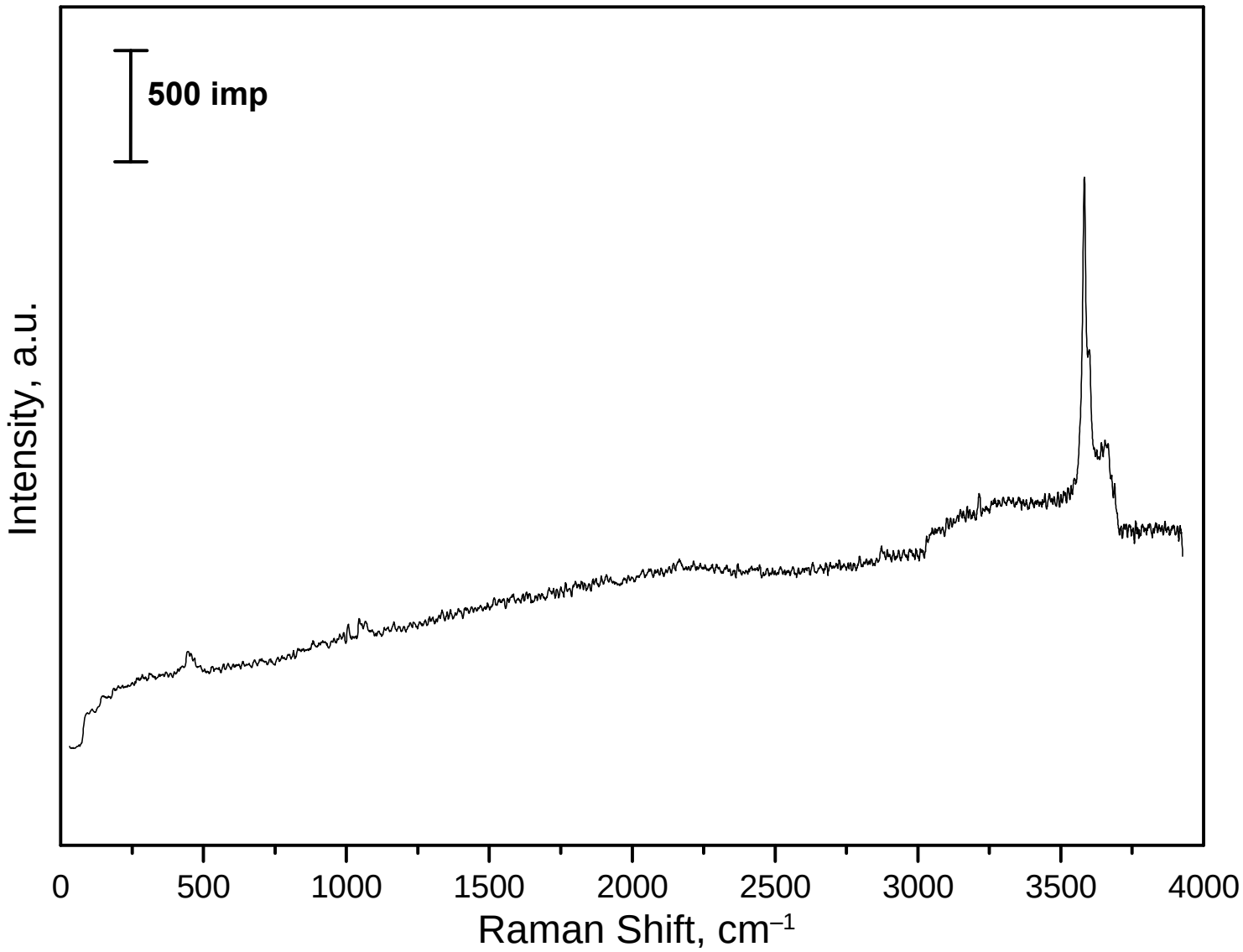

Figure S15. Raman spectrum of $Ni(OH)_2$ isolated from the reaction mixture after heating compound **6a** with 3M aqueous KOH solution in 1,4-dioxane at 100 ºC within 20 h.

The Raman spectrum is analogous to the literature data for the disordered β-$Ni(OH)_2$.[1,2] The 3680 cm^{-1} peak is associated with the stretching of the free OH^- groups of the outer part of the crystallites of $Ni(OH)_2$. The 3570 cm^{-1} intense peak is assigned to the free OH^-, while the 3580 cm^{-1} shoulder to the linked OH^- groups in the crystalline bulk [2].

[1] Cornilsen, B. C.; Karjala, P. J.; Loyselle, P. L. *J. Power Sources* **1988**, *22*, 351-357.
[2] Bernard, M. C.; Cortes, R.; Keddam, M.; Takenouti, H.; Bernard, P.; Senyarich, S. *J. Power Sources* **1996,** *63*, 247-254.

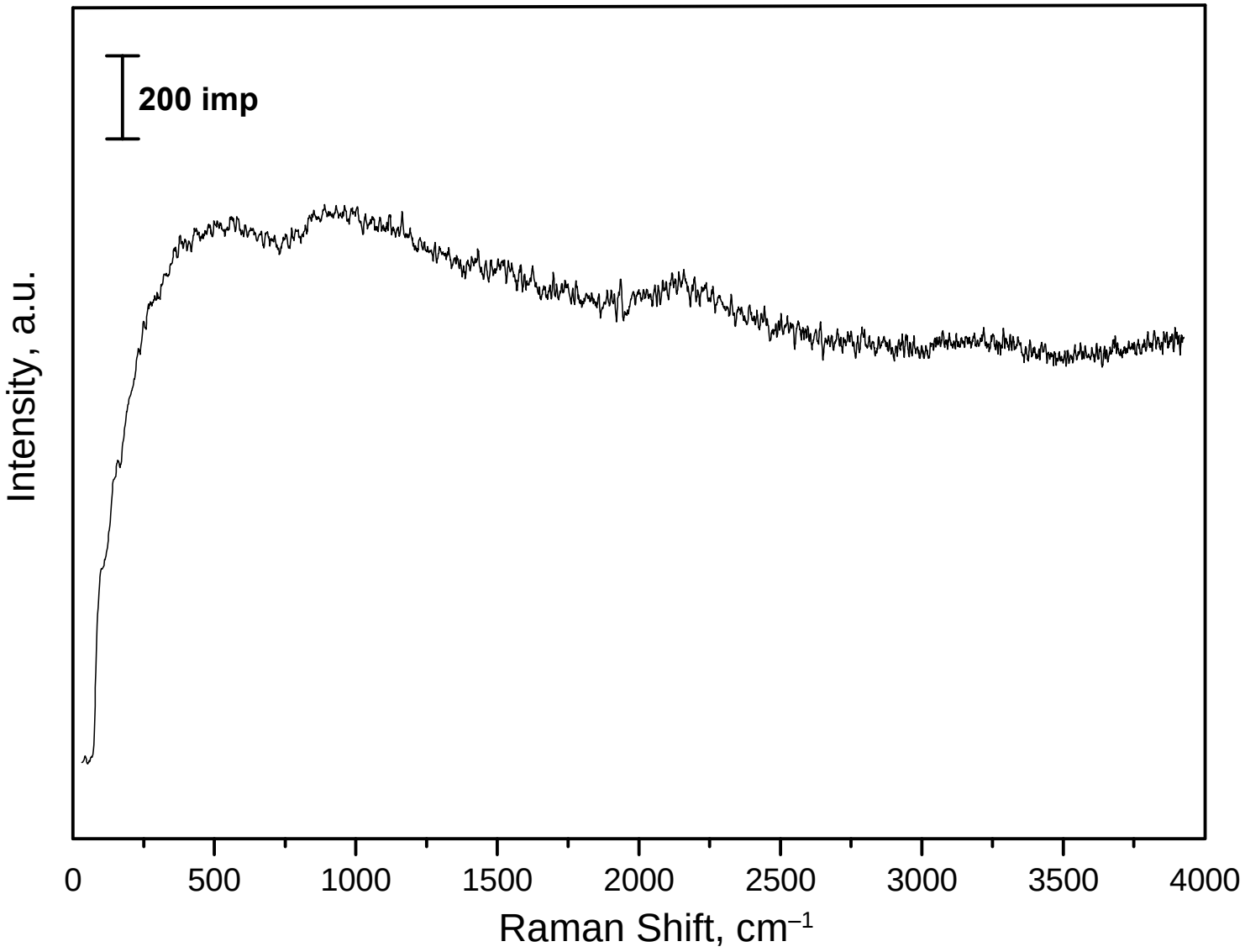

Figure S16. Raman spectrum of nickel black isolated from the reaction mixture after heating compound **6a** with *t*-BuOK in 1,4-dioxane at 100 ºC within 20 h.
The absence of strong enough Raman signals in the range of 30 – 4000 cm^{-1} corroborates the absence of any notable amounts of Ni oxides, hydroxides or complexes in the analytic sample.

S5. NMR spectra, ESI-MS and GC-MS data

^{1}H and ^{13}C NMR,[a] HRMS spectra

[a]Small impurity signals were observed in the NMR spectra of Pd-PEPPSI complexes **2b,c,e,g** in $CDCl_3$. Analogous signals were also observed previously in NMR spectra of Pd-NHC complexes and reported in the literature: a) Yen, S. K.; Koh, L. L.; Huynh, H. V.; Hor, T. S. A. *Aust. J. Chem.* **2009,** *62*, 1047-1053; (b) Teci, M.; Brenner, E.; Matt, D.; Toupet, L. *Eur. J. Inorg. Chem.* **2013,** *2013*, 2841-2848; (c) Rottschäfer, D.; Schürmann, C. J.; Lamm, J.-H.; Paesch, A. N.; Neumann, B.; Ghadwal, R. S. *Organometallics* **2016,** *35*, 3421-3429; (d) Steeples, E.; Kelling, A.; Schilde, U.; Esposito, D. *New J. Chem.* **2016,** *40*, 4922-4930; (e) Astakhov, A. V.; Khazipov, O. V.; Chernenko, A. Y.; Pasyukov, D. V.; Kashin, A. S.; Gordeev, E. G.; Khrustalev, V. N.; Chernyshev, V. M.; Ananikov, V. P. *Organometallics* **2017,** *36*, 1981-1992.

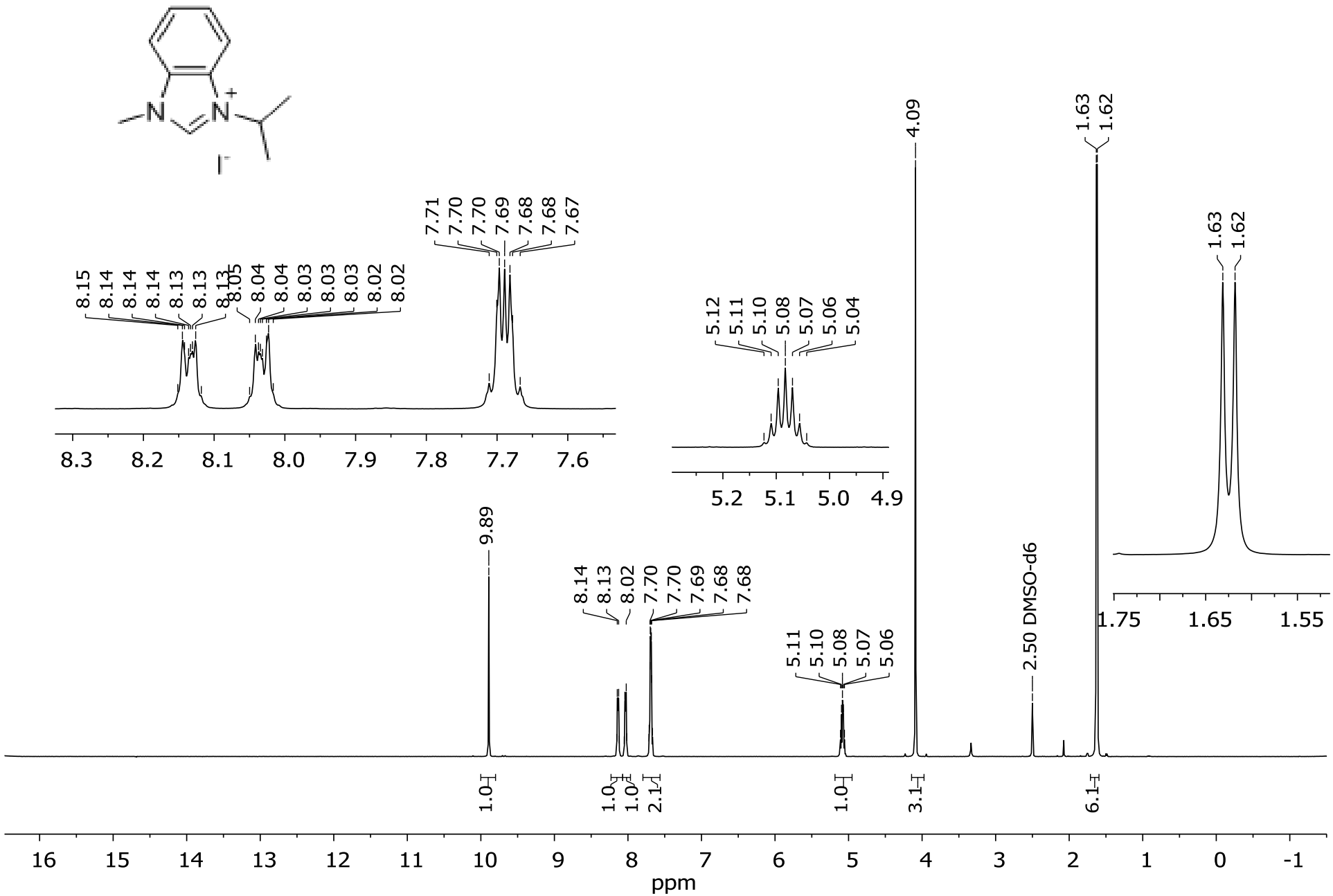

Figure S17. ^{1}H NMR spectrum of compound **1e** (DMSO-d_6, 500 MHz).

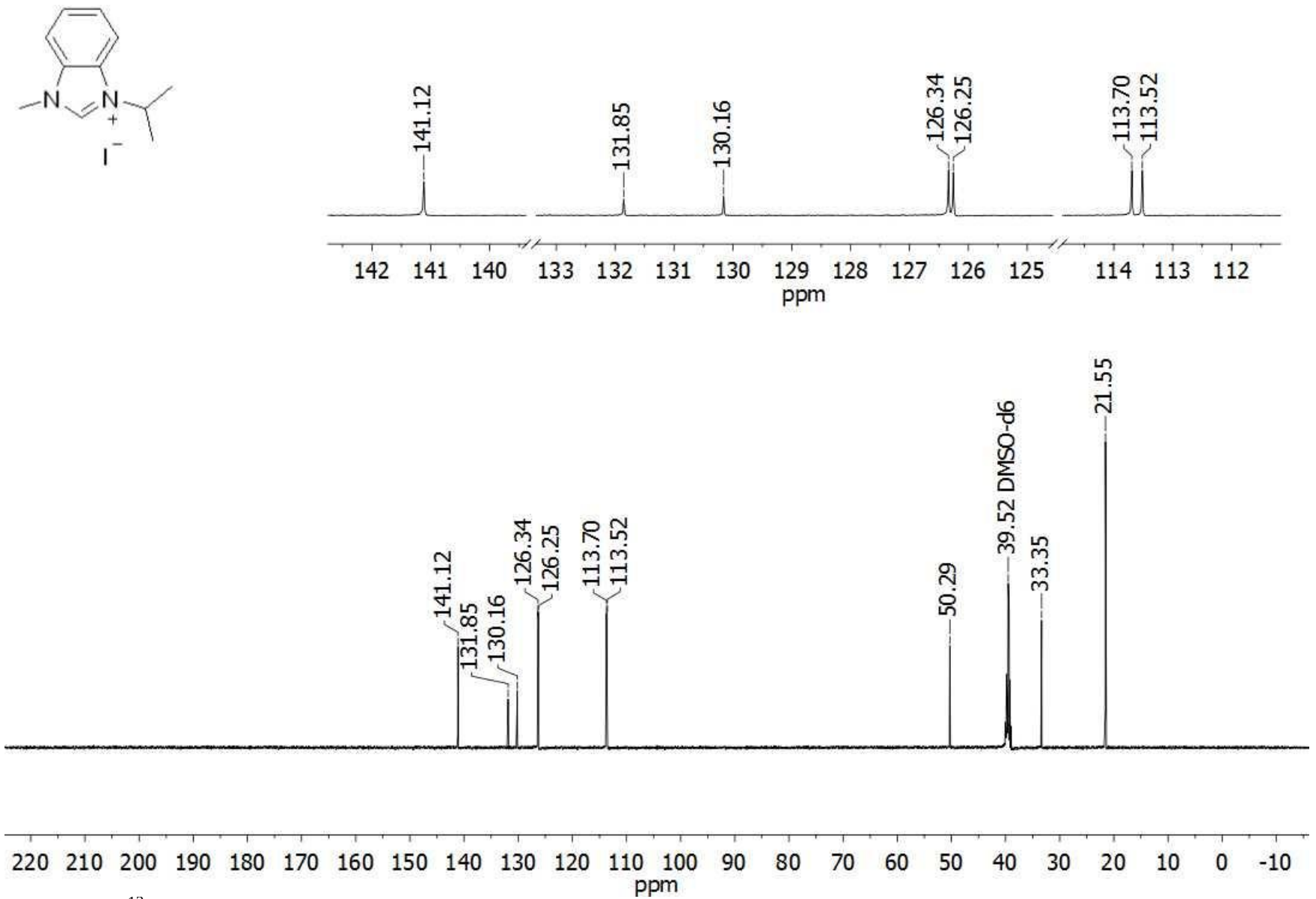

Figure S18. ^{13}C NMR spectrum of compound **1e** (DMSO-d_6, 500 MHz).

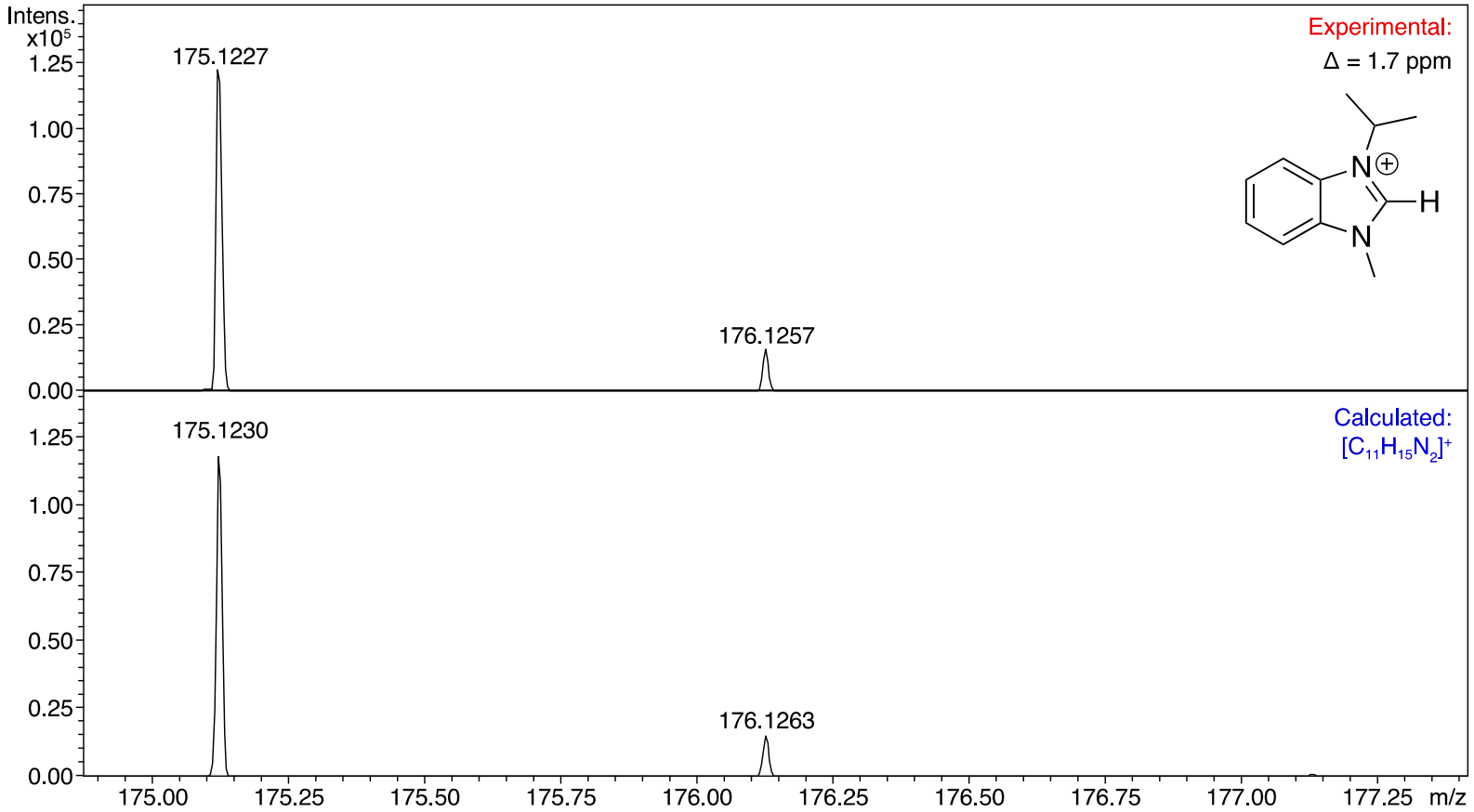

Figure S19. ESI-(+)MS spectrum of compound **1e** in CH_3CN solution, expanded to the $[M]^+$ region.

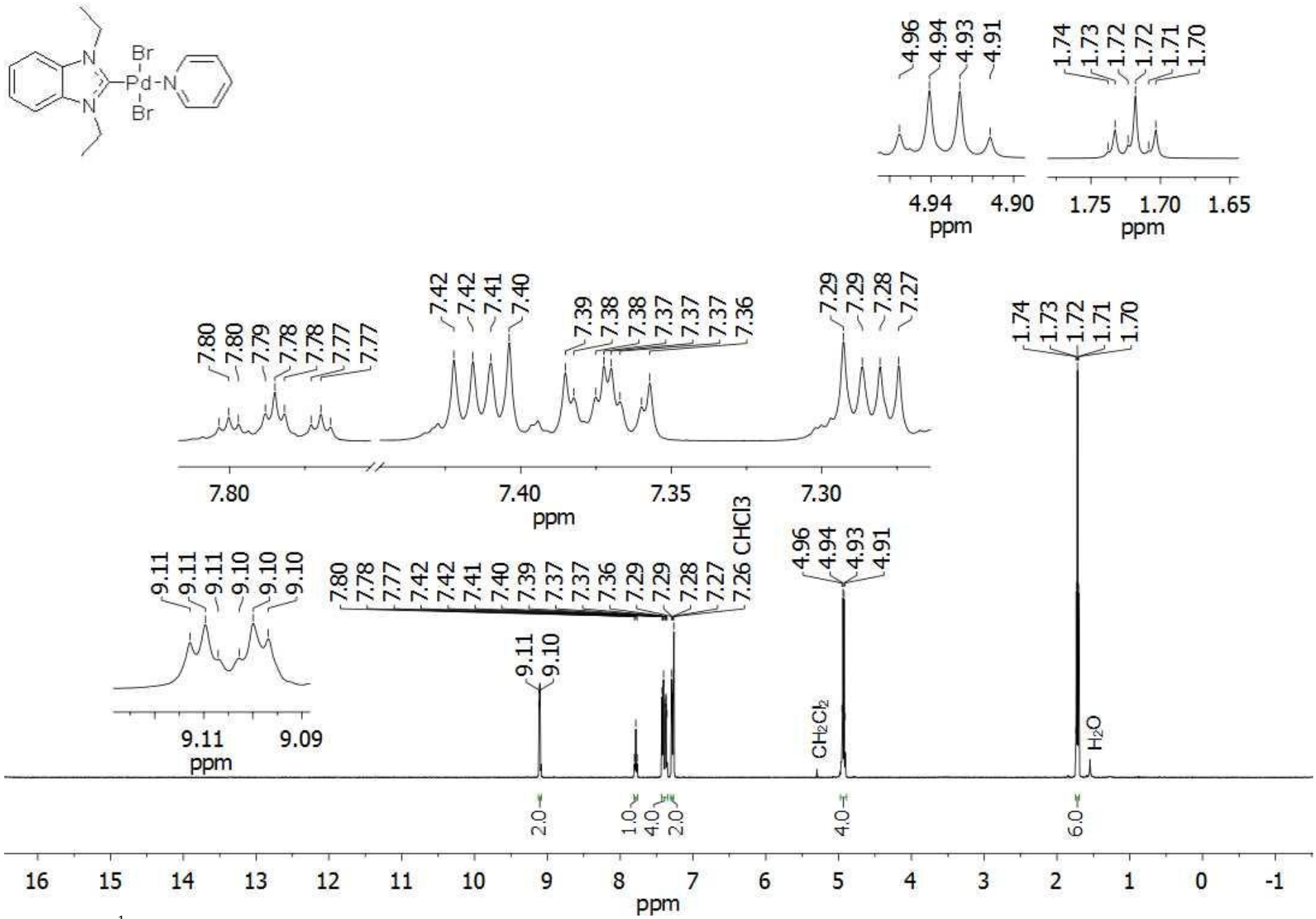

Figure S20. ^{1}H NMR spectrum of compound **2b** ($CDCl_3$, 500 MHz).

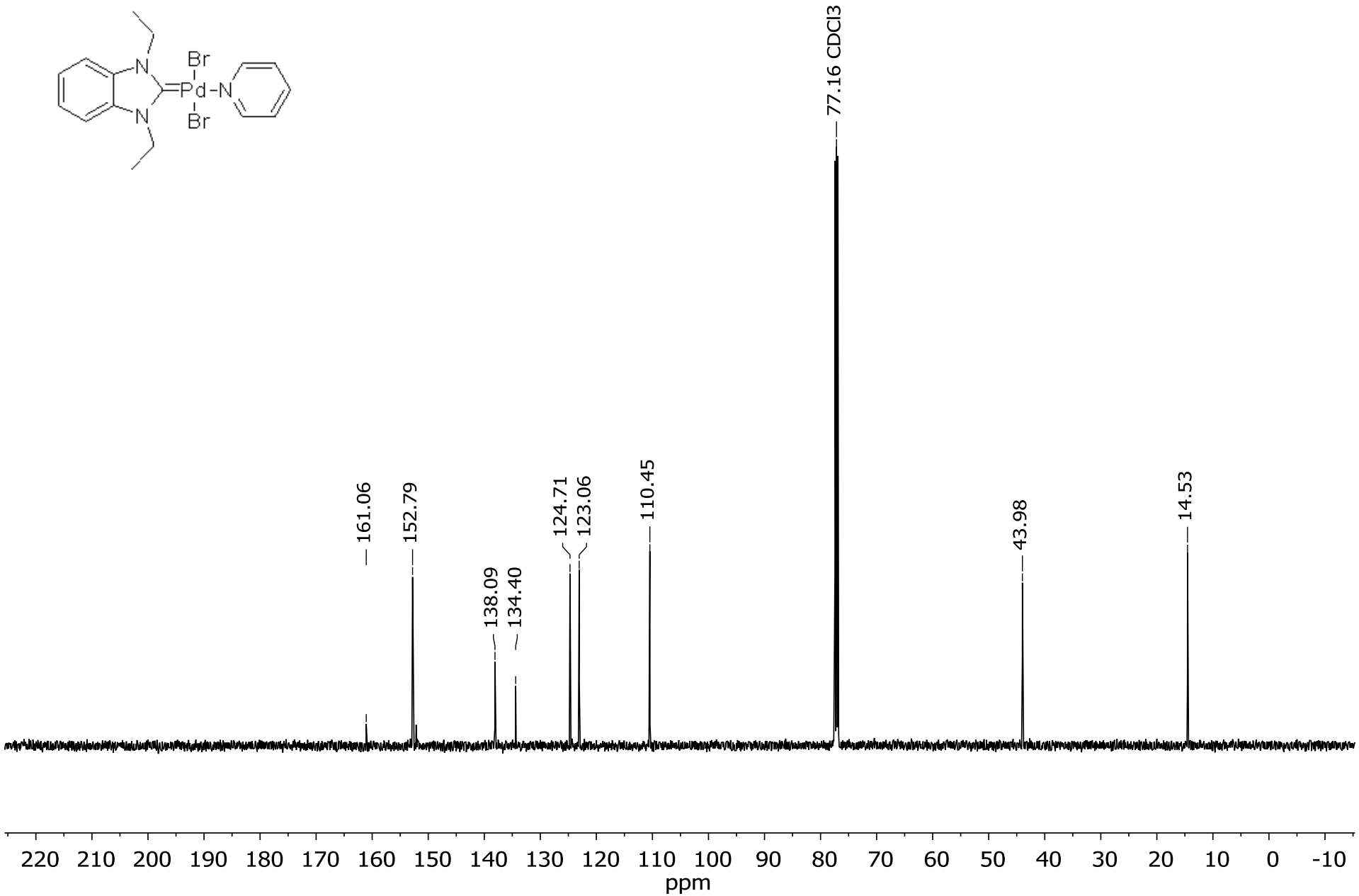

Figure S21. ^{13}C NMR spectrum of compound **2b** ($CDCl_3$, 125 MHz).

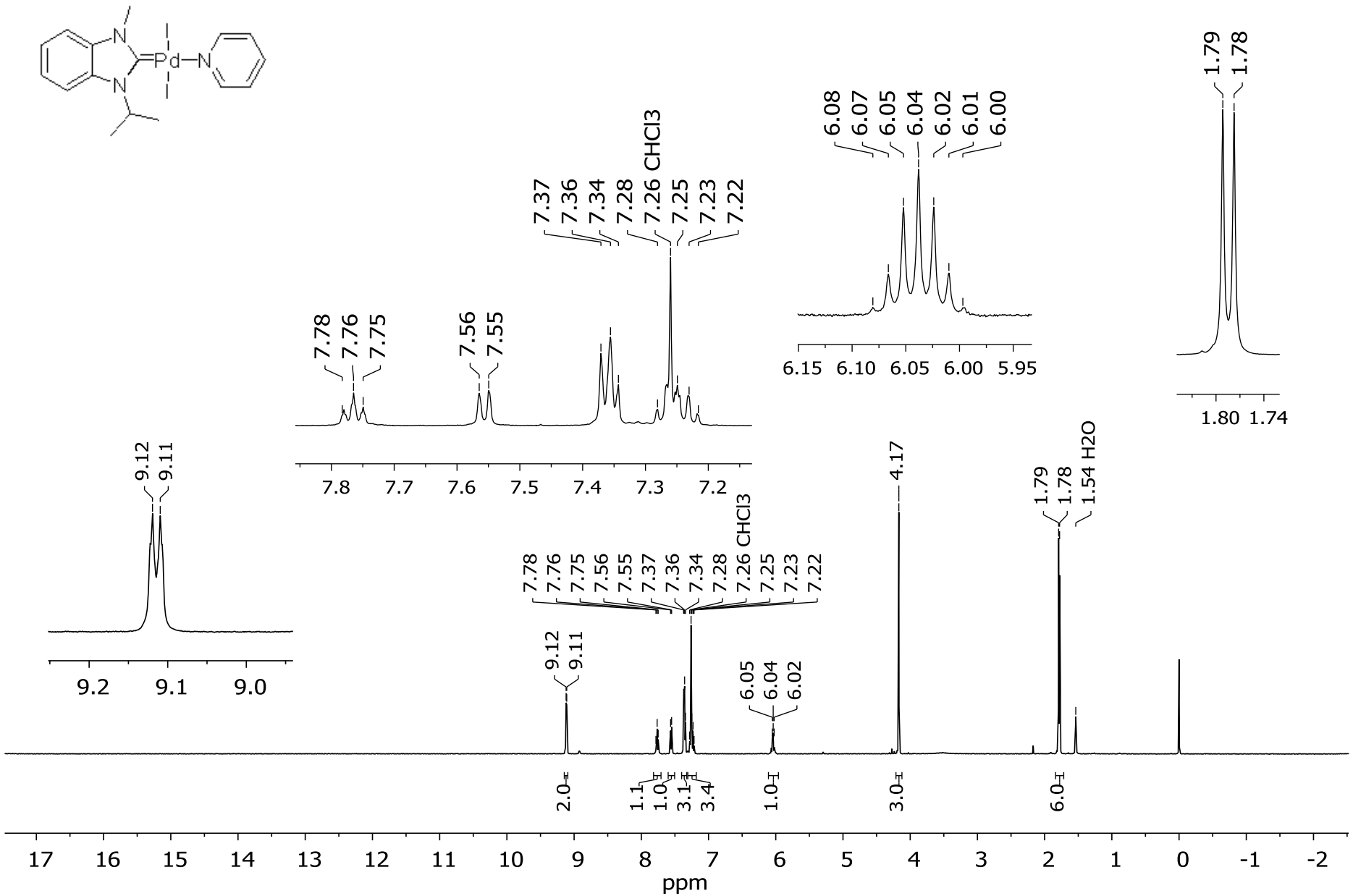

Figure S22. ^{1}H NMR spectrum of compound **2e** ($CDCl_3$, 500 MHz).

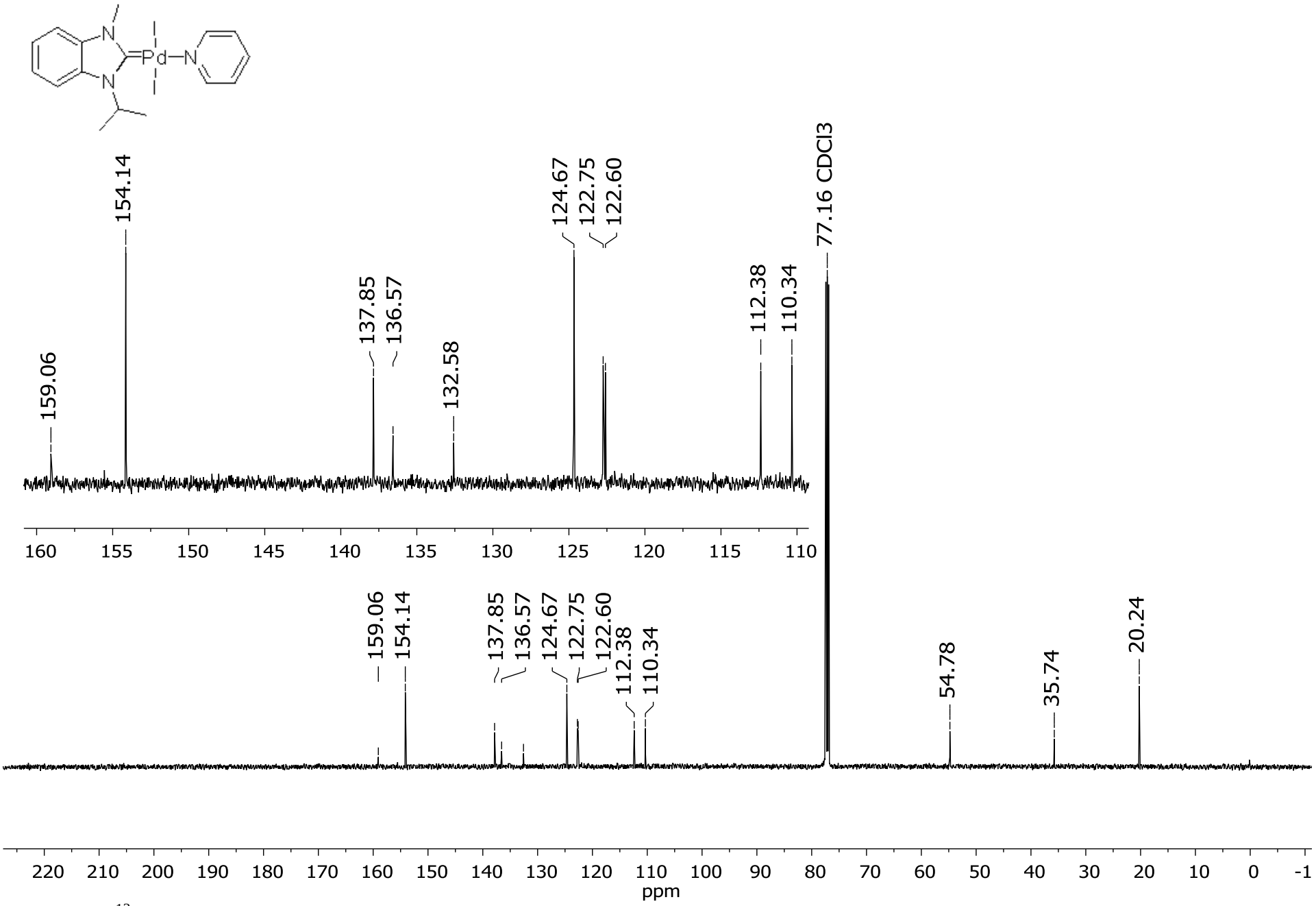

Figure S23. ^{13}C NMR spectrum of compound **2e** ($CDCl_3$, 125 MHz).

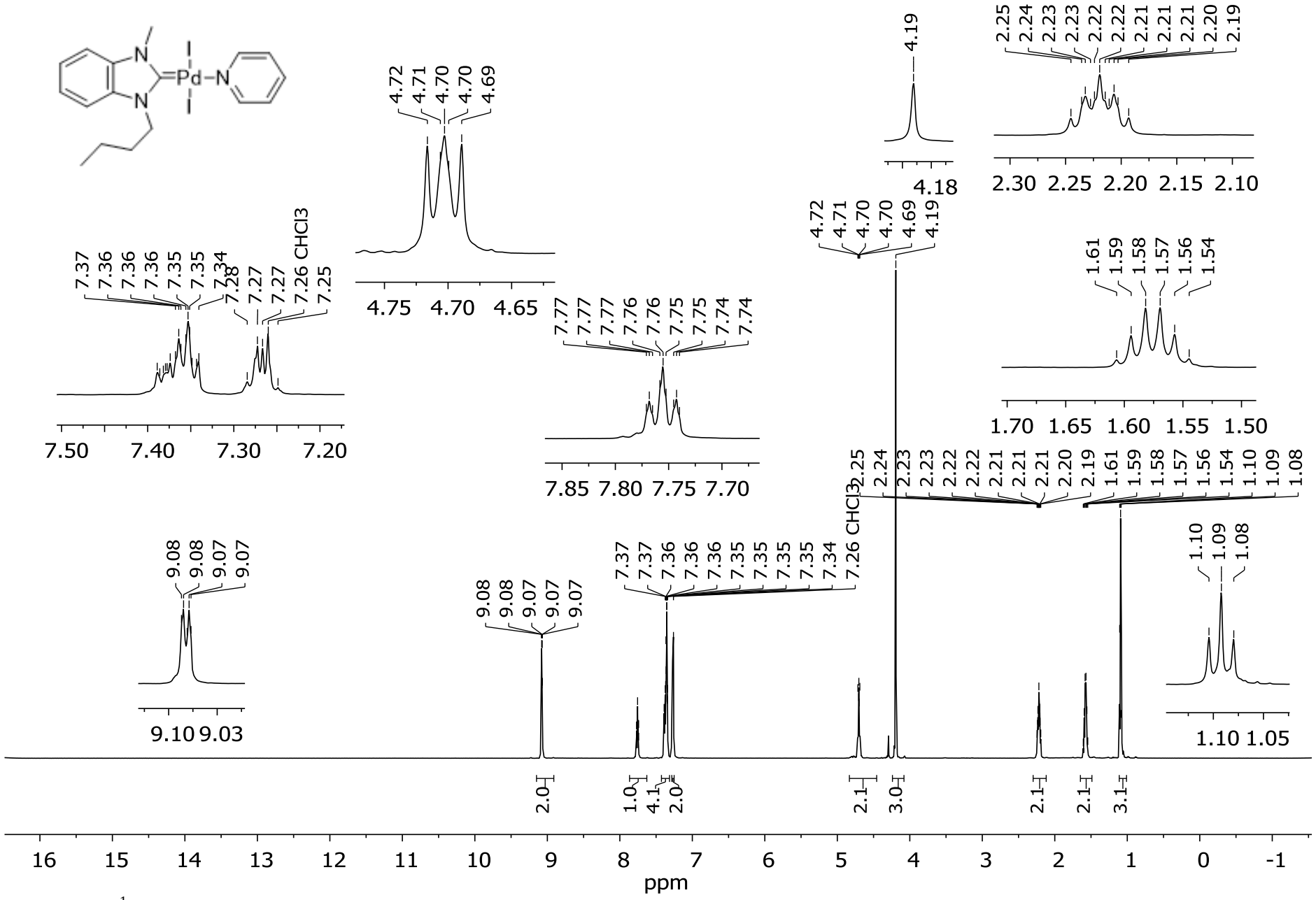

Figure S24. ^{1}H NMR spectrum of compound **2g** ($CDCl_3$, 500 MHz).

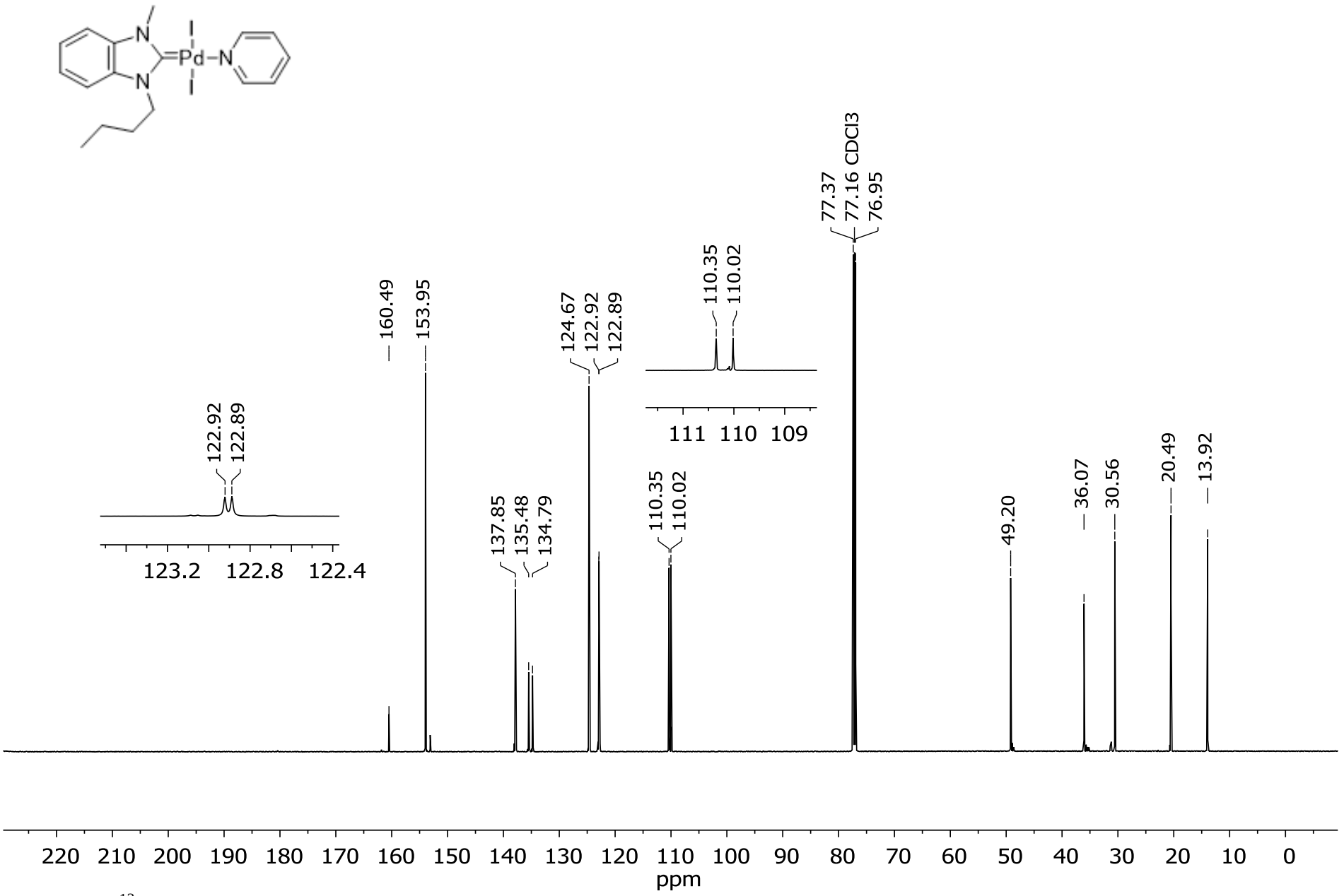

Figure S25. ^{13}C NMR spectrum of compound **2g** ($CDCl_3$, 125 MHz).

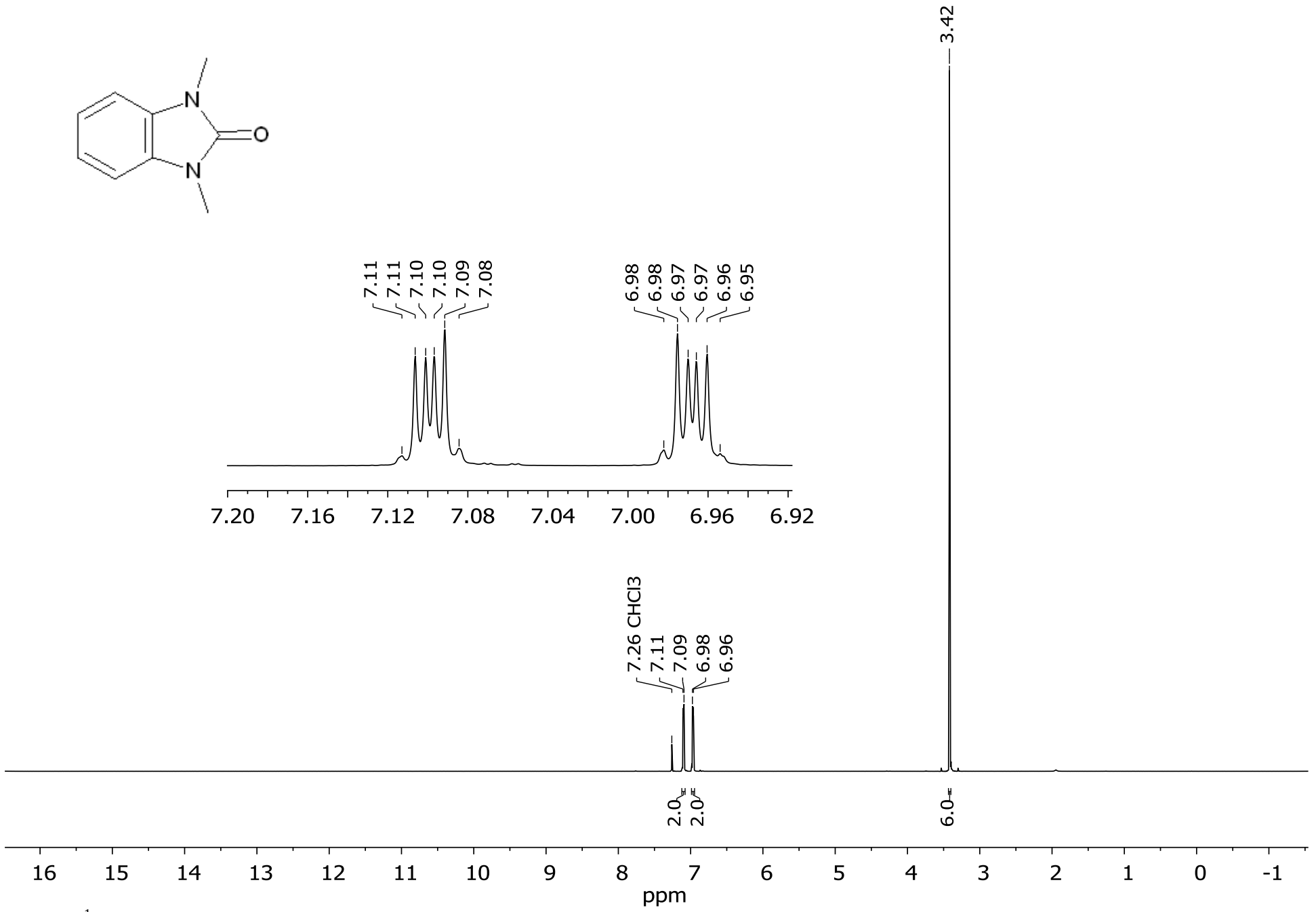

Figure S26. ^{1}H NMR spectrum of compound **7a** ($CDCl_3$, 500 MHz).

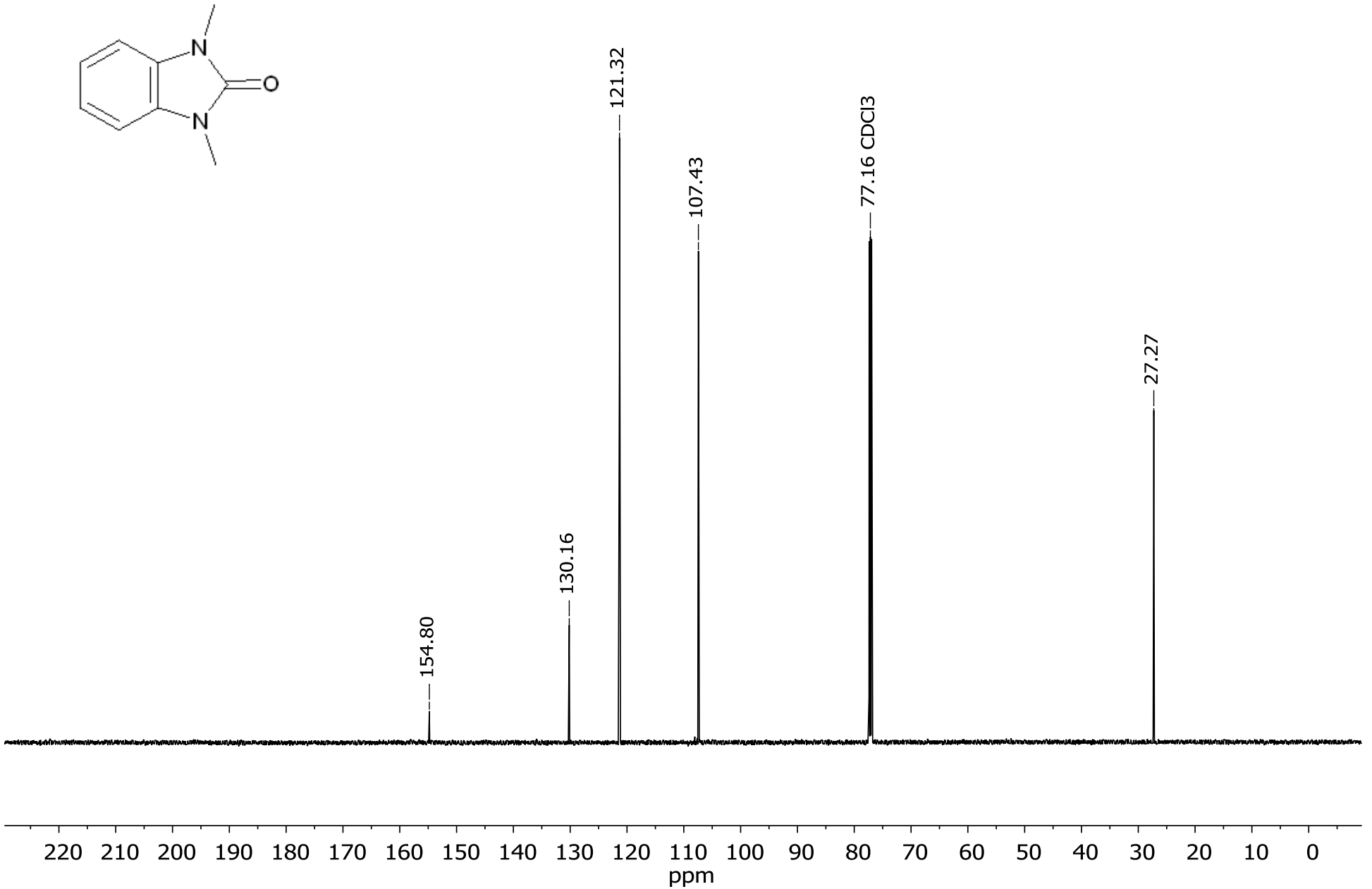

Figure S27. ^{13}C NMR spectrum of compound **7a** ($CDCl_3$, 125 MHz).

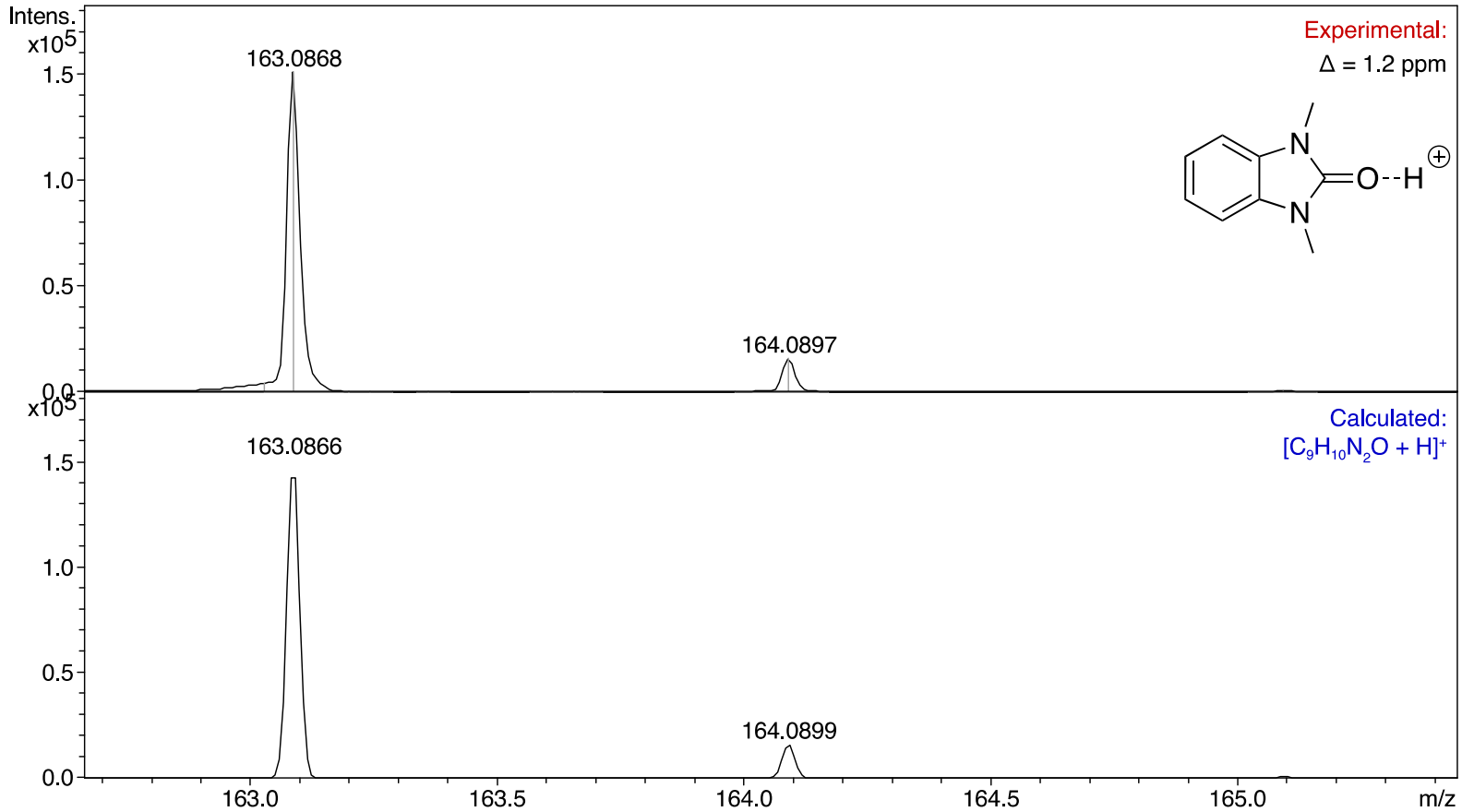

Figure S28. ESI-(+)MS spectrum of compound **7a** in CH_3CN solution, expanded to the $[M + H]^+$ region.

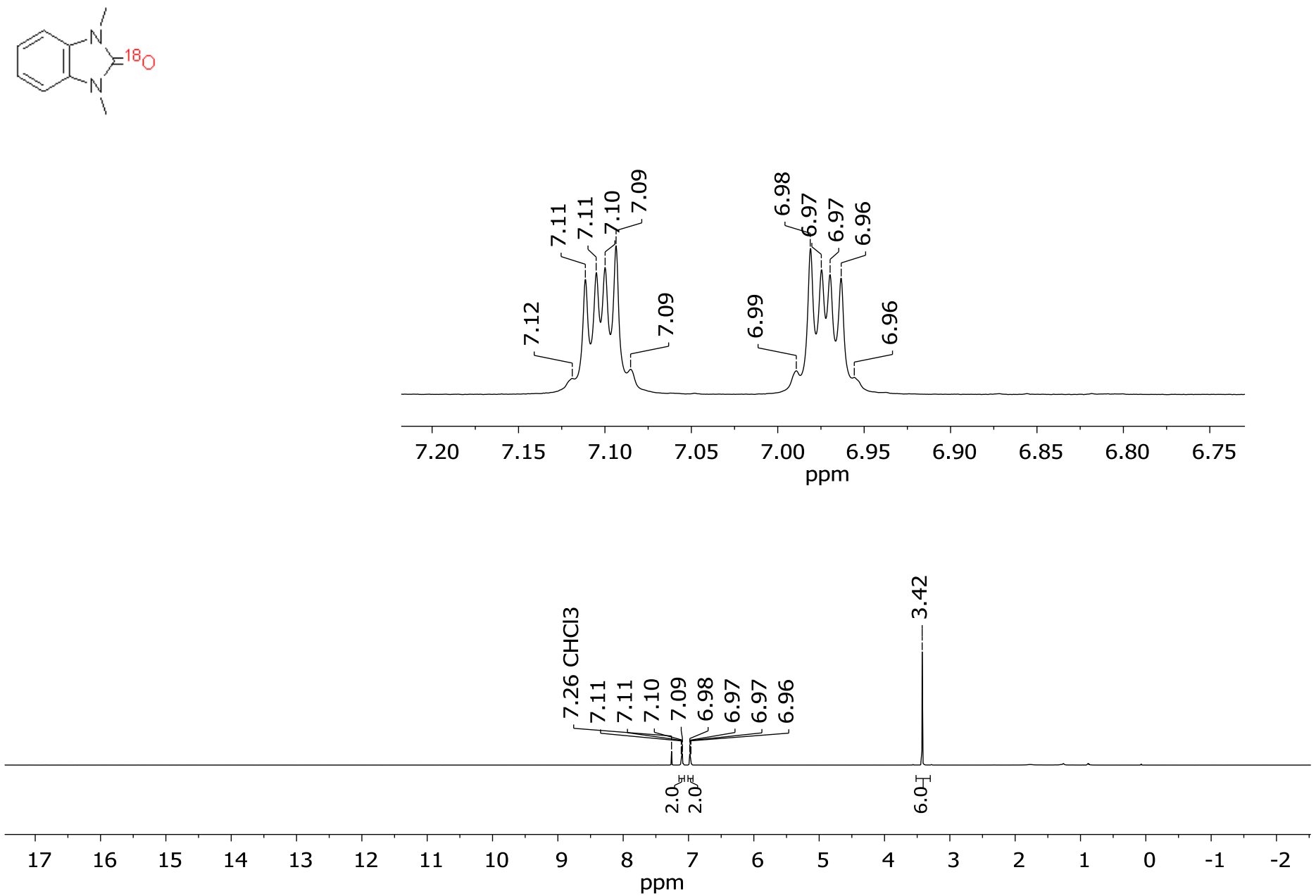

Figure S29. ^{1}H NMR spectrum of compound **7a-^{18}O** ($CDCl_3$, 500 MHz).

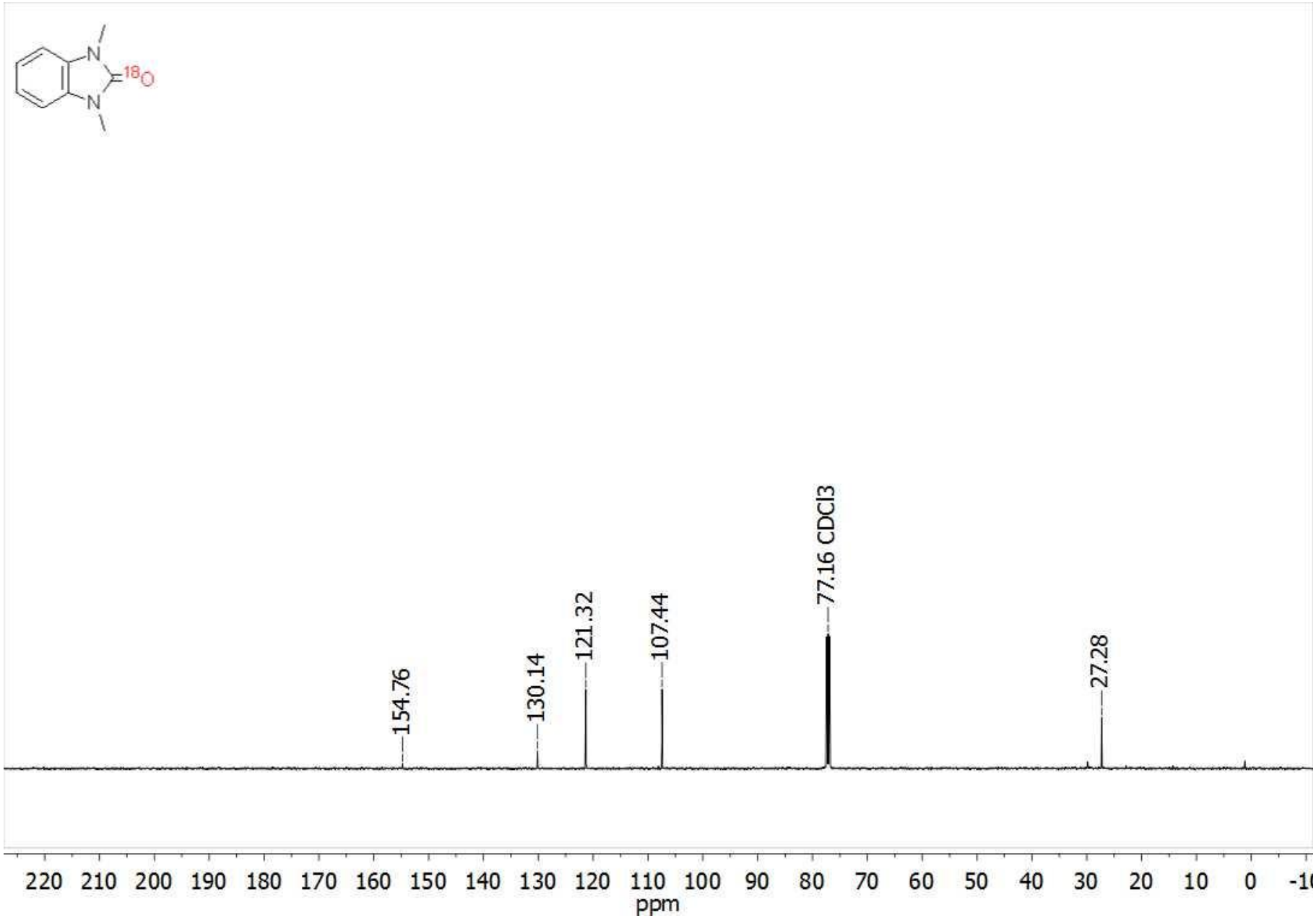

Figure S30. ^{13}C NMR spectrum of compound **7a-^{18}O** ($CDCl_3$, 125 MHz).

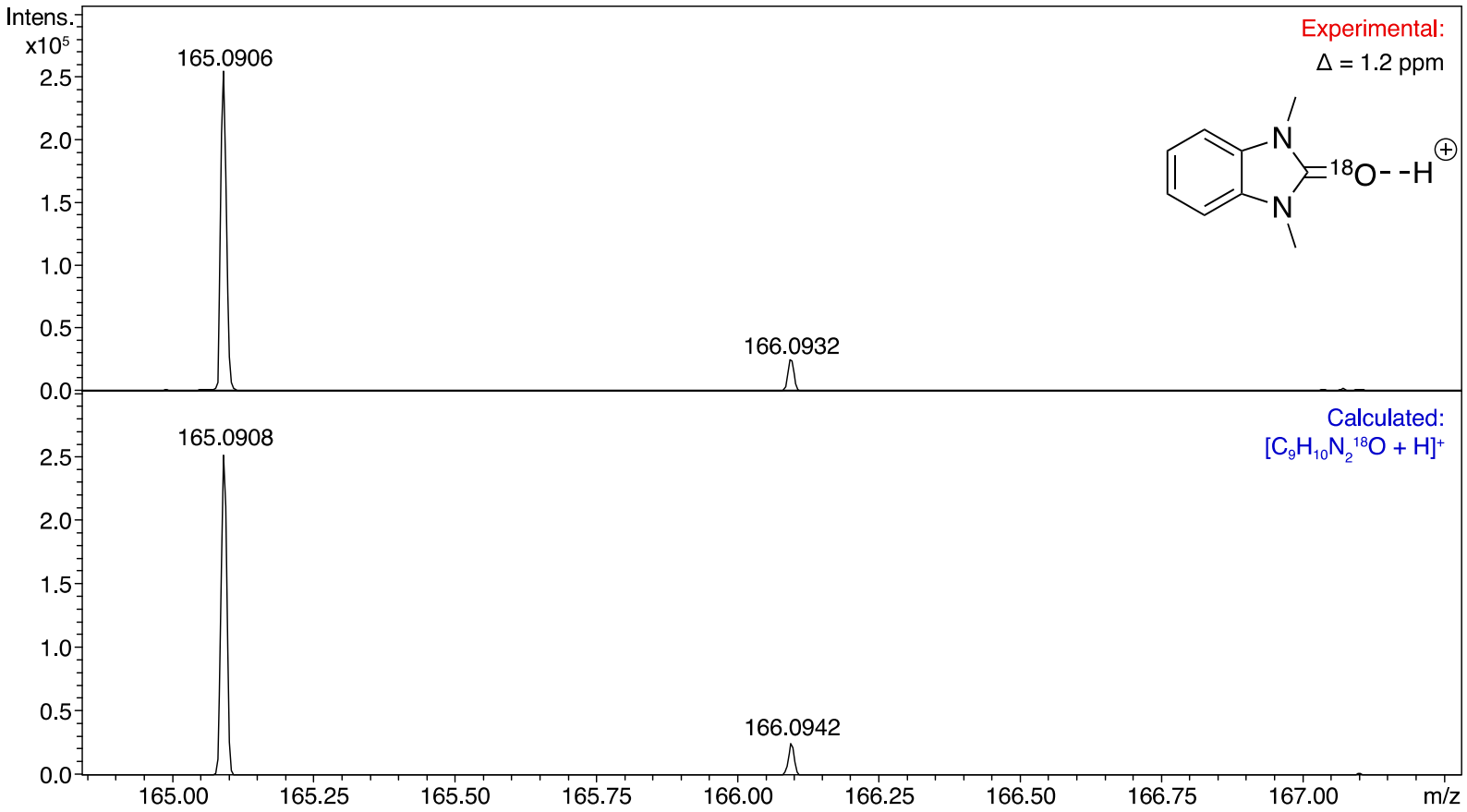

Figure S31. ESI-(+)MS spectrum of 1,3-dimethyl-1,3-dihydro-2*H*-benzimidazol-2-one-^{18}O (**7a-^{18}O**) in CH_3CN solution expanded to the $[M + H]^+$ region.

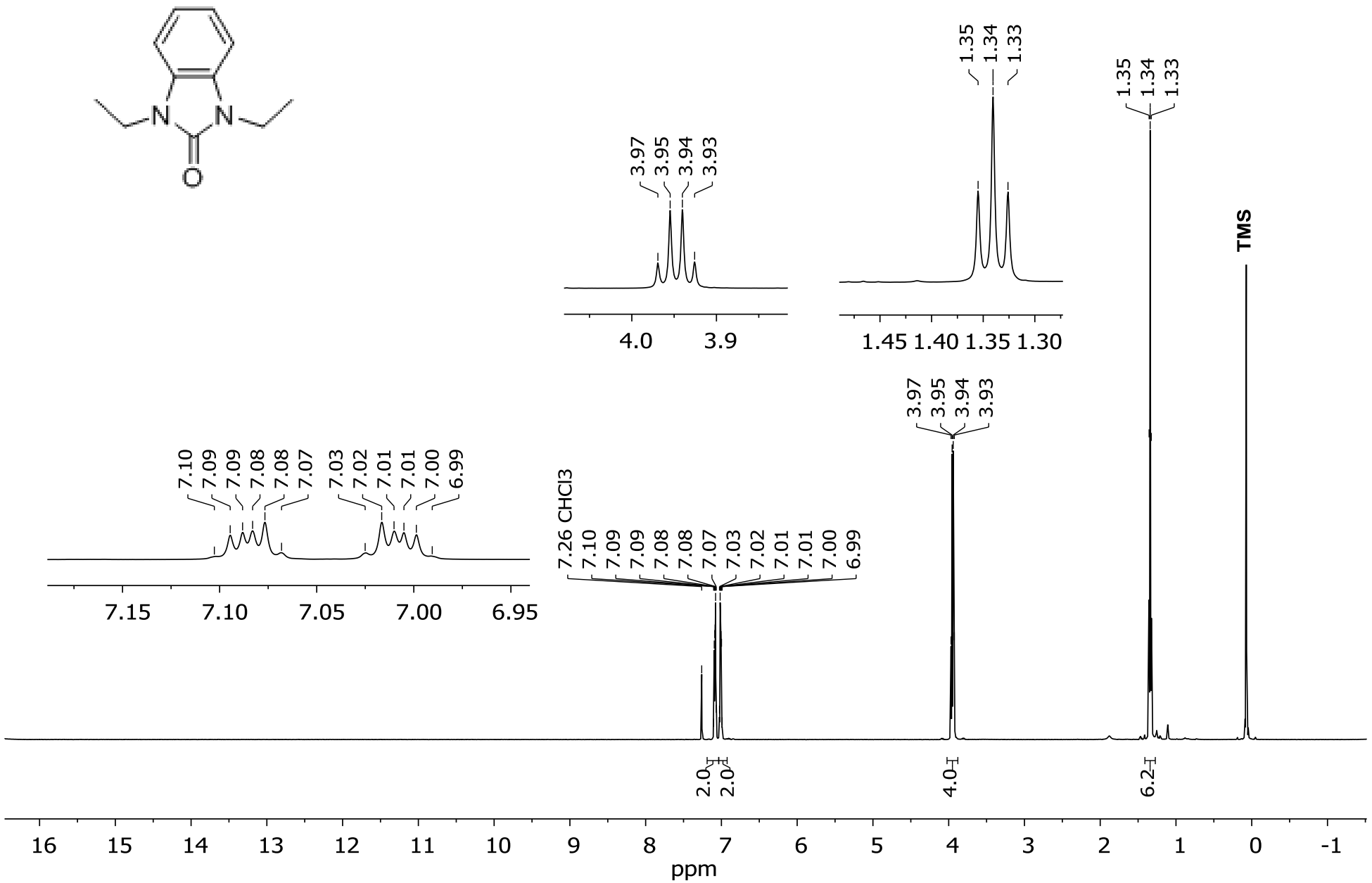

Figure S32. ^{1}H NMR spectrum of compound **7b** ($CDCl_3$, 500 MHz).

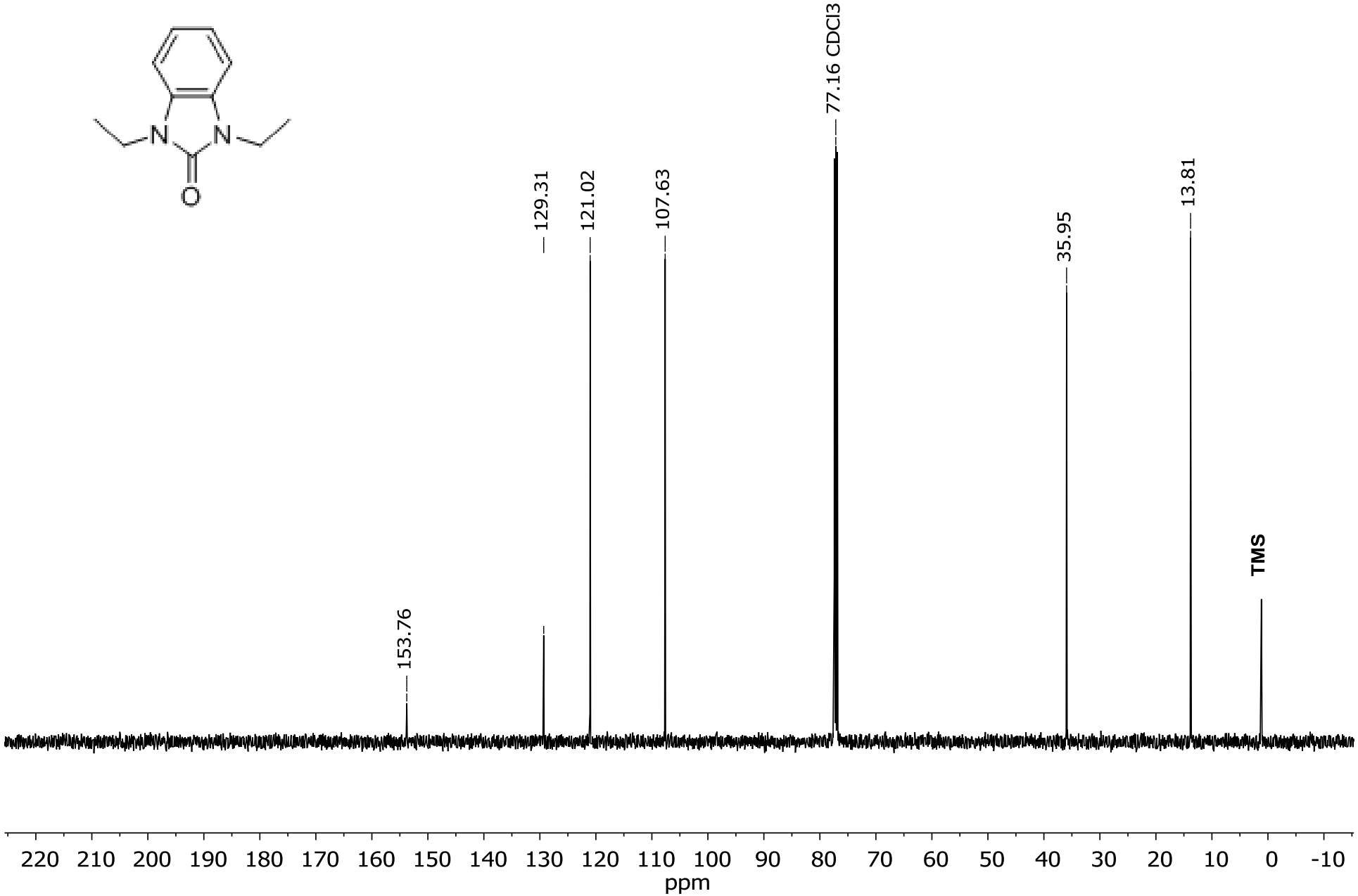

Figure S33. ^{13}C NMR spectrum of compound **7b** ($CDCl_3$, 125 MHz).

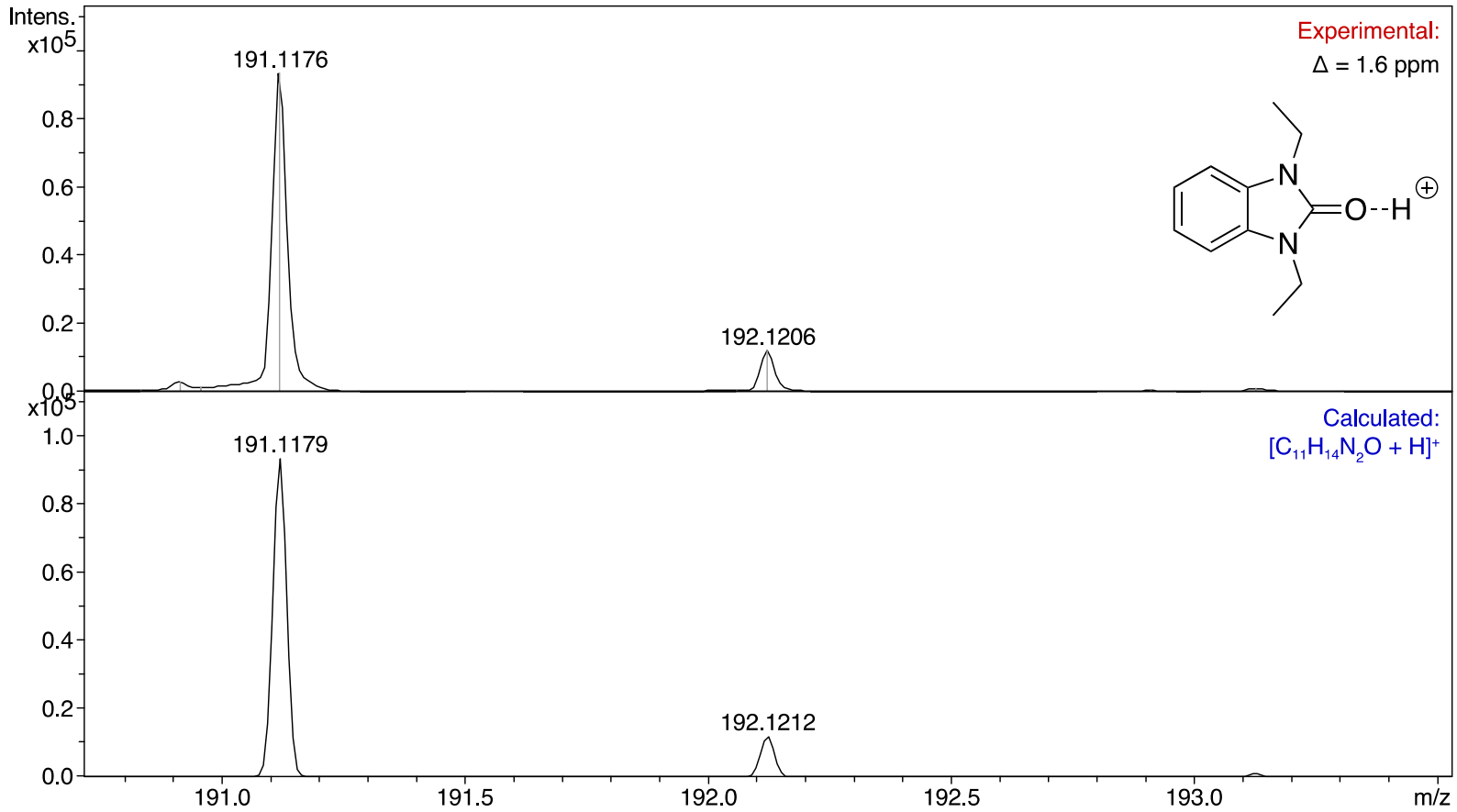

Figure S34. ESI-(+)MS spectrum of compound **7b** in CH_3CN solution expanded to the $[M + H]^+$ region.

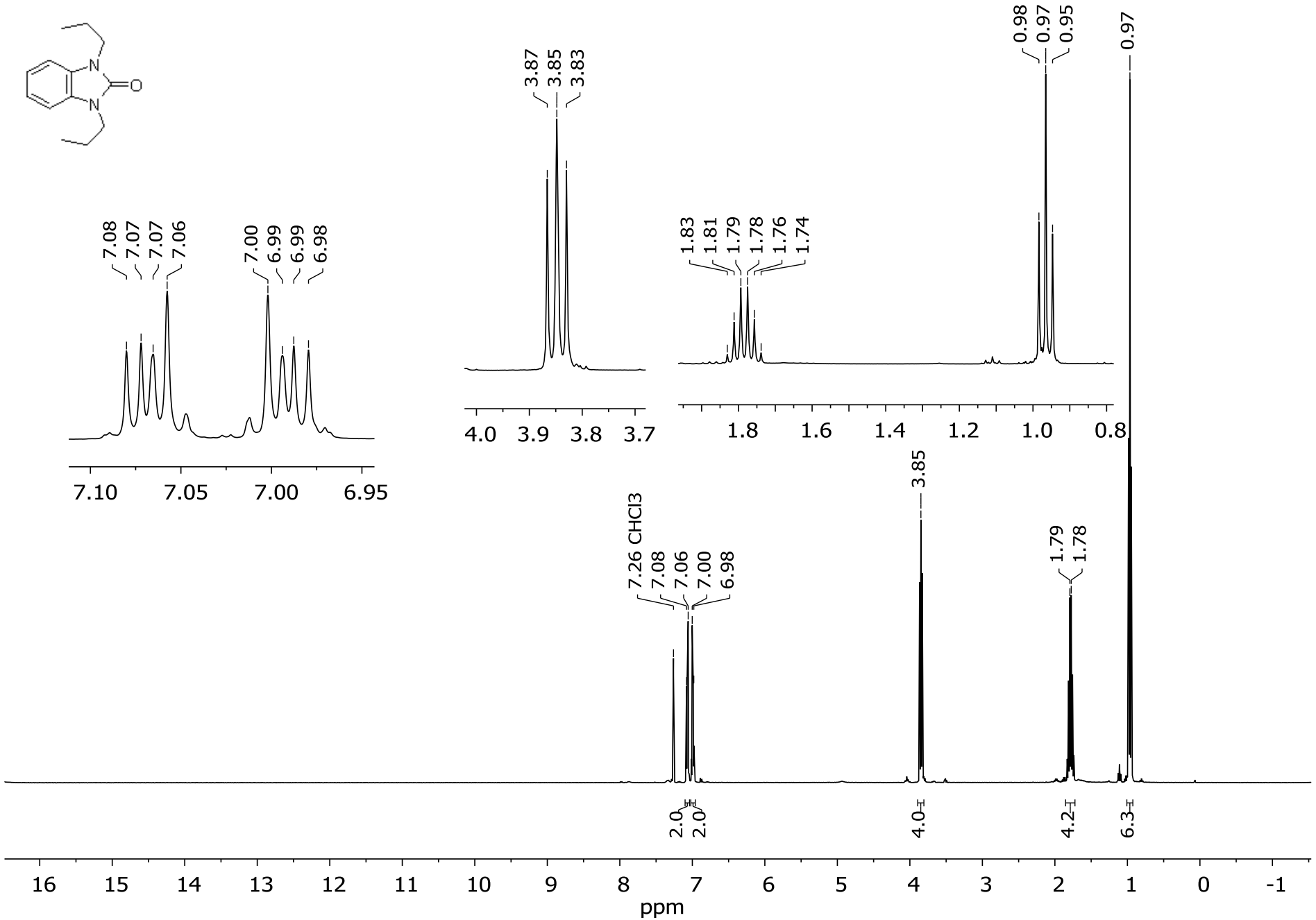

Figure S35. ^{1}H NMR spectrum of compound **7c** ($CDCl_3$, 400 MHz).

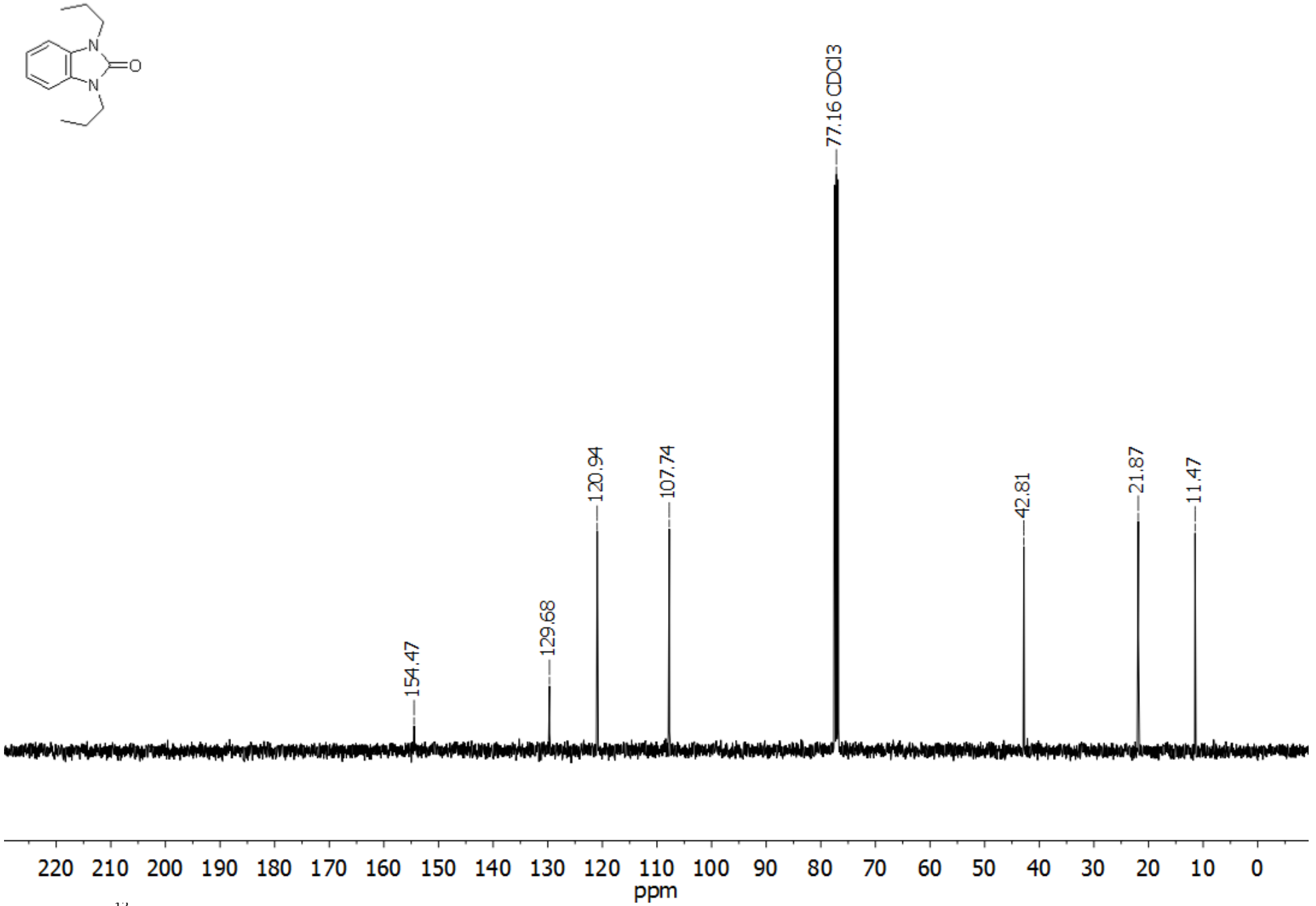

Figure S36. ^{13}C NMR spectrum of compound **7c** ($CDCl_3$, 100 MHz).

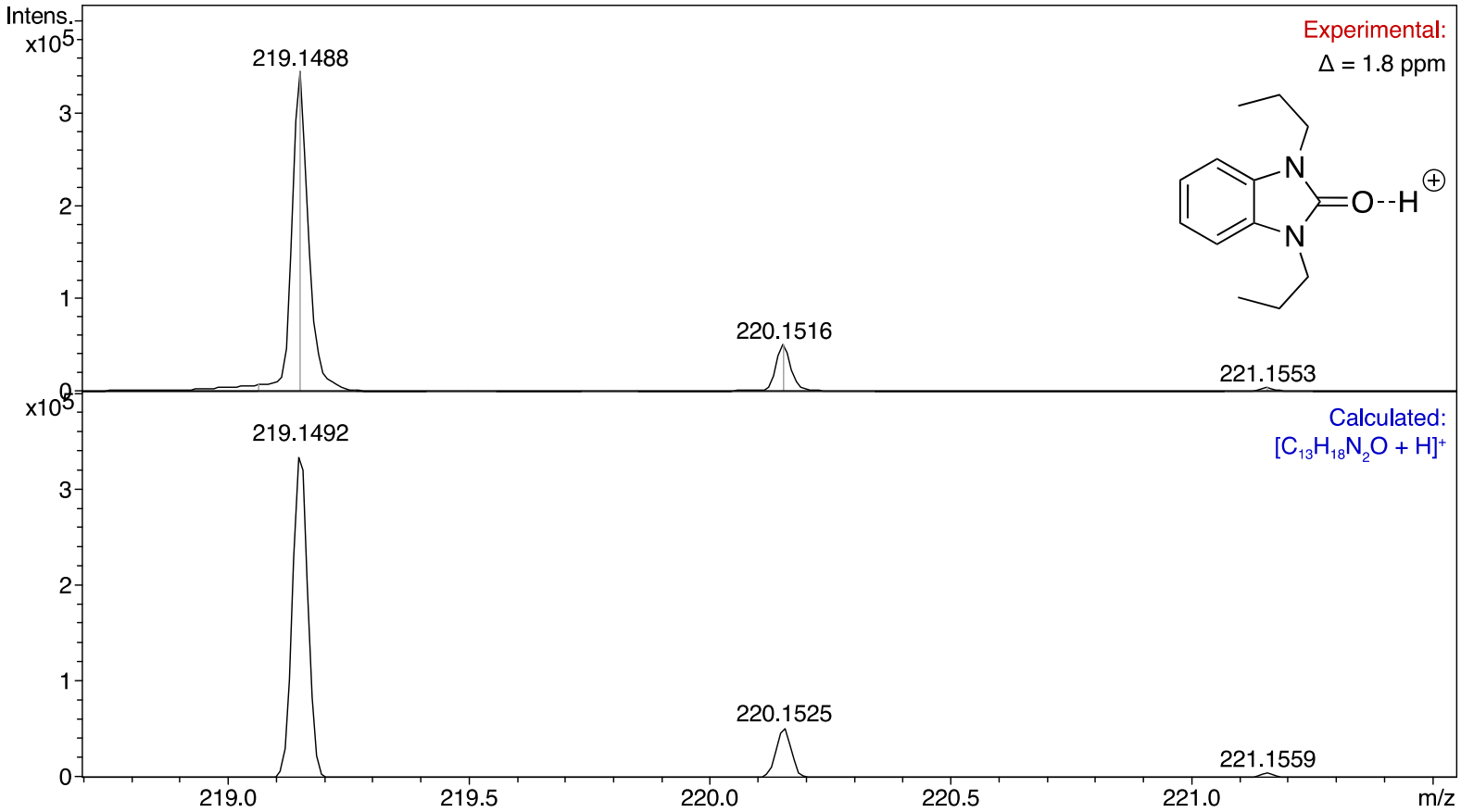

Figure S37. ESI-(+)MS spectrum of compound **7c** in CH_3CN solution expanded to the $[M + H]^+$ region.

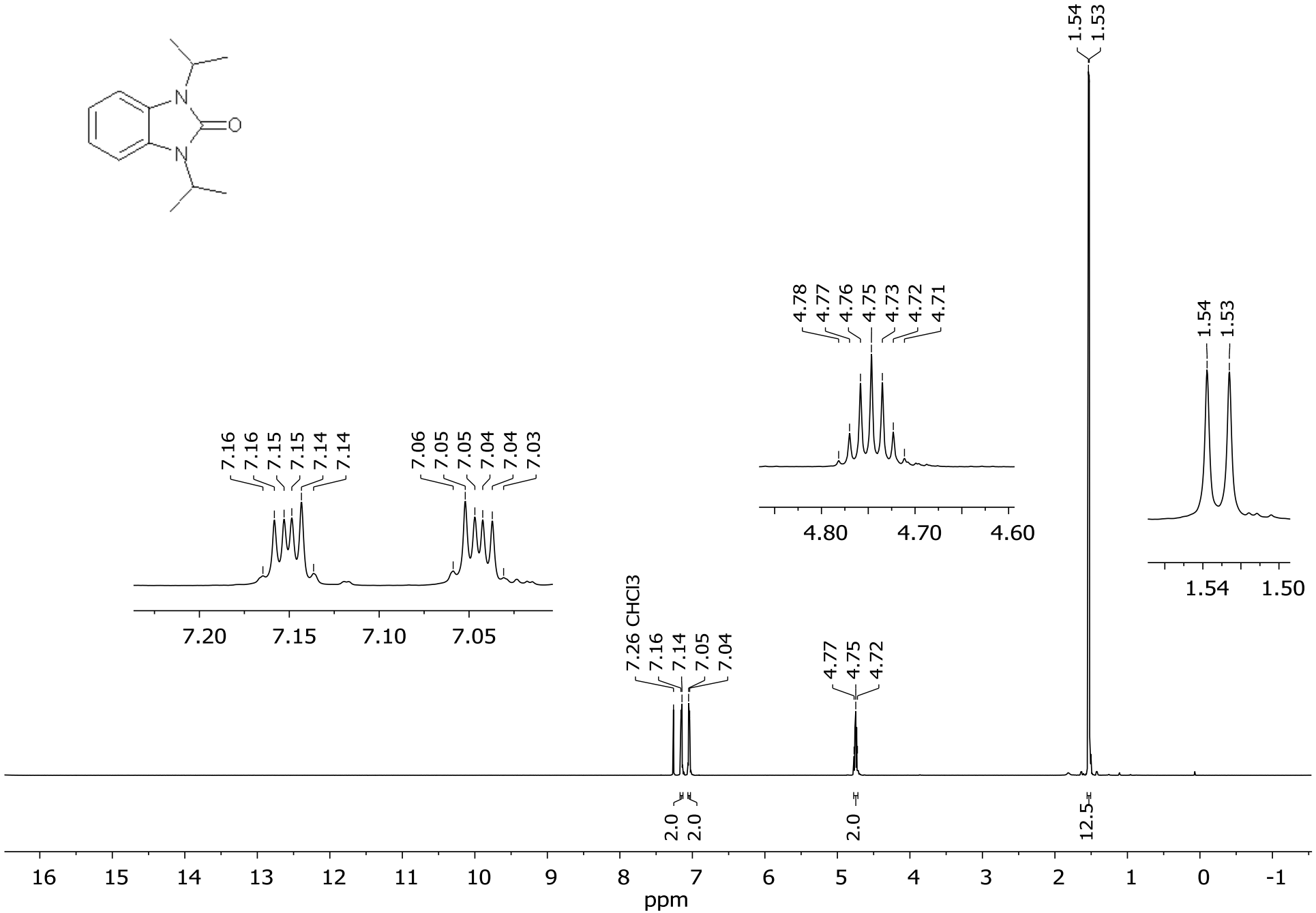

Figure S38. ^{1}H NMR spectrum of compound **7d** ($CDCl_3$, 500 MHz).

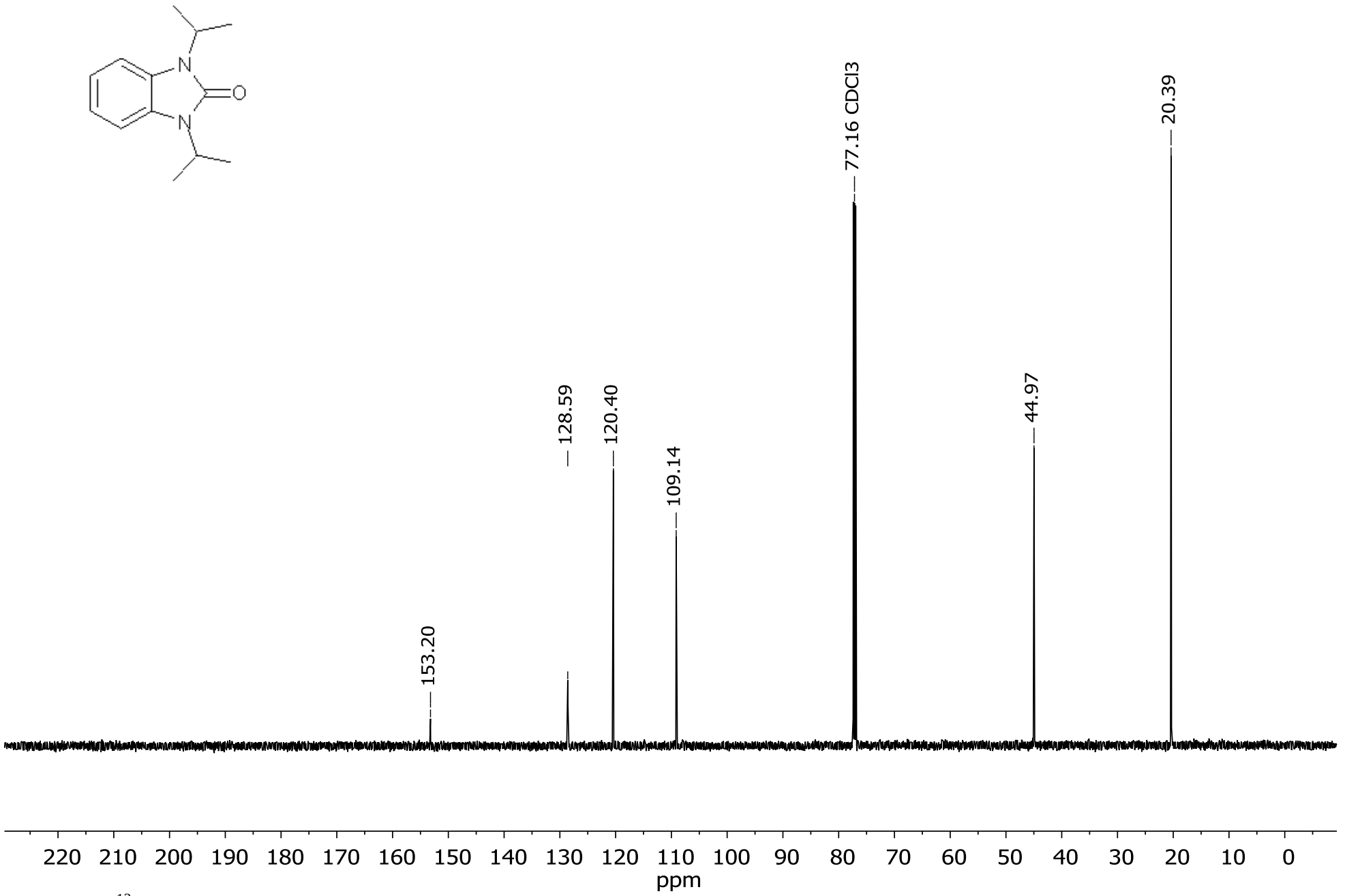

Figure S39. ^{13}C NMR spectrum of compound **7d** ($CDCl_3$, 125 MHz).

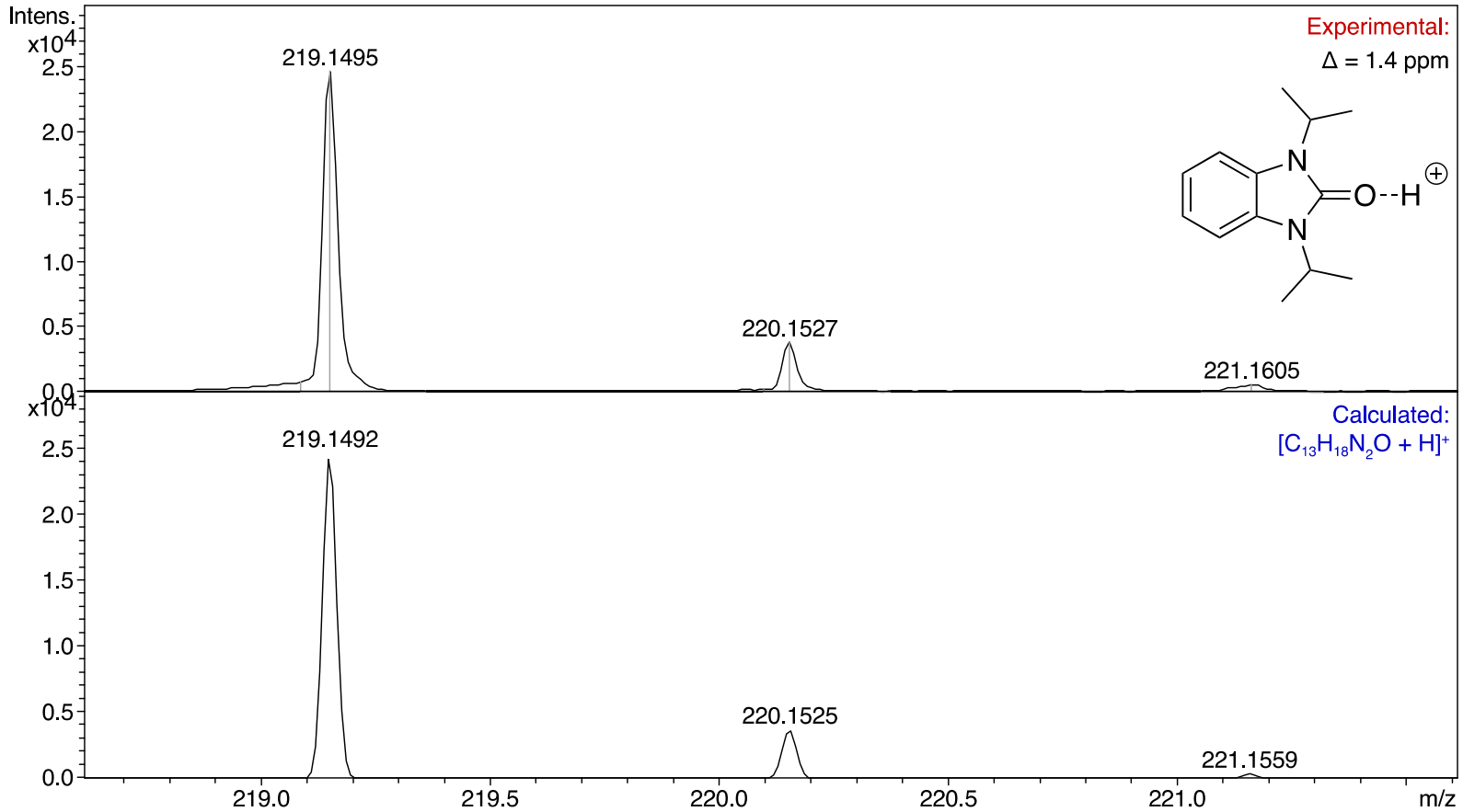

Figure S40. ESI-(+)MS spectrum of compound **7d** in CH_3CN solution expanded to the $[M + H]^+$ region.

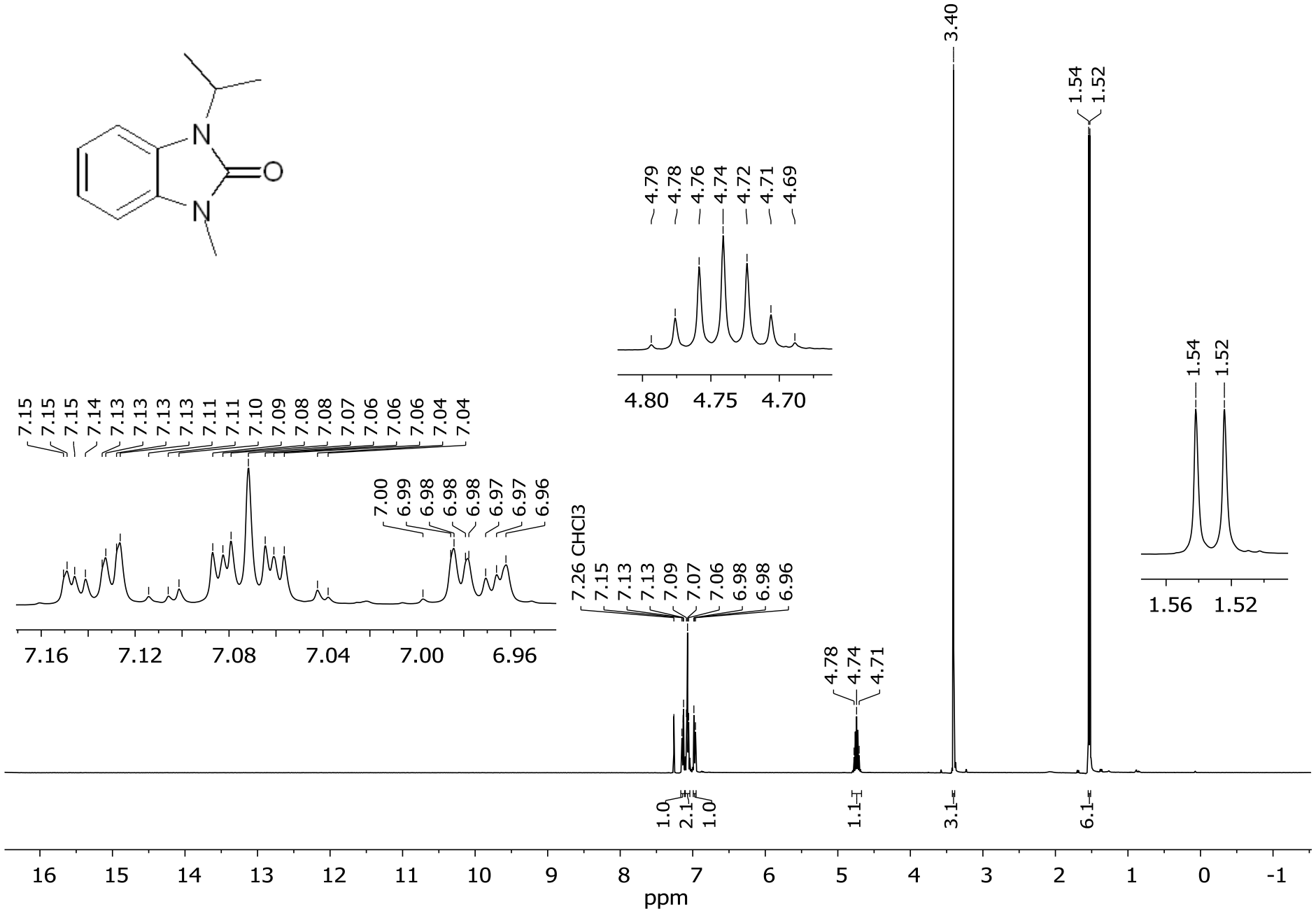

Figure S41. ^{1}H NMR spectrum of compound **7e** ($CDCl_3$, 500 MHz).

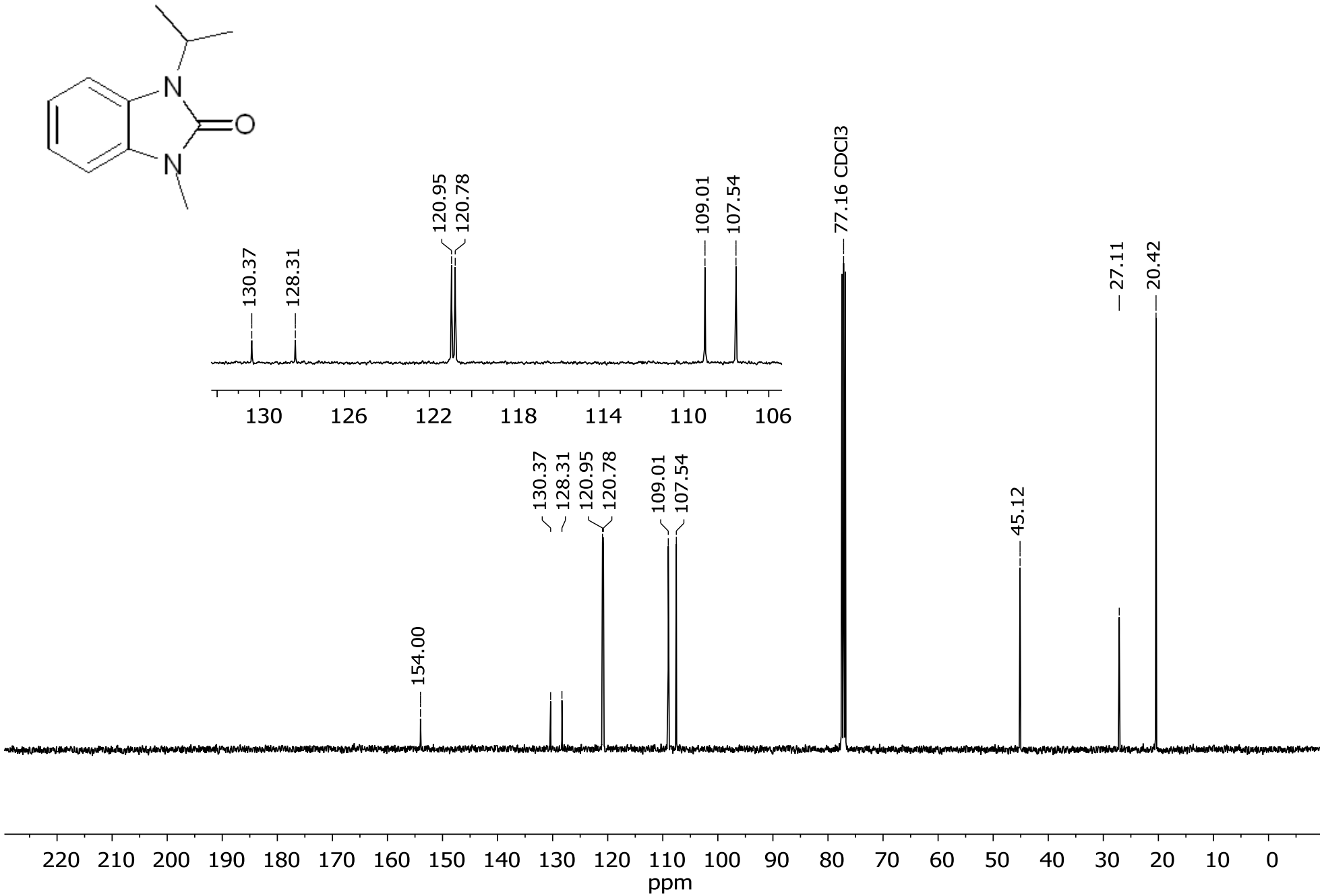

Figure S42. ^{13}C NMR spectrum of compound **7e** ($CDCl_3$, 125 MHz).

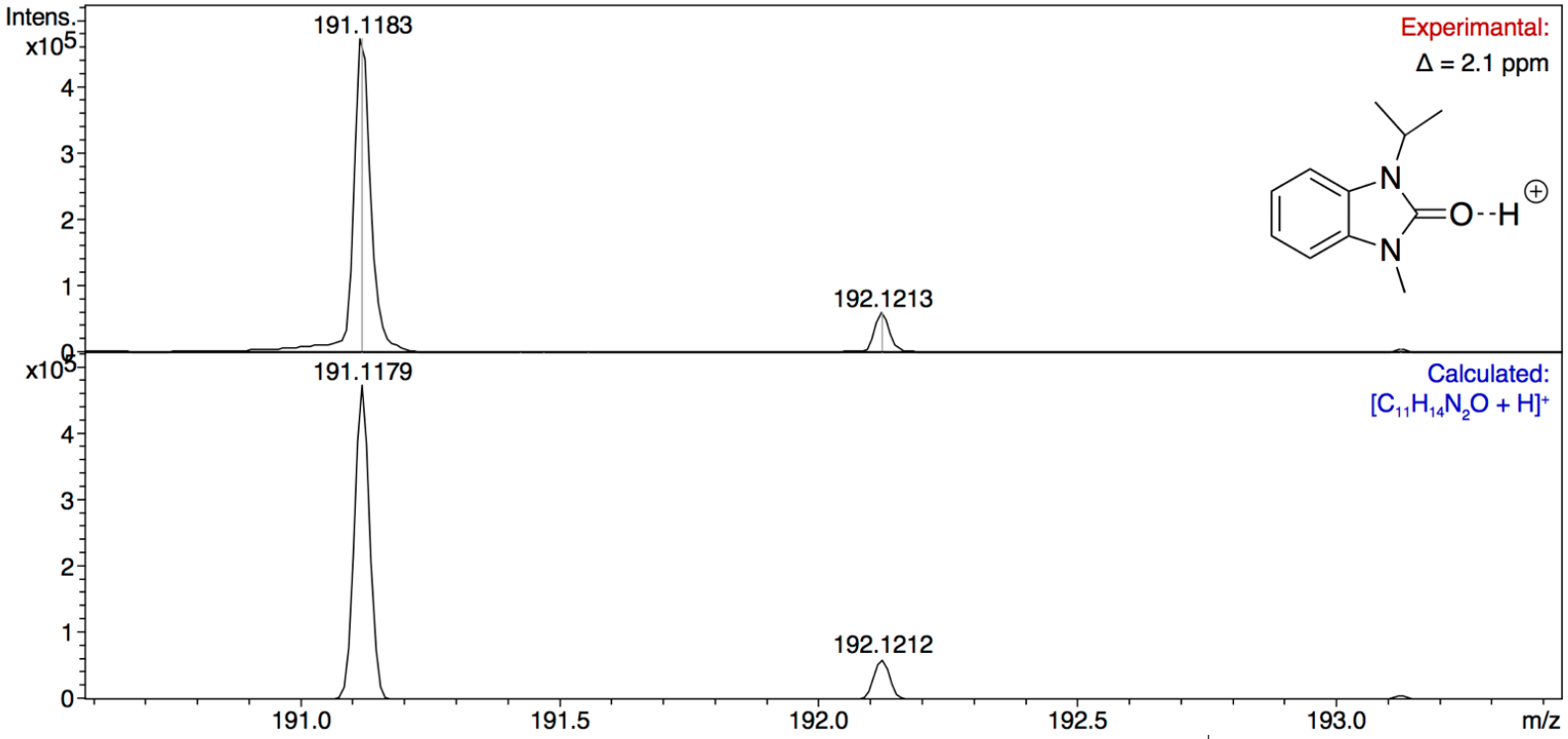

Figure S43. ESI-(+)MS spectrum of compound **7e** in CH_3CN solution expanded to the $[M + H]^+$ region.

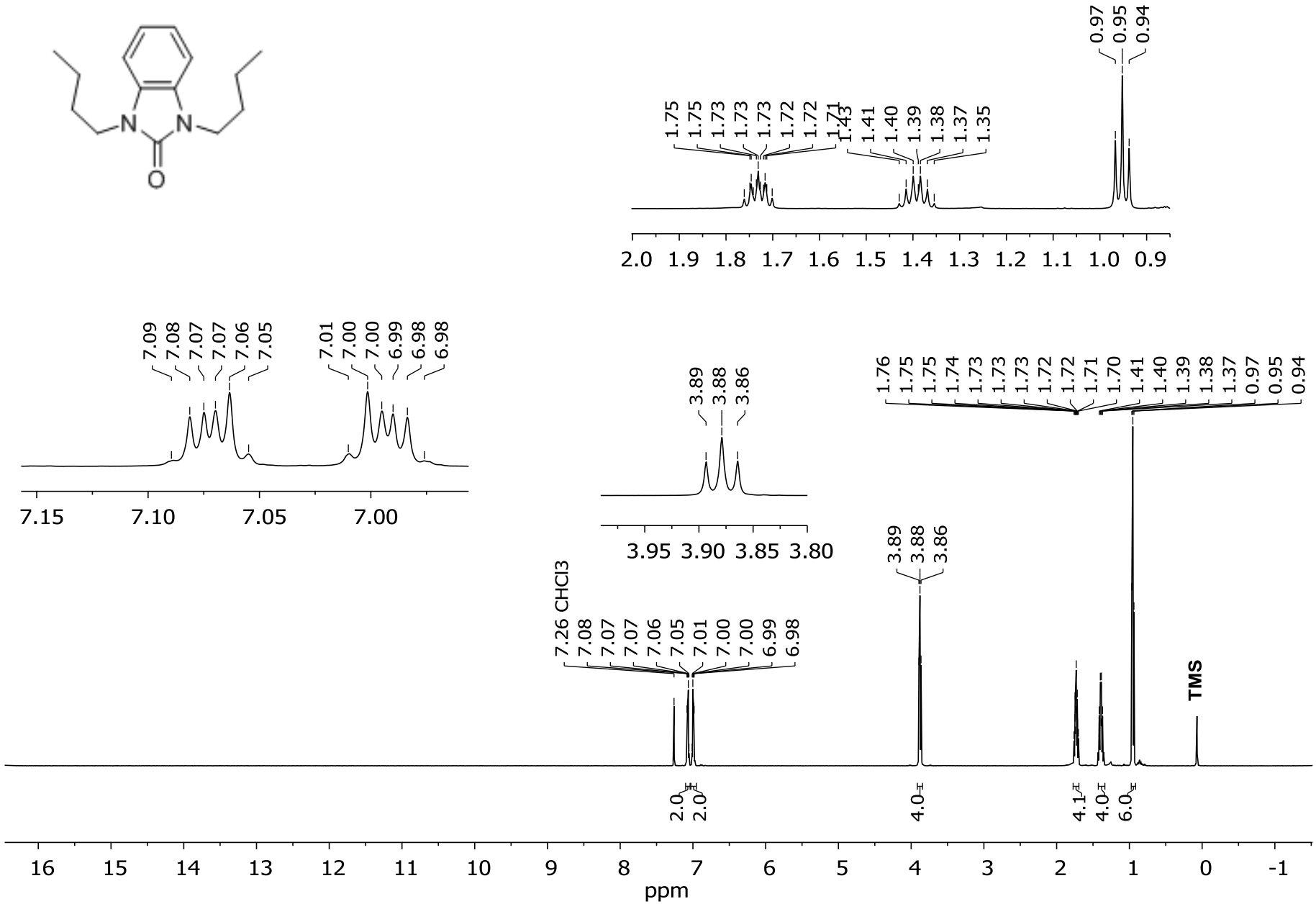

Figure S44. ^{1}H NMR spectrum of compound **7f** ($CDCl_3$, 500 MHz).

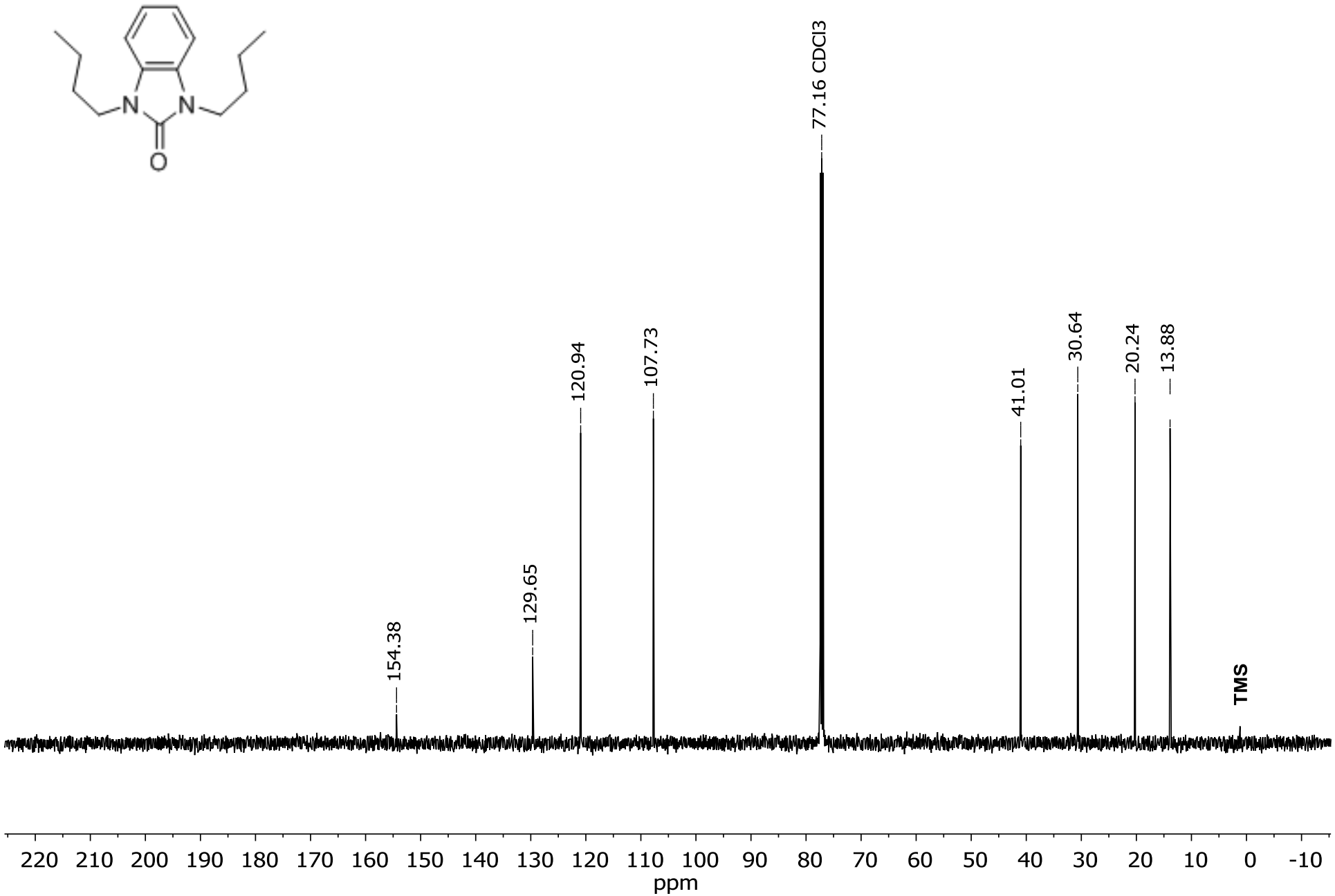

Figure S45. ^{13}C NMR spectrum of compound **7f** ($CDCl_3$, 125 MHz).

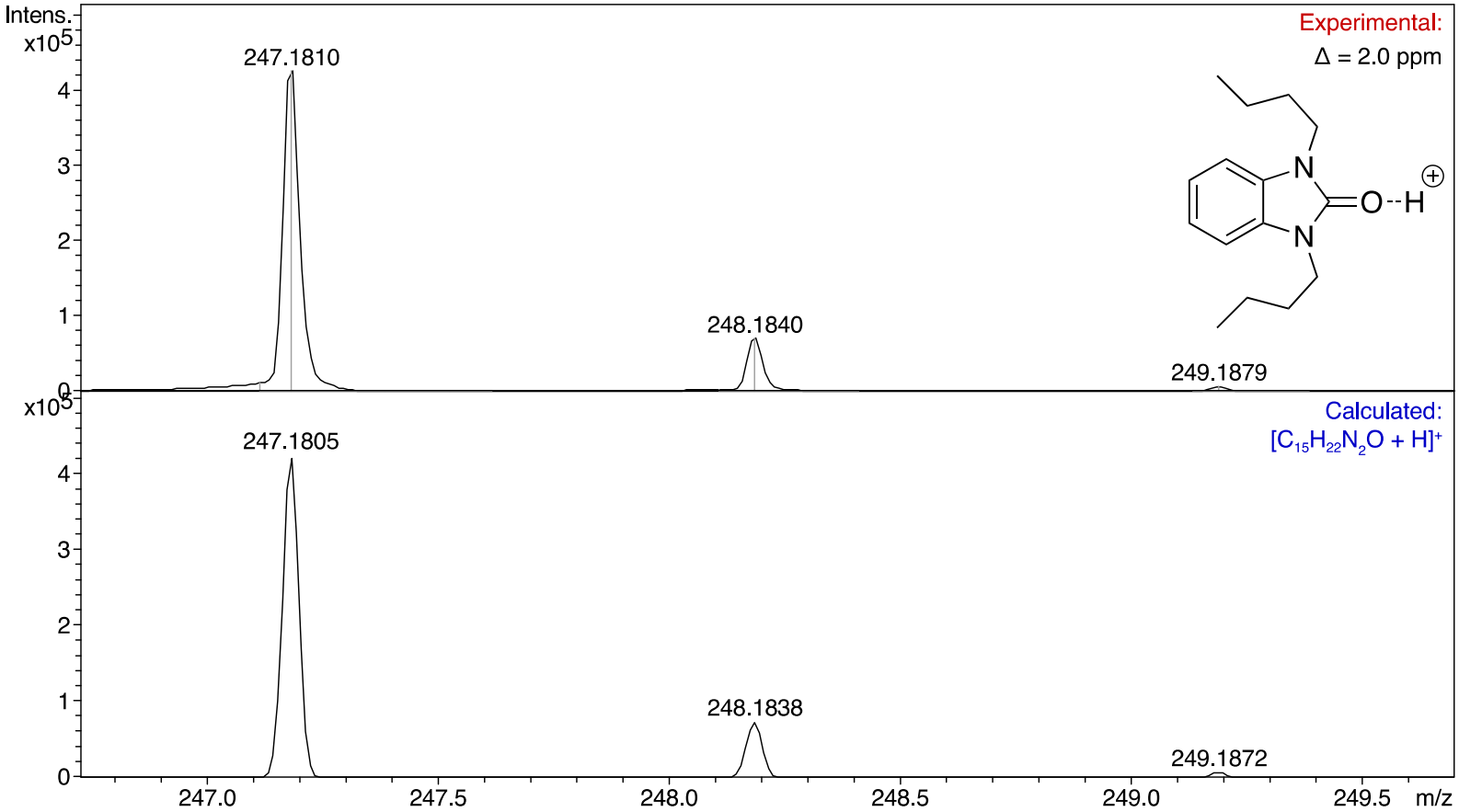

Figure S46. ESI-(+)MS spectrum of compound **7f** in CH_3CN solution expanded to the $[M + H]^+$ region.

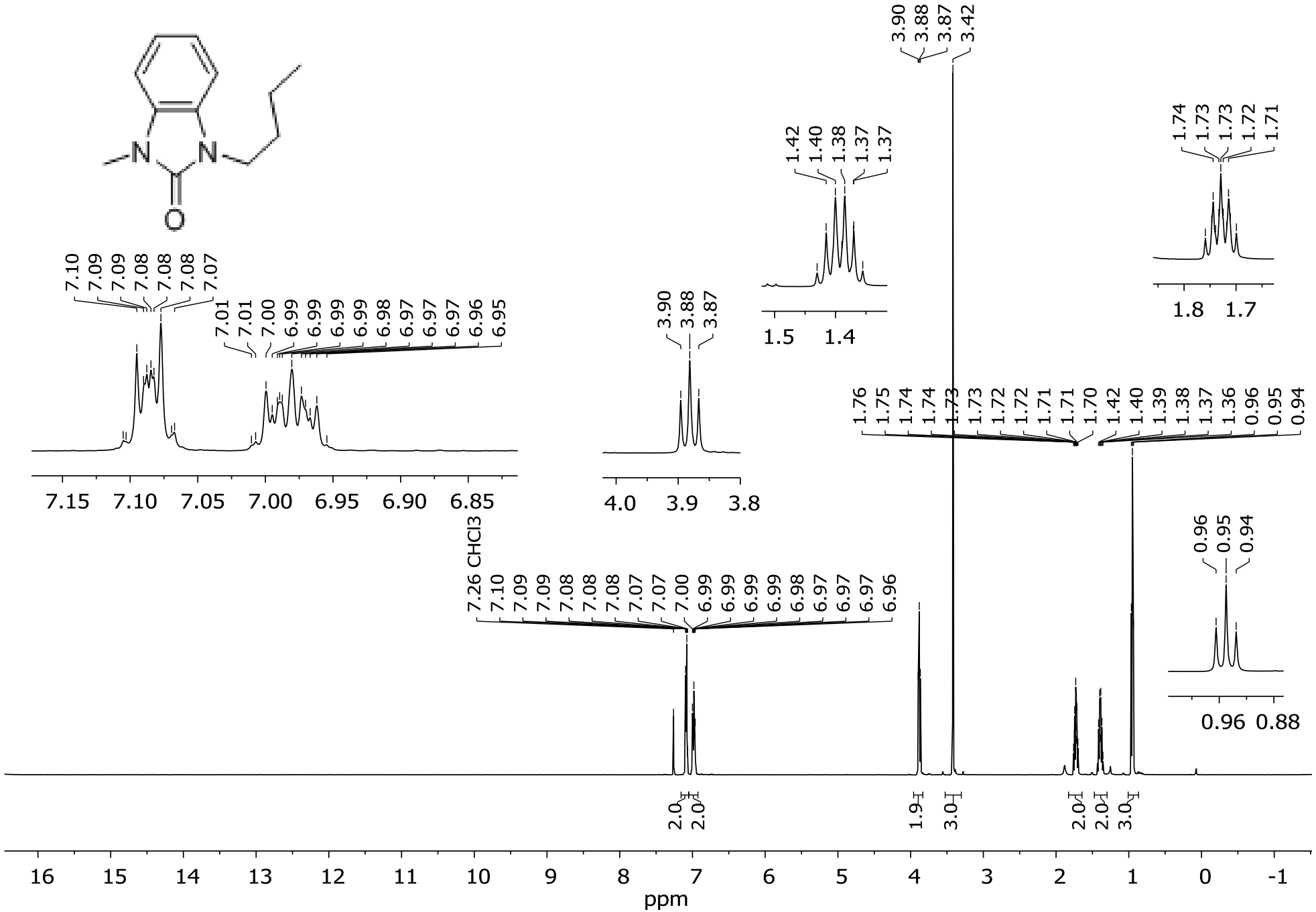

Figure S47. ^{1}H NMR spectrum of compound **7g** ($CDCl_3$, 500 MHz).

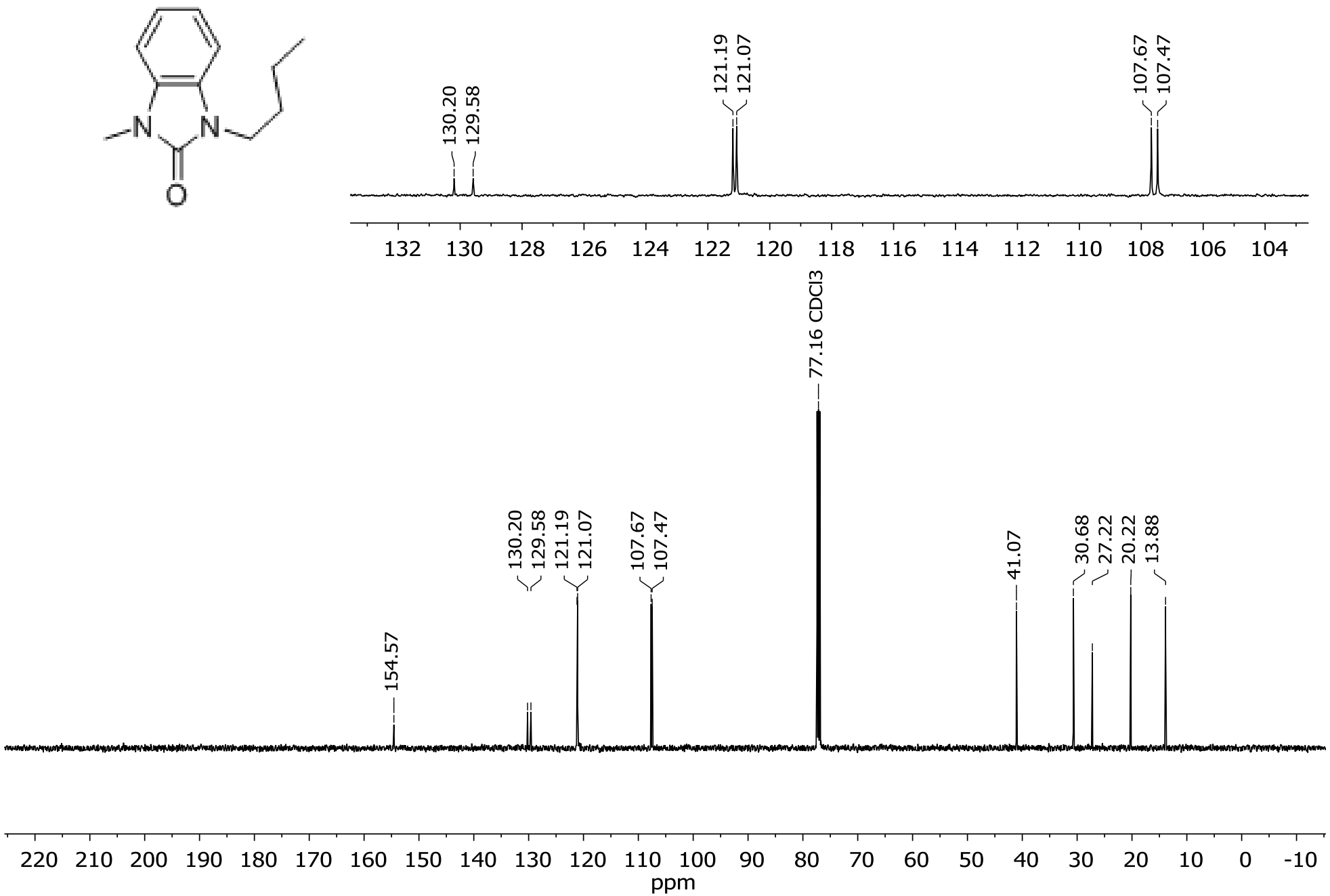

Figure S48. ^{13}C NMR spectrum of compound **7g** ($CDCl_3$, 125 MHz).

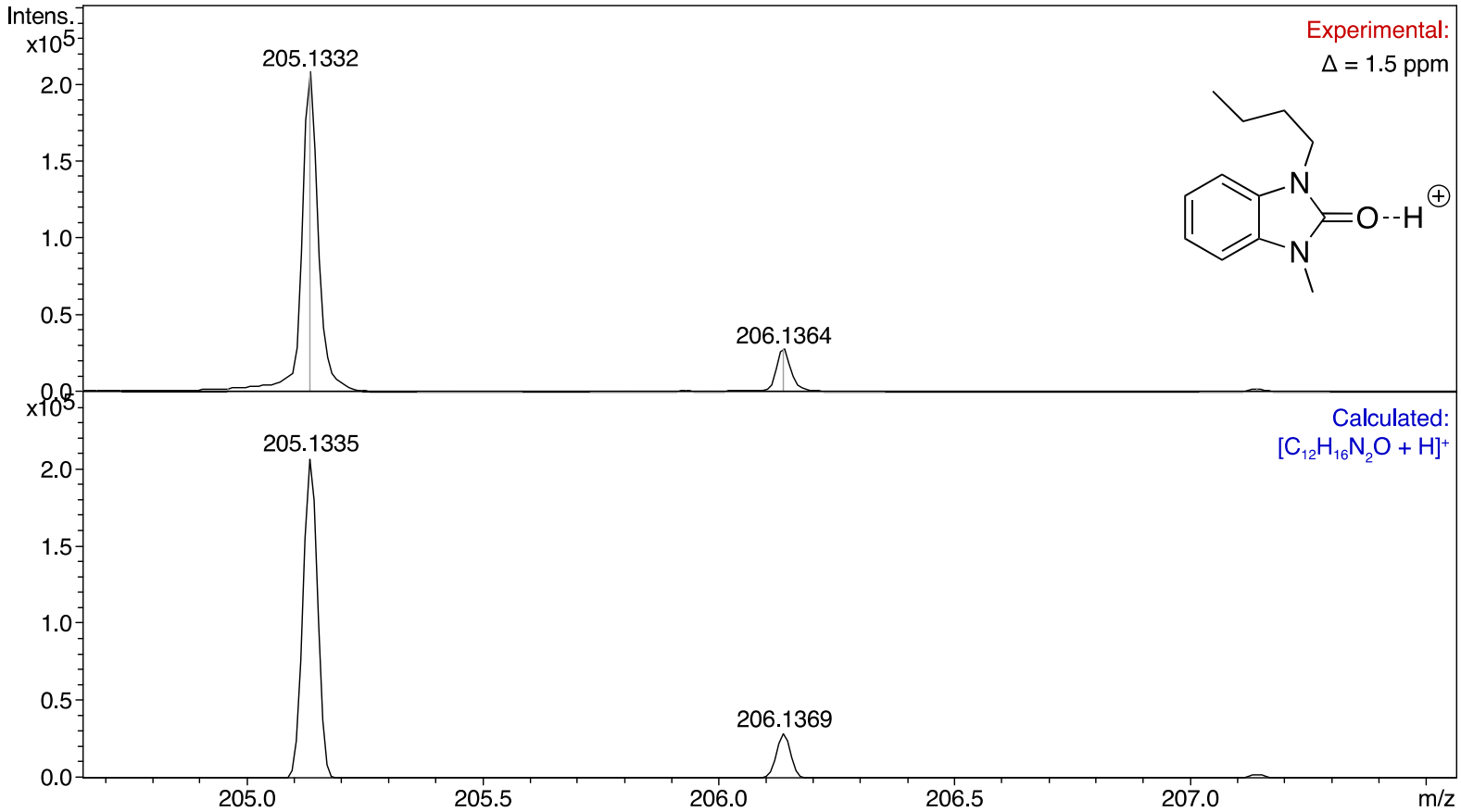

Figure S49. ESI-(+)MS spectrum of compound **7g** in CH_3CN solution expanded to the $[M + H]^+$ region.

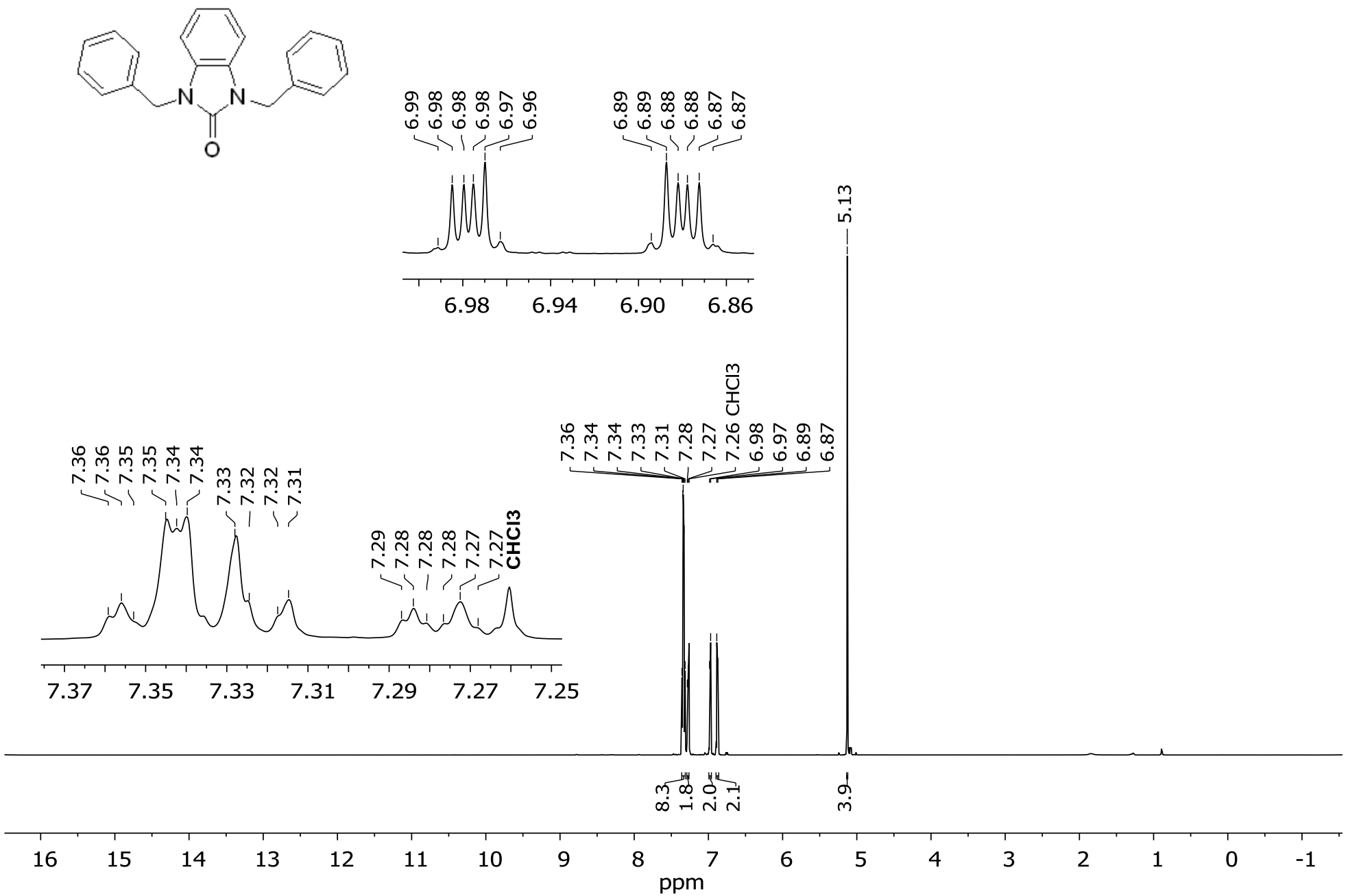

Figure S50. ^{1}H NMR spectrum of compound **7h** ($CDCl_3$, 500 MHz).

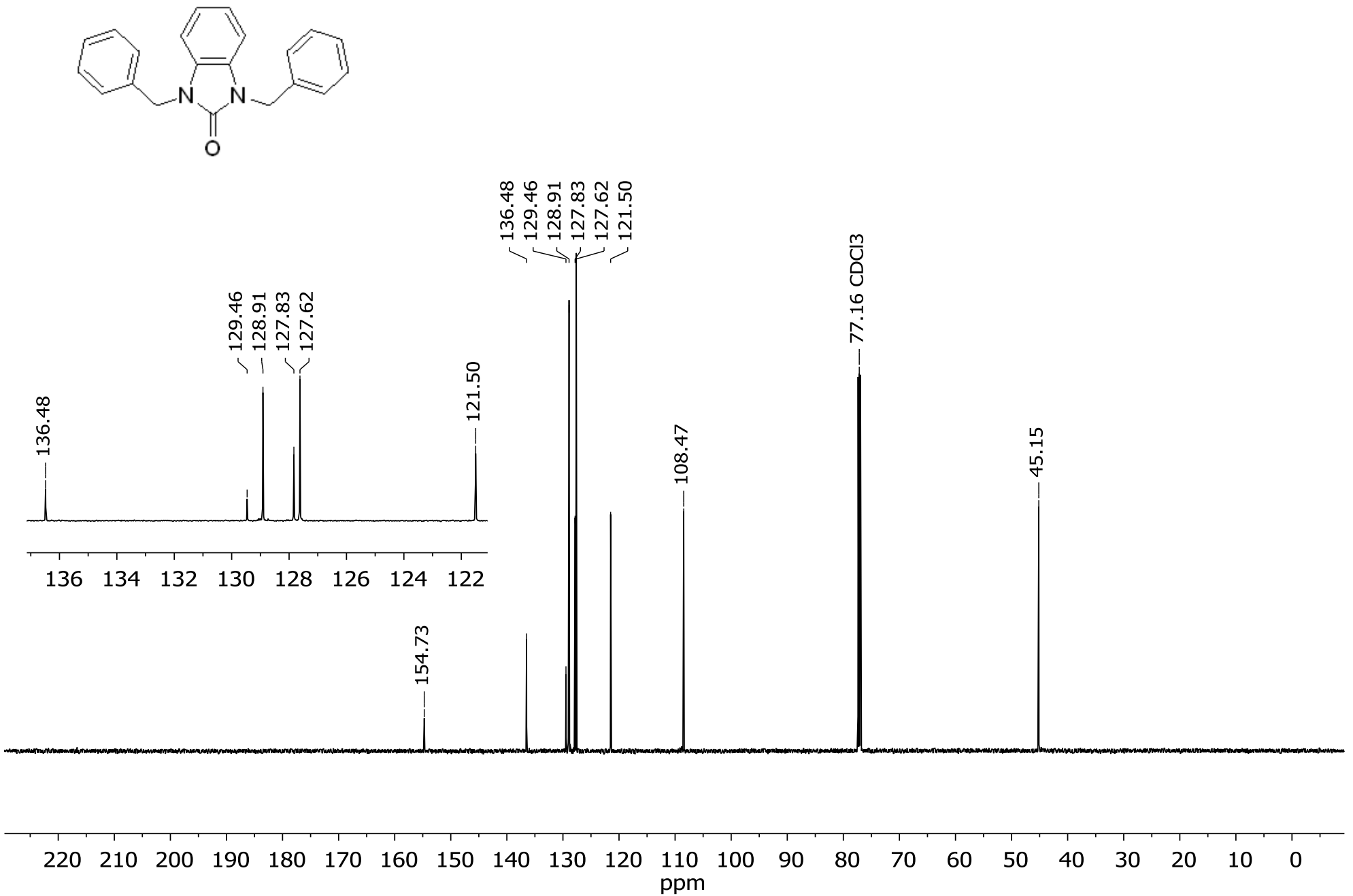

Figure S51. ^{13}C NMR spectrum of compound **7h** ($CDCl_3$, 125 MHz).

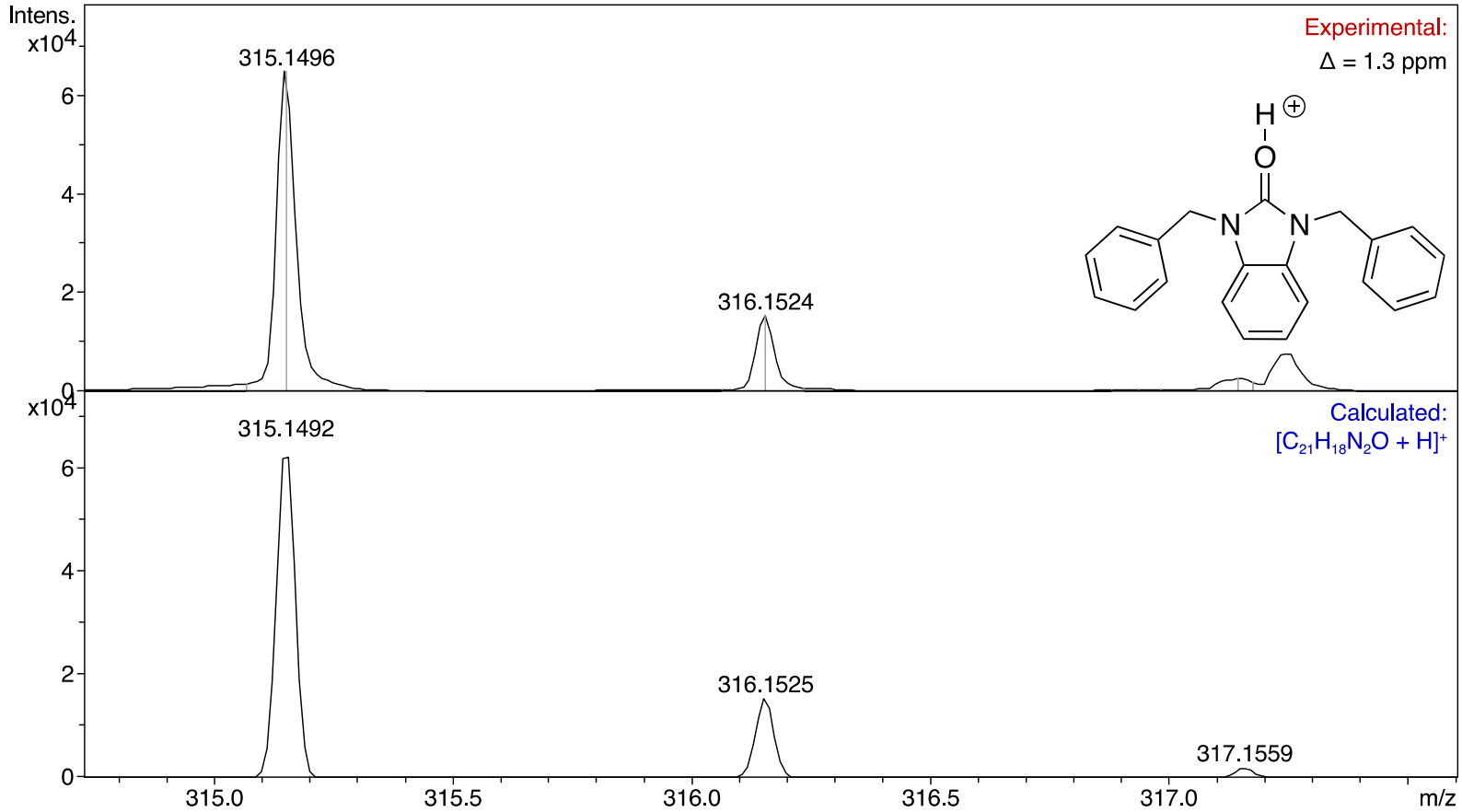

Figure S52. ESI-(+)MS spectrum of compound **7h** in CH_3CN solution expanded to the $[M + H]^+$ region.

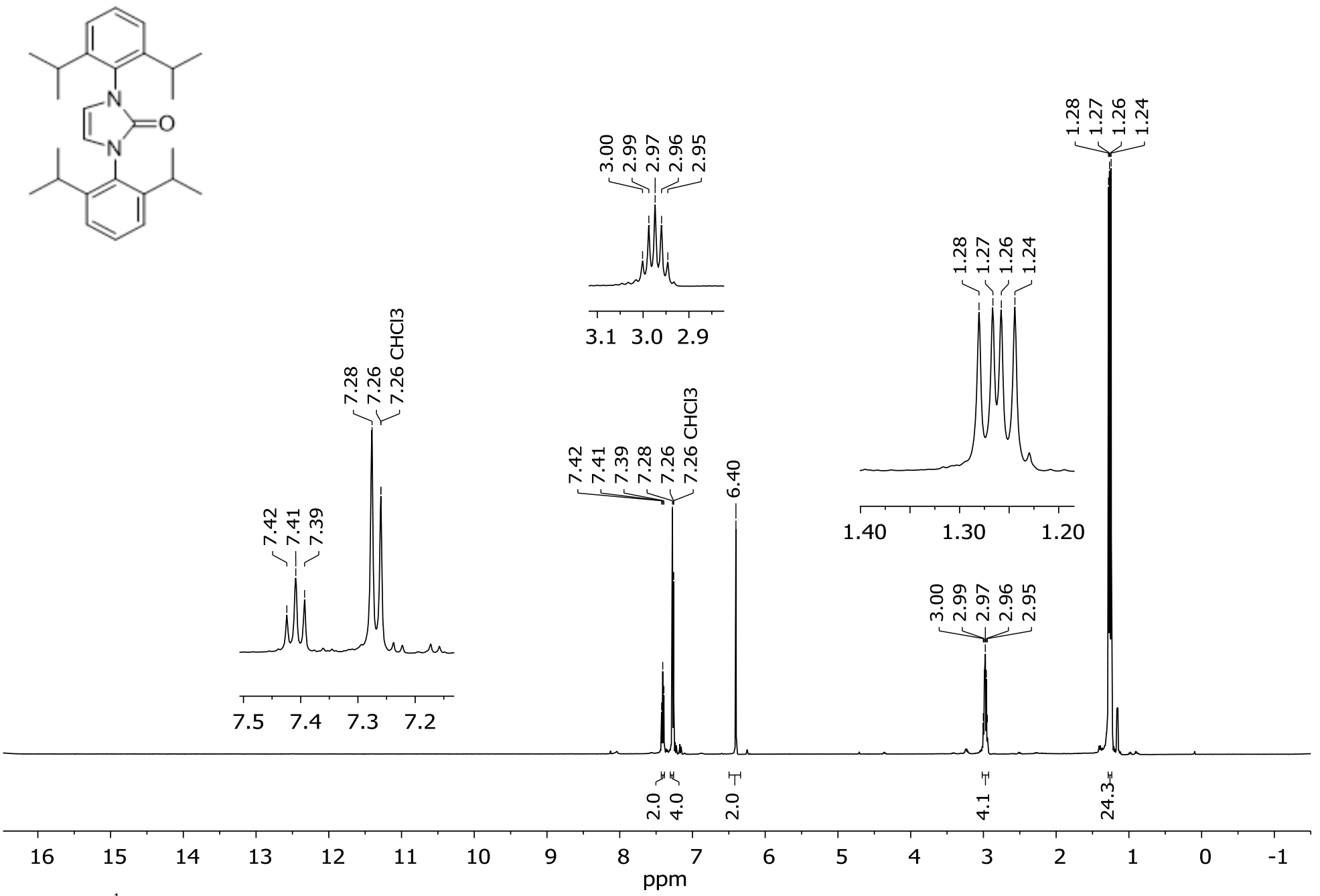

Figure S53. ^{1}H NMR spectrum of compound **7i** ($CDCl_3$, 500 MHz).

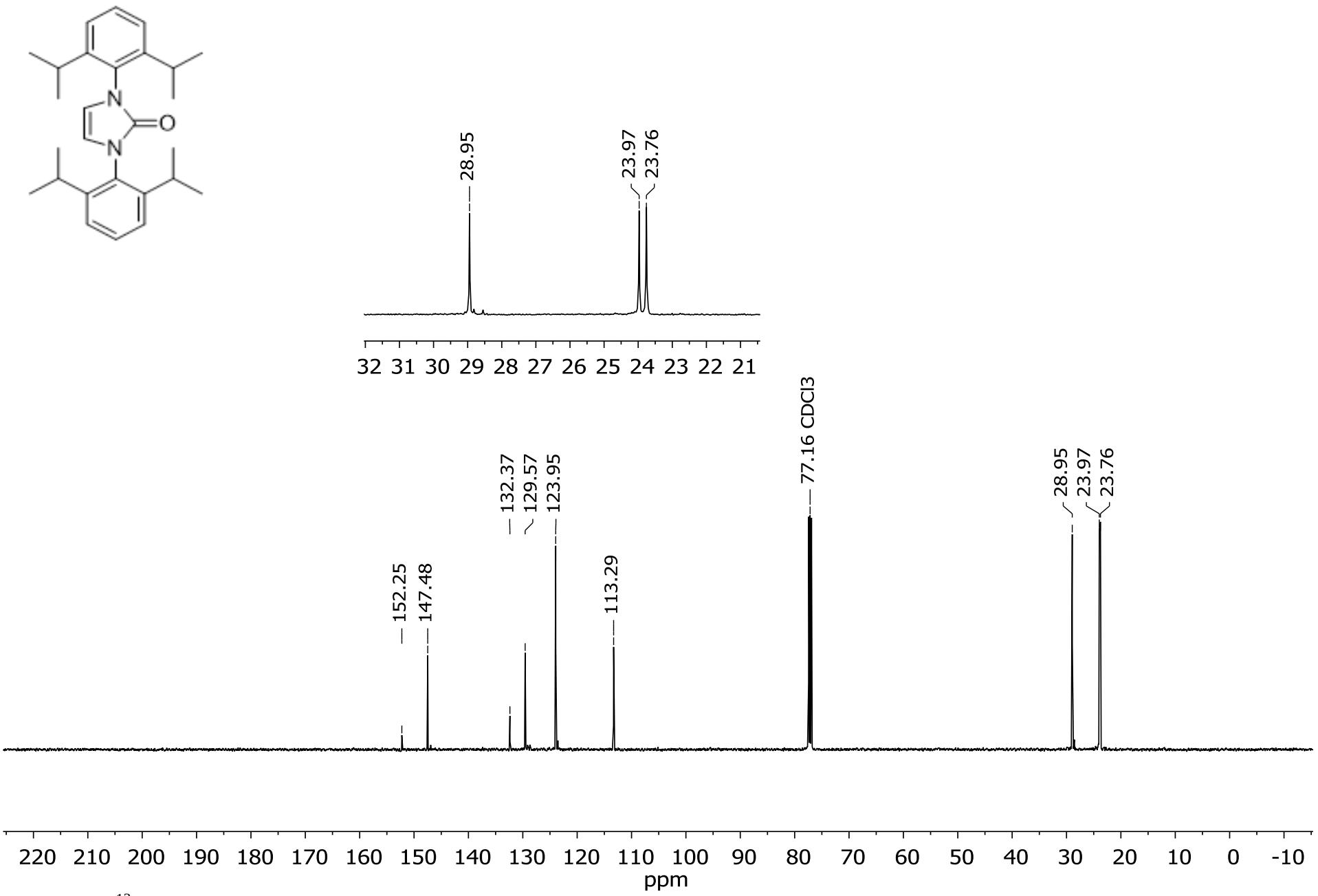

Figure S54. ^{13}C NMR spectrum of compound **7i** ($CDCl_3$, 125 MHz).

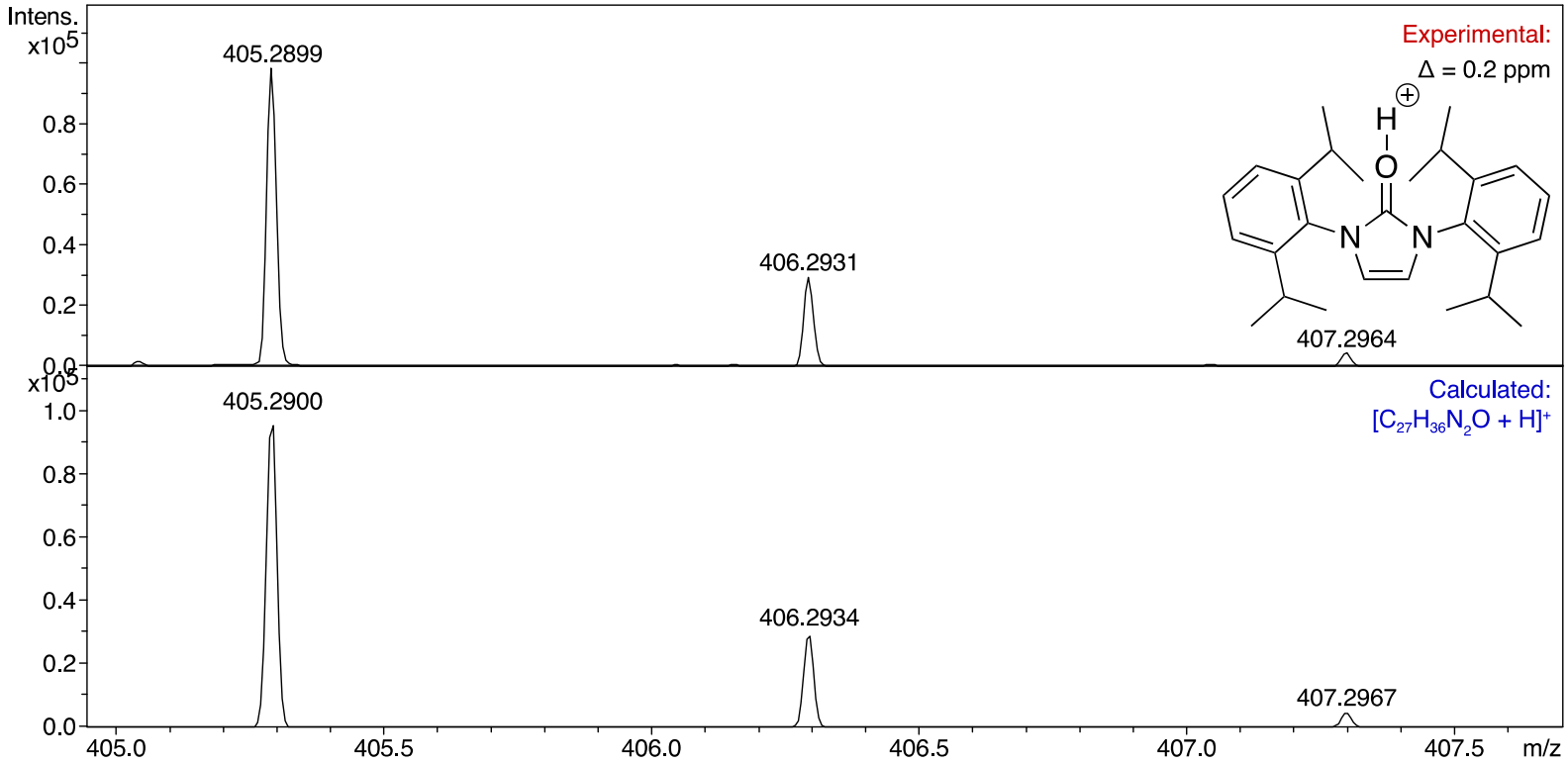

Figure S55. ESI-(+)MS spectrum of compound **7i** in CH_3CN solution expanded to the $[M + H]^+$ region.

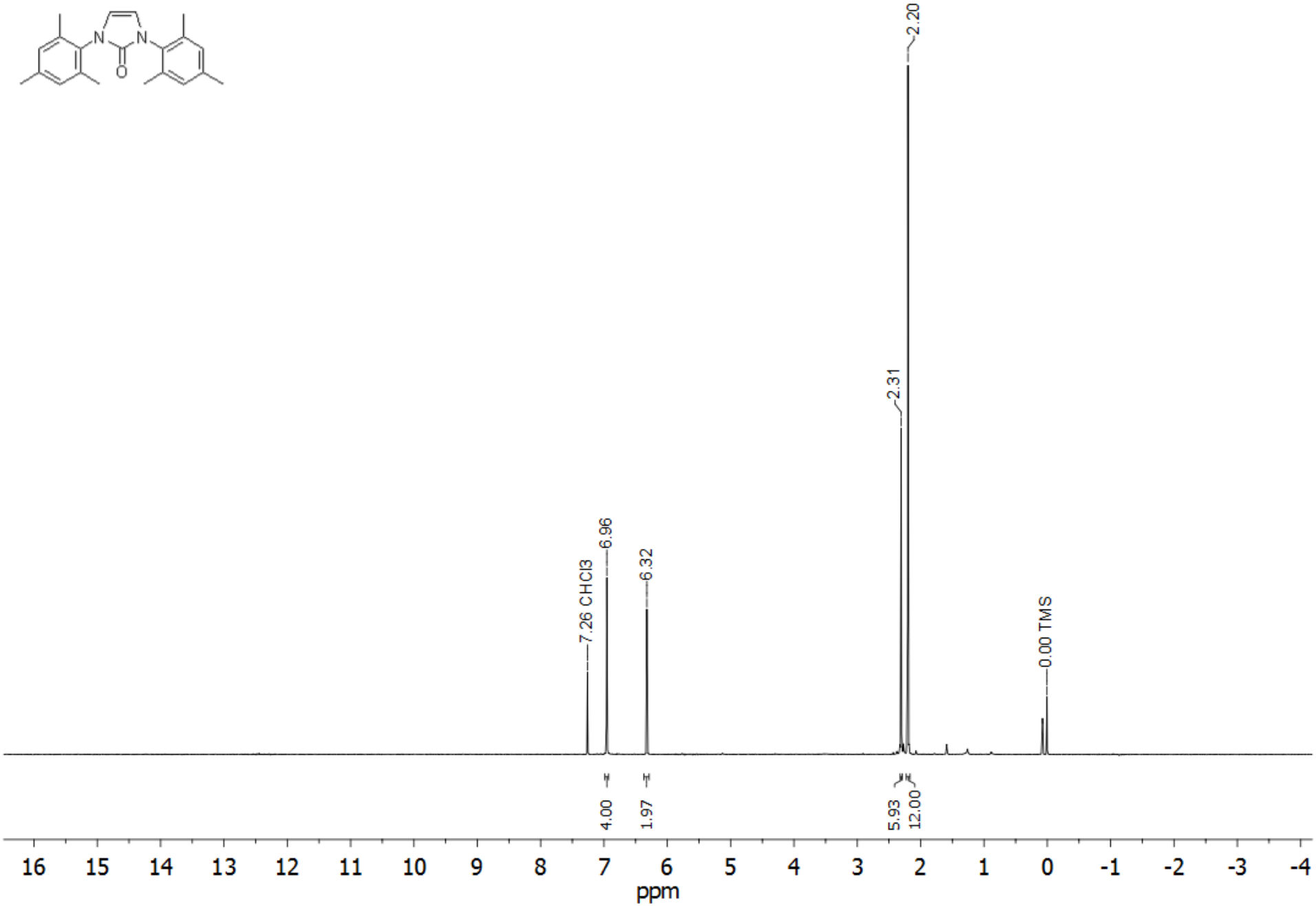

Figure S56. ^{1}H NMR spectrum of compound **7j** ($CDCl_3$, 500 MHz).

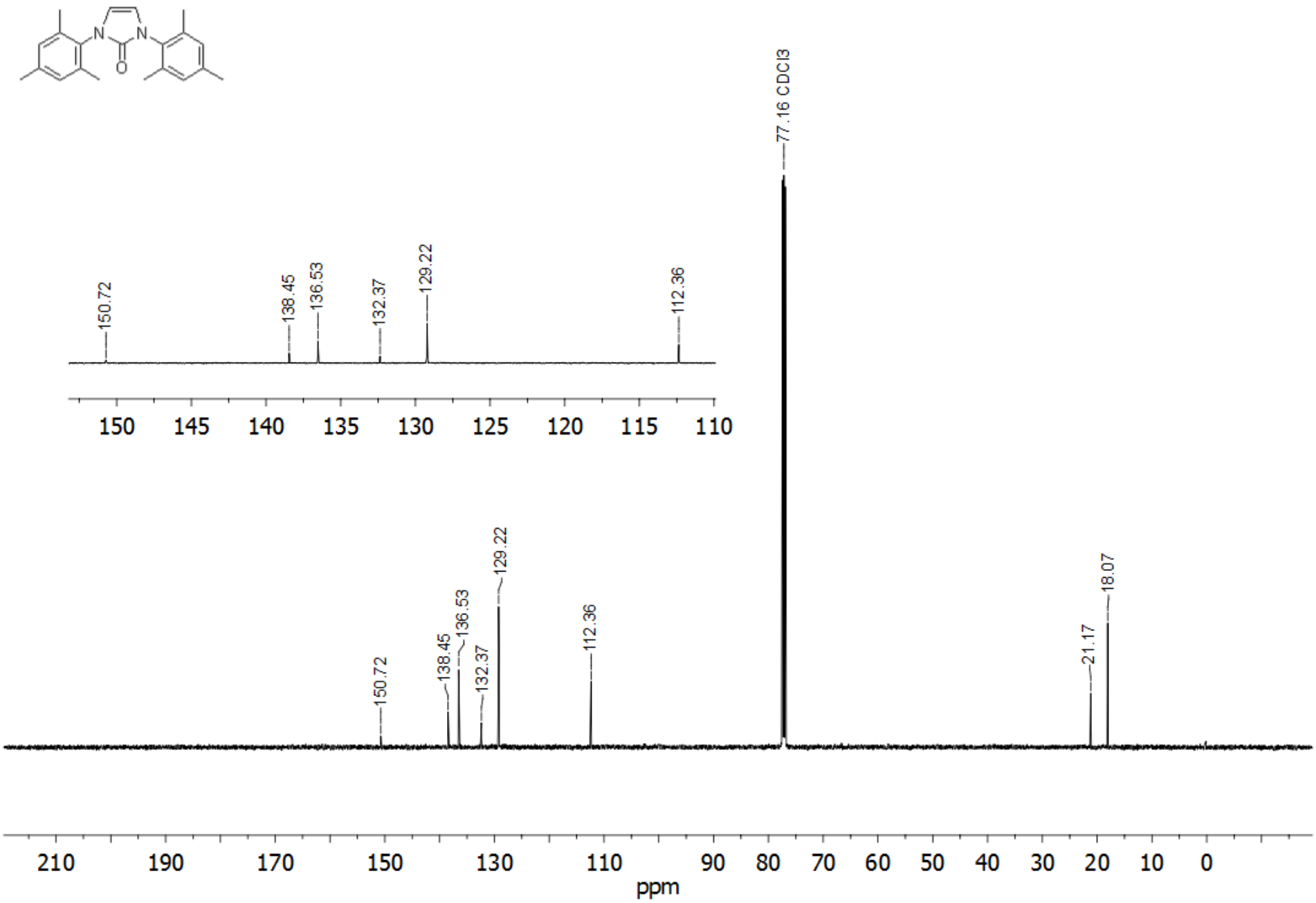

Figure S57. ^{13}C NMR spectrum of compound **7j** ($CDCl_3$, 125 MHz).

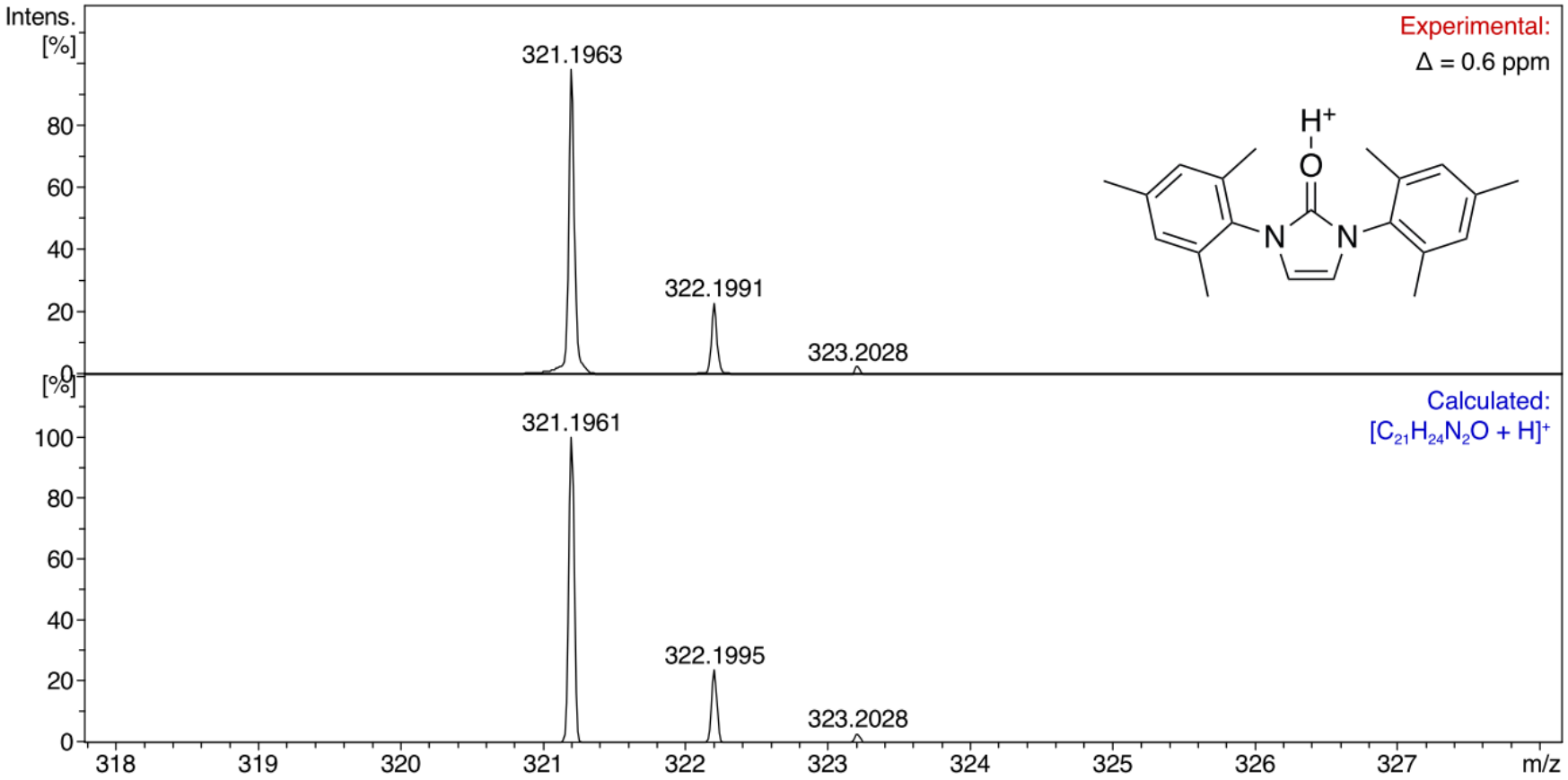

Figure S58. ESI-(+)MS spectrum of compound **7j** in CH_3CN solution expanded to the $[M + H]^+$ region.

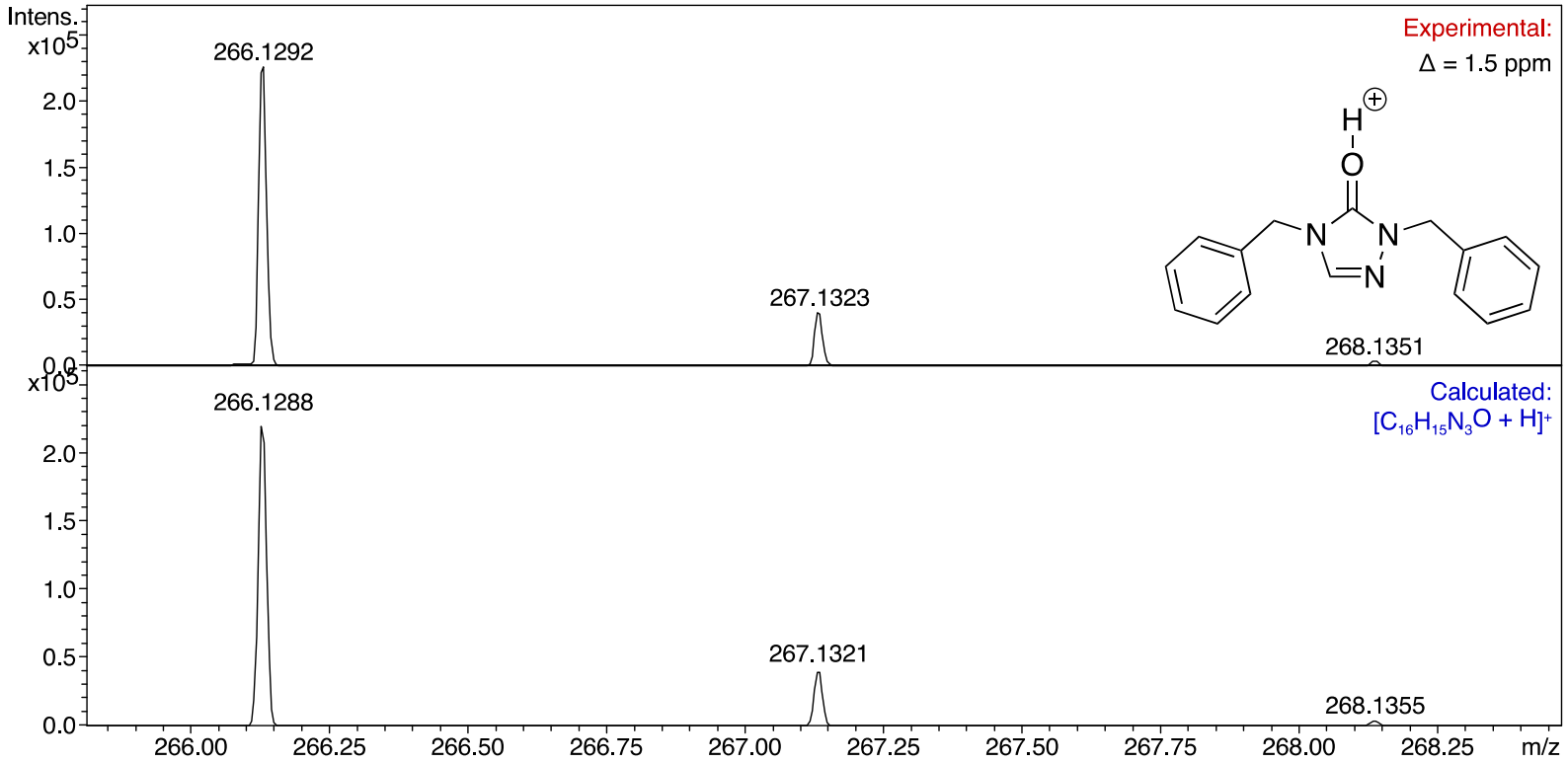

Figure S59. ESI-(+)MS spectrum of compound **7n** in CH_3CN solution, expanded to the $[M + H]^+$ region.

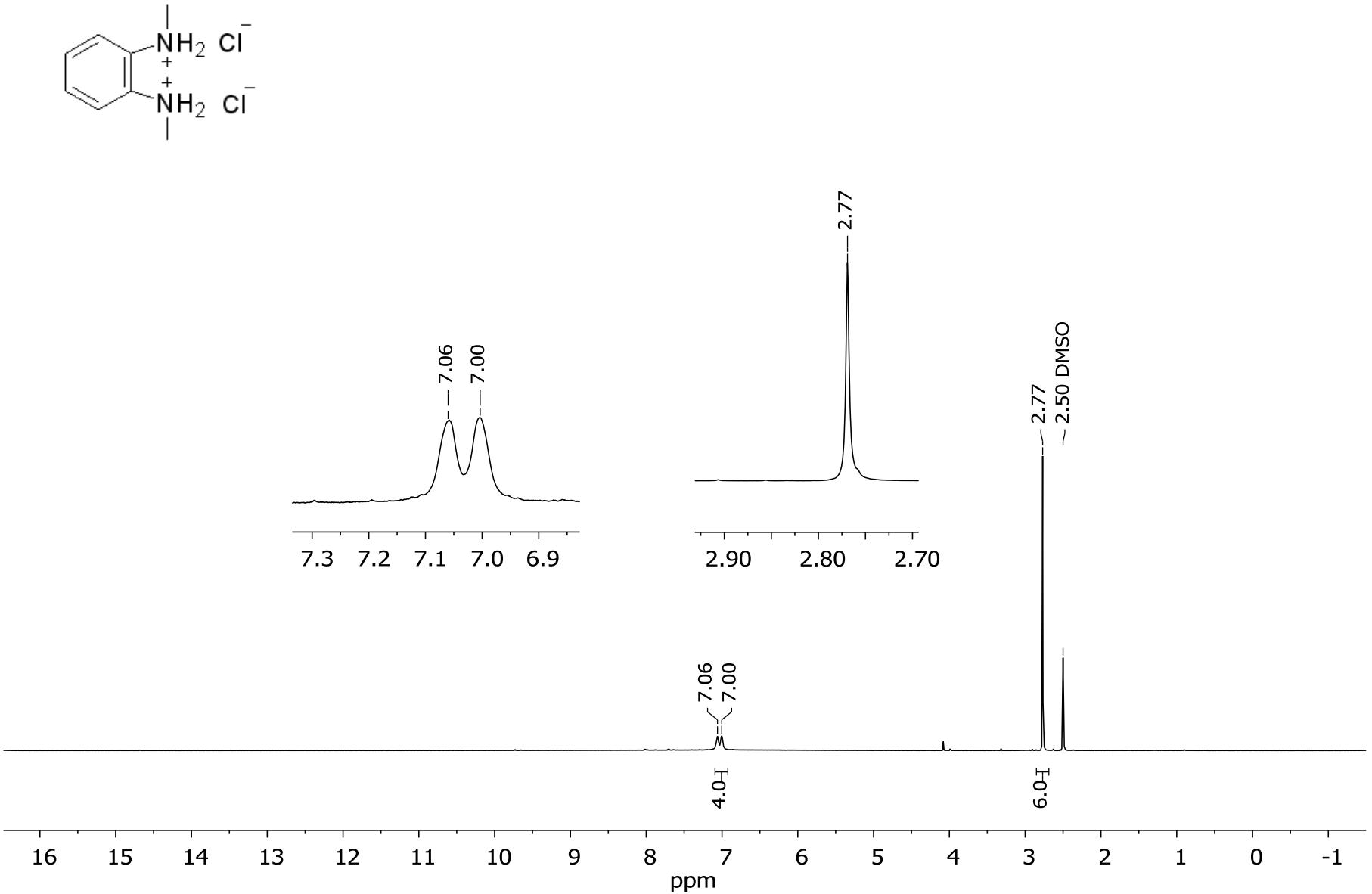

Figure S60. ^{1}H NMR spectrum of dihydrochloride of compound **8a×2HCl** (DMSO-d_6, 500 MHz).

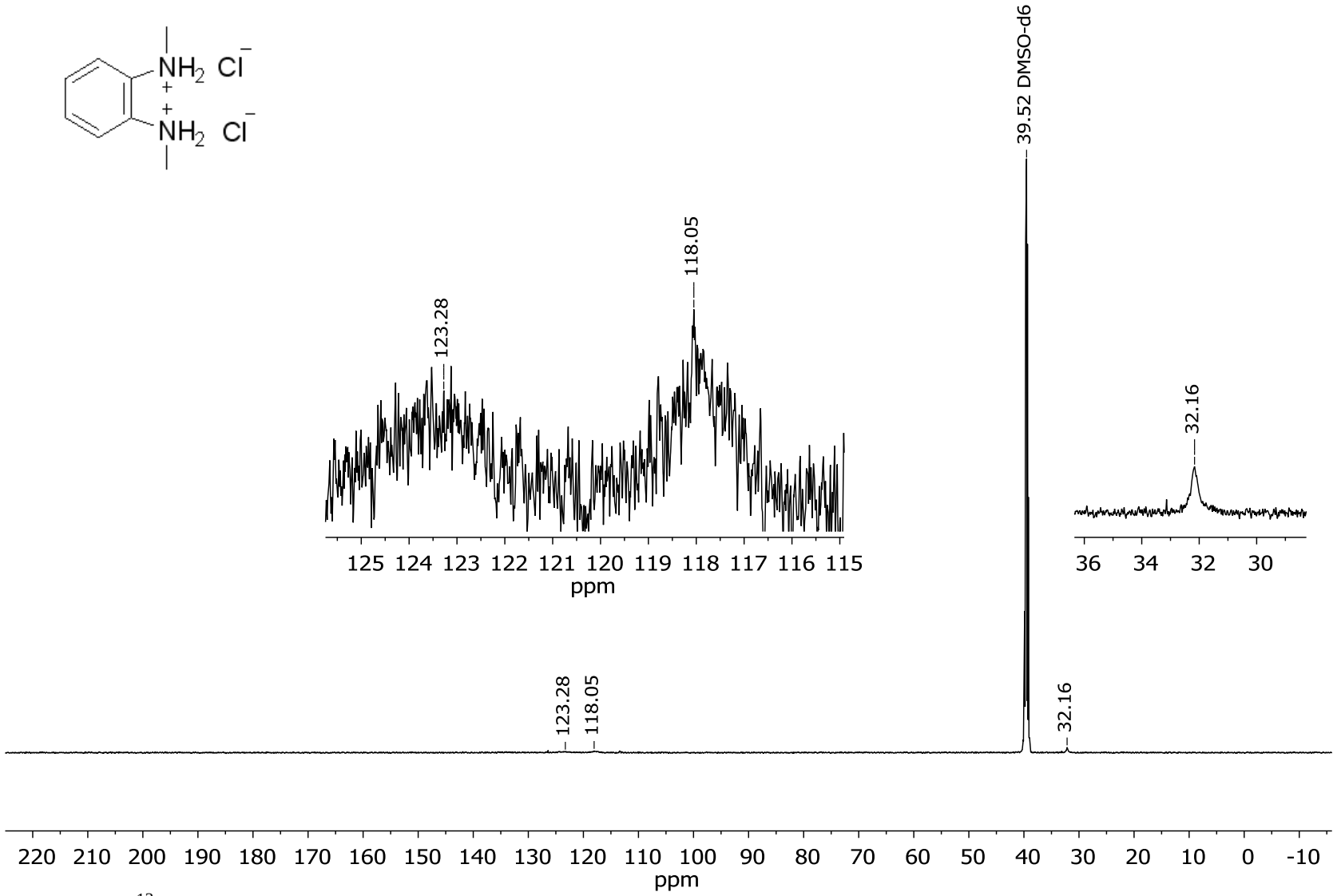

Figure S61. ^{13}C NMR spectrum of dihydrochloride of compound **8a×2HCl** (DMSO-d_6, 125 MHz)

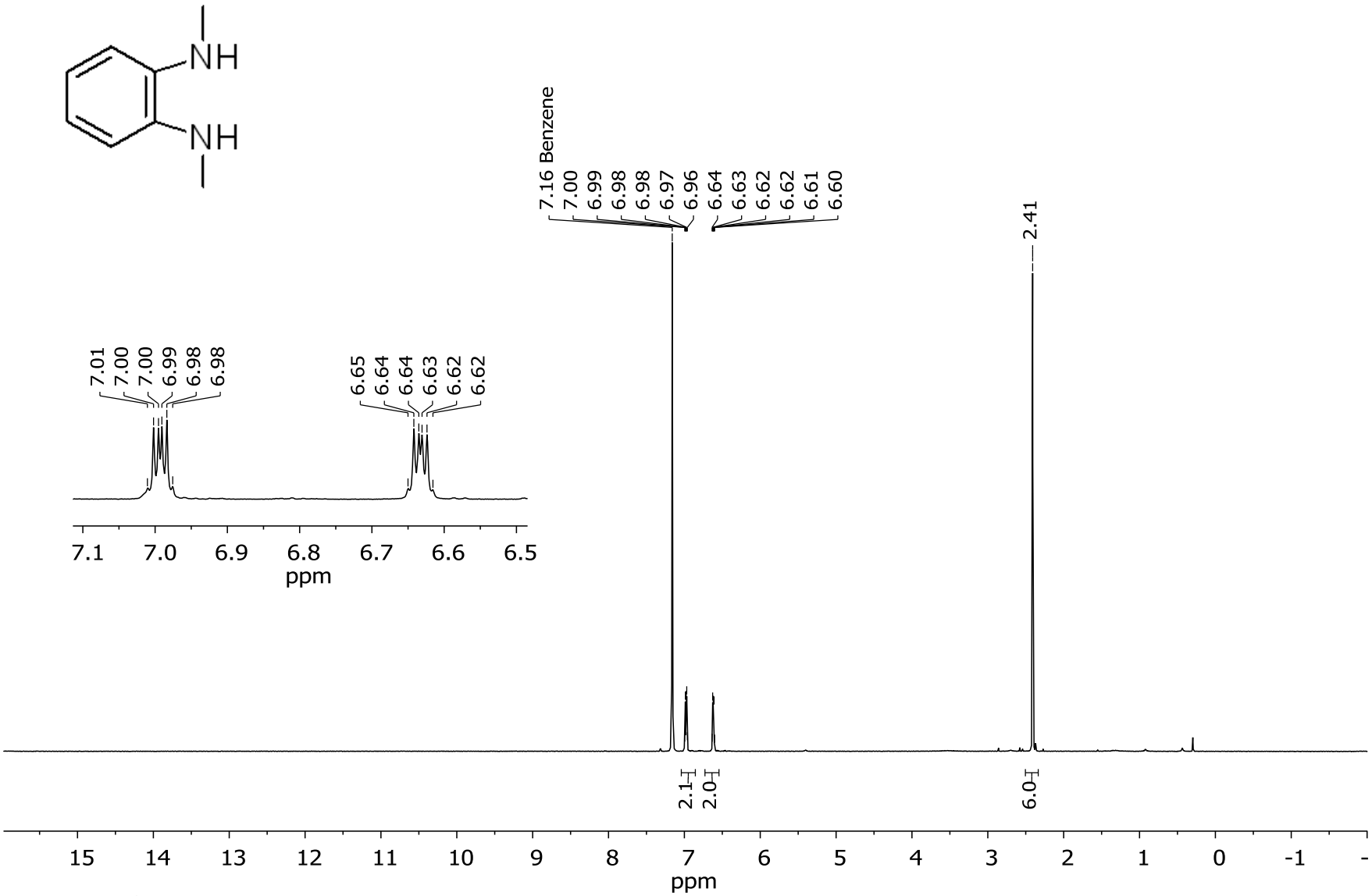

Figure S62. ^{1}H NMR spectrum of compound **8a** (C_6D_6, 500 MHz)

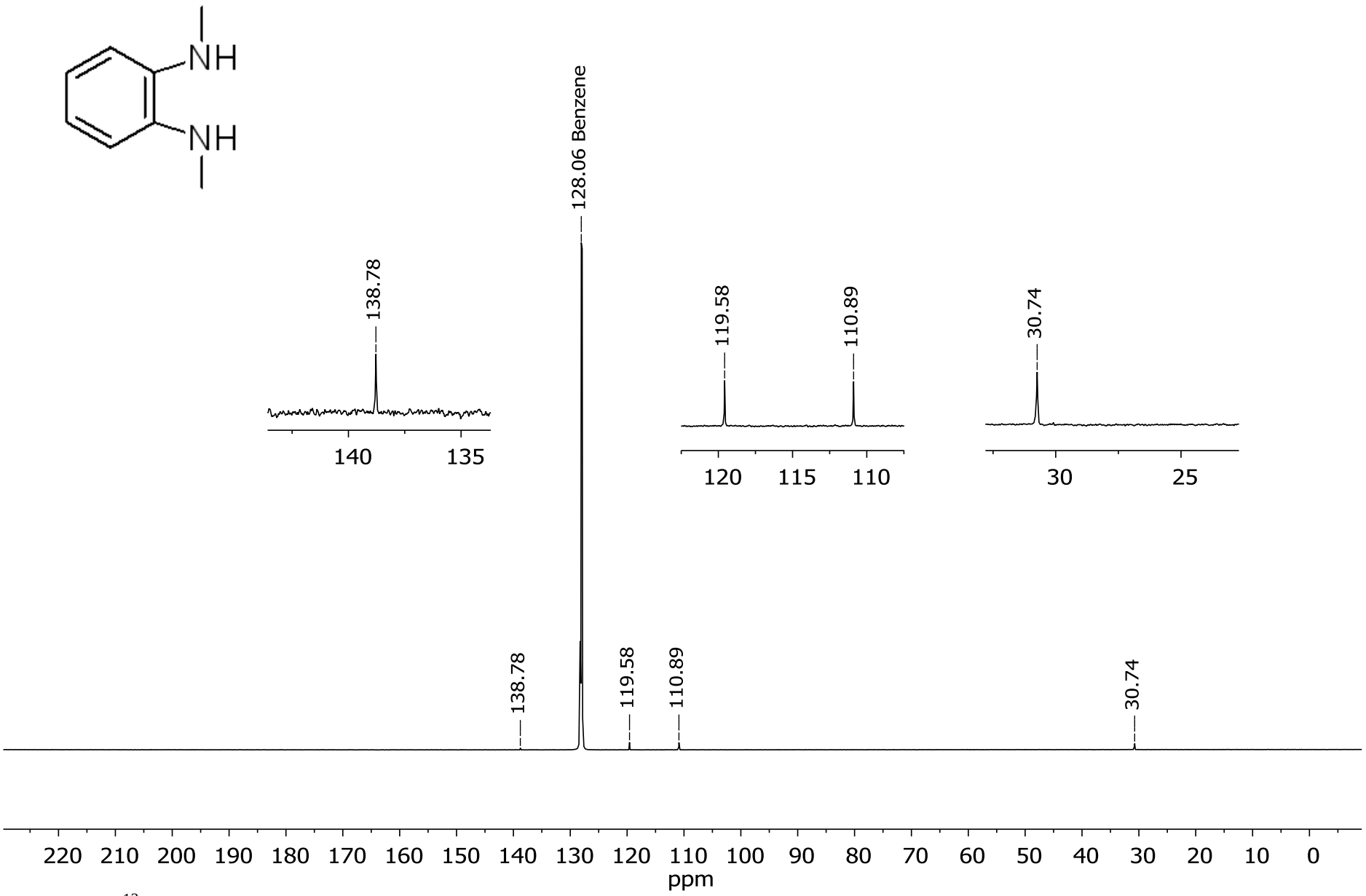

Figure S63. ^{13}C NMR spectrum of compound **8a** (C_6D_6, 125 MHz)

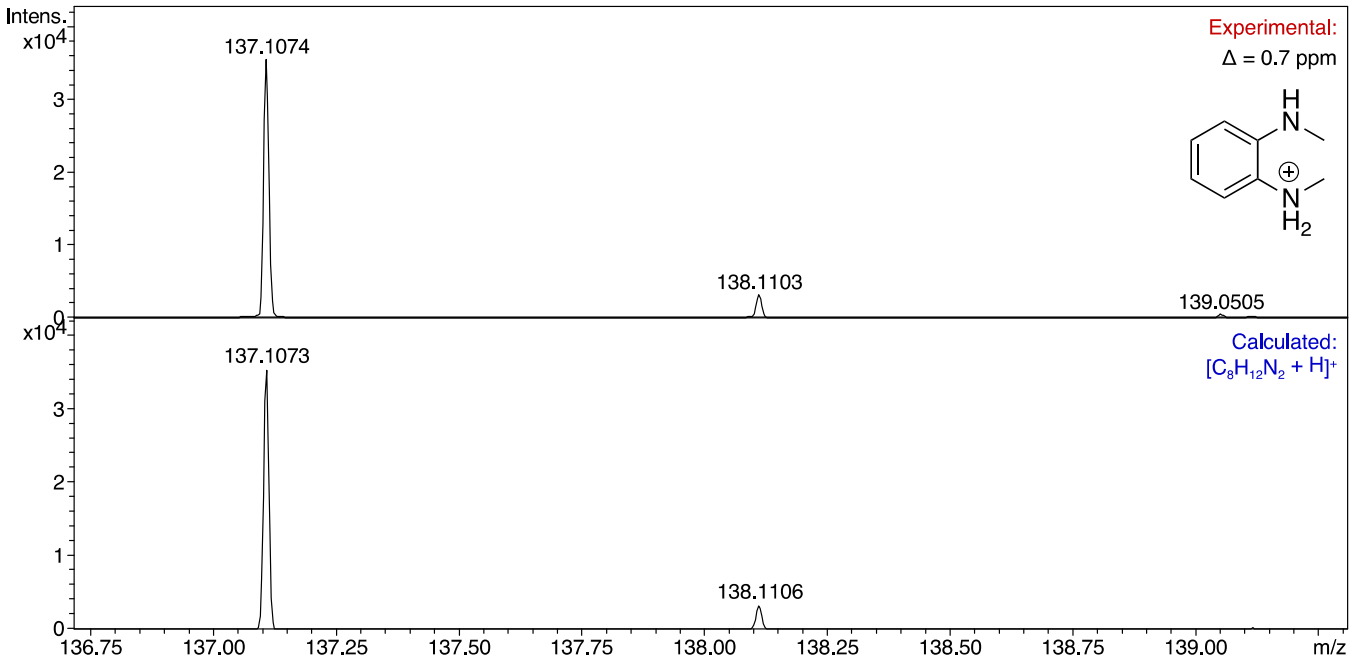

Figure S64. ESI-(+)MS spectrum of the dihydrochloride of compound **8a×2HCl** in CH_3CN solution expanded to the $[M - HCl - Cl]^+$ region.

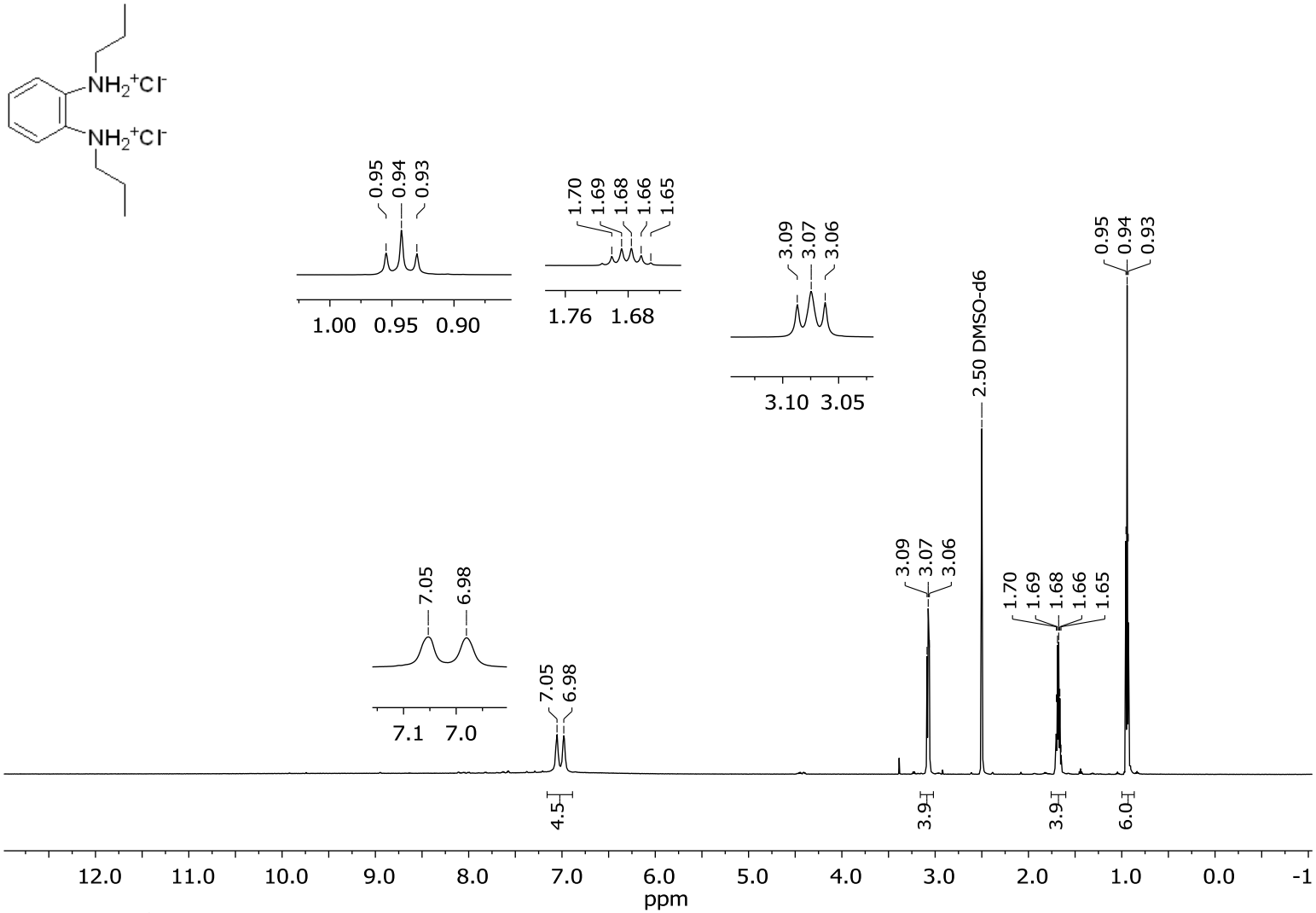

Figure S65. ^{1}H NMR spectrum of dihydrochloride of compound **8b×2HCl** (DMSO-d_6, 500 MHz).

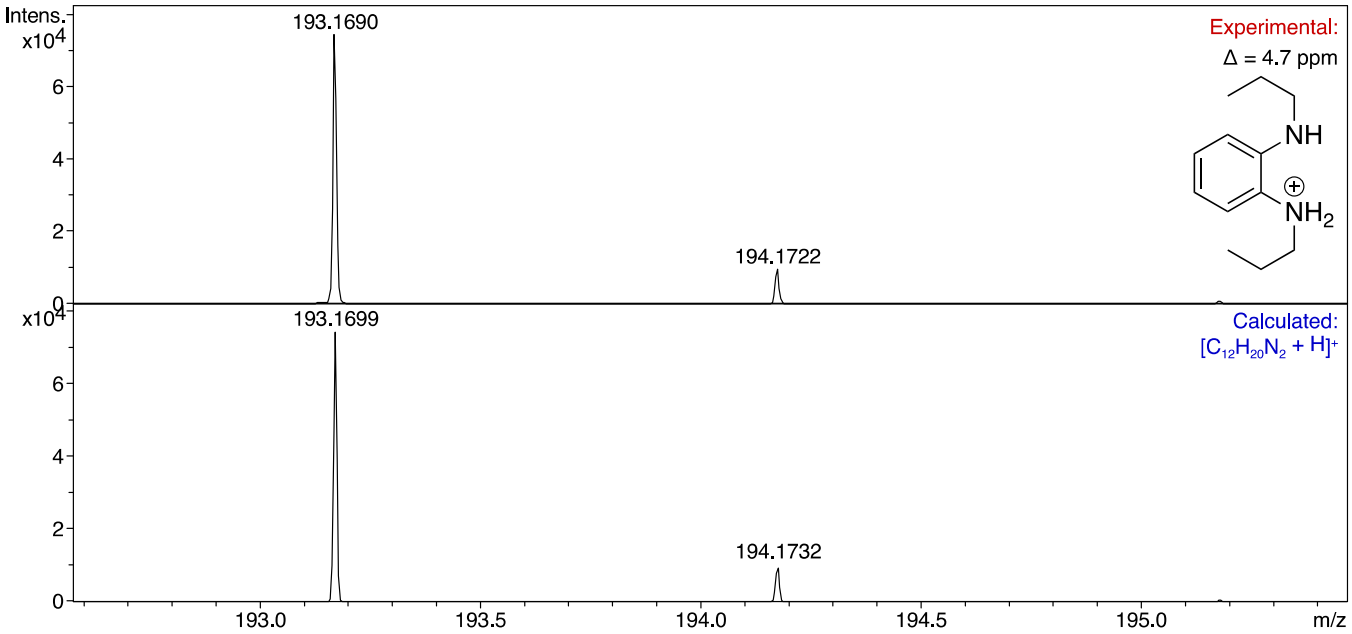

Figure S66. ESI-(+)MS spectrum of the dihydrochloride of compound **8b×2HCl** in CH_3CN solution expanded to the $[M – HCl – Cl]^+$ region.

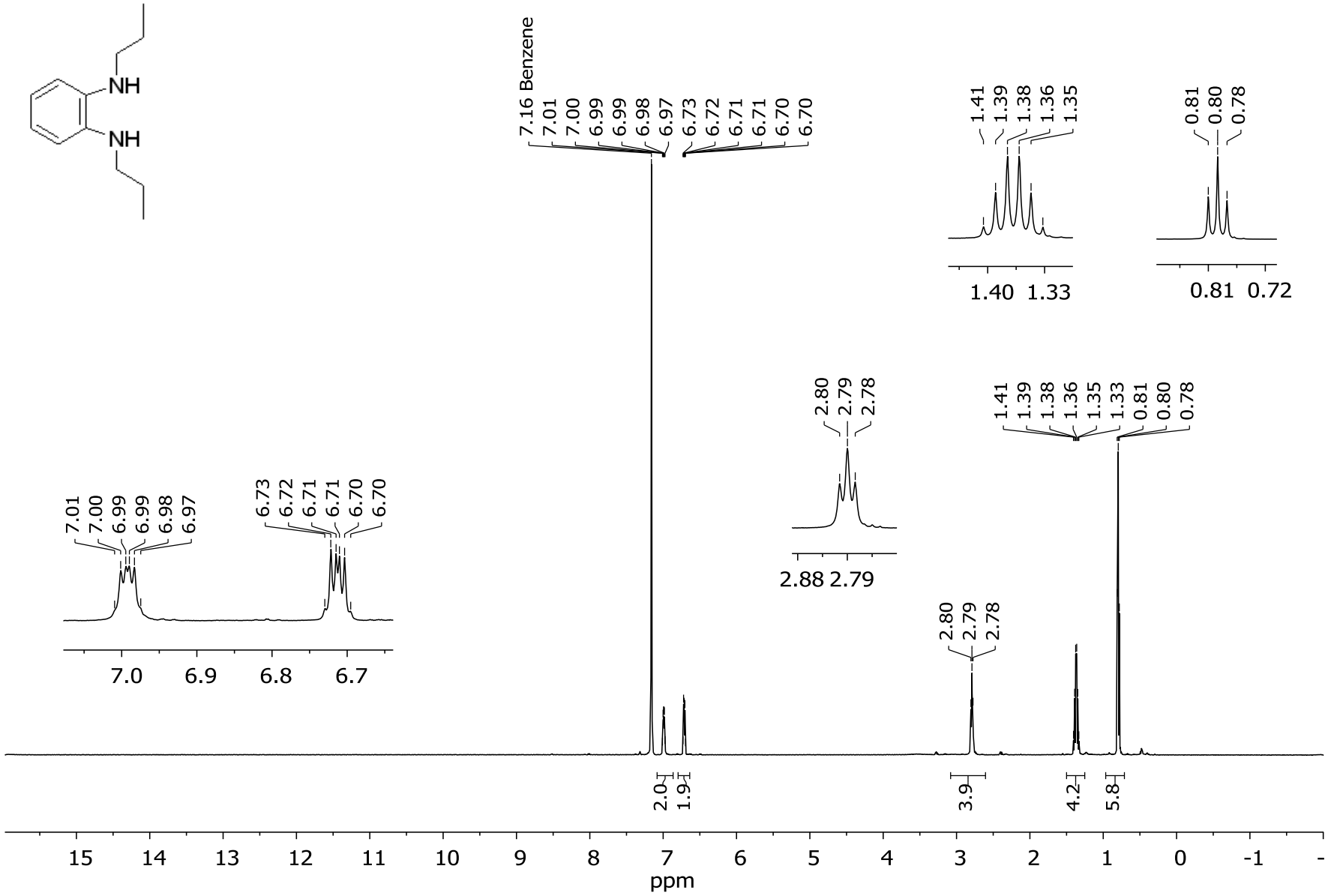

Figure S67. ^{1}H NMR spectrum of compound **8b** (C_6D_6, 500 MHz)

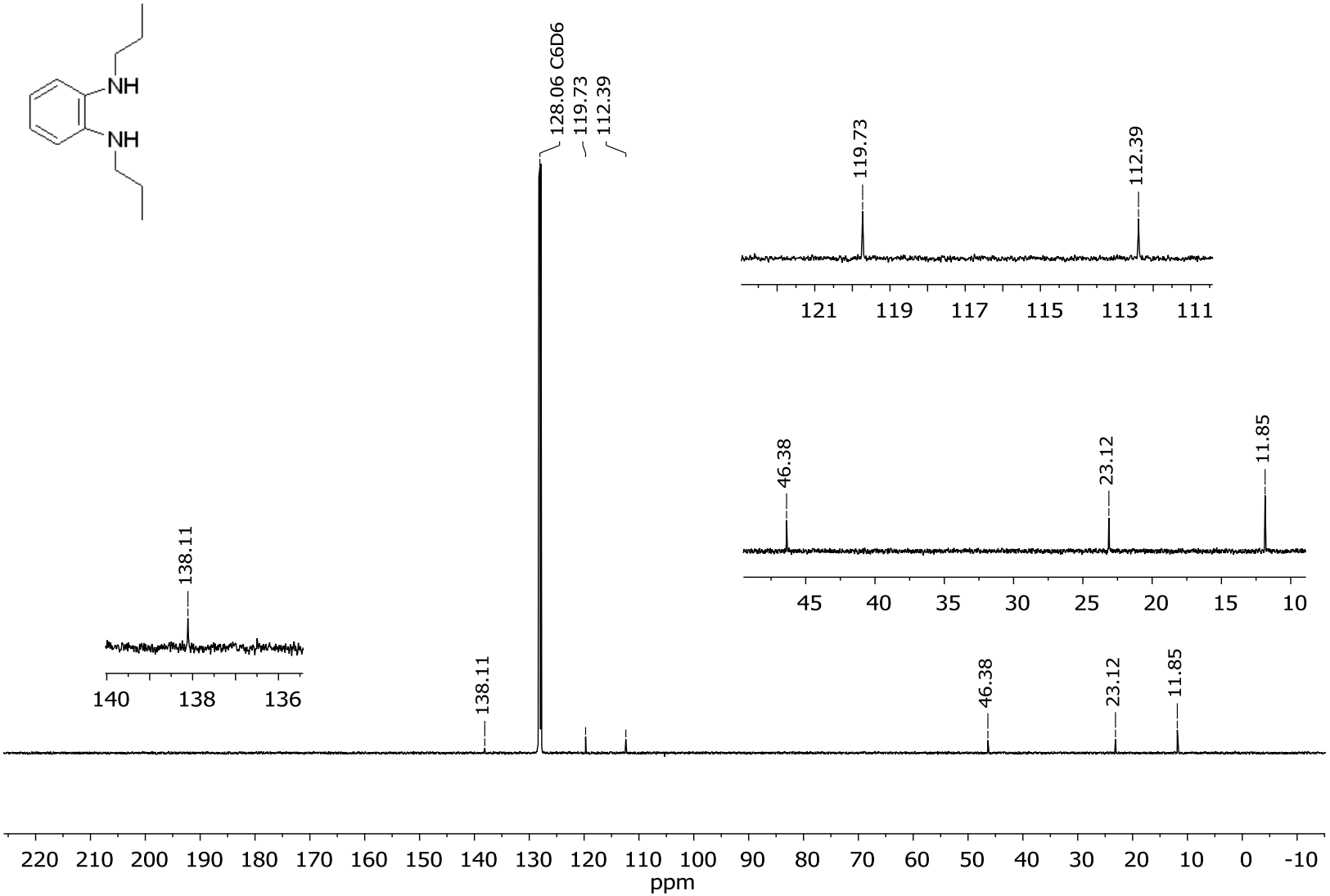

Figure S68. ^{13}C NMR spectrum of compound **8b** (C_6D_6, 125 MHz)

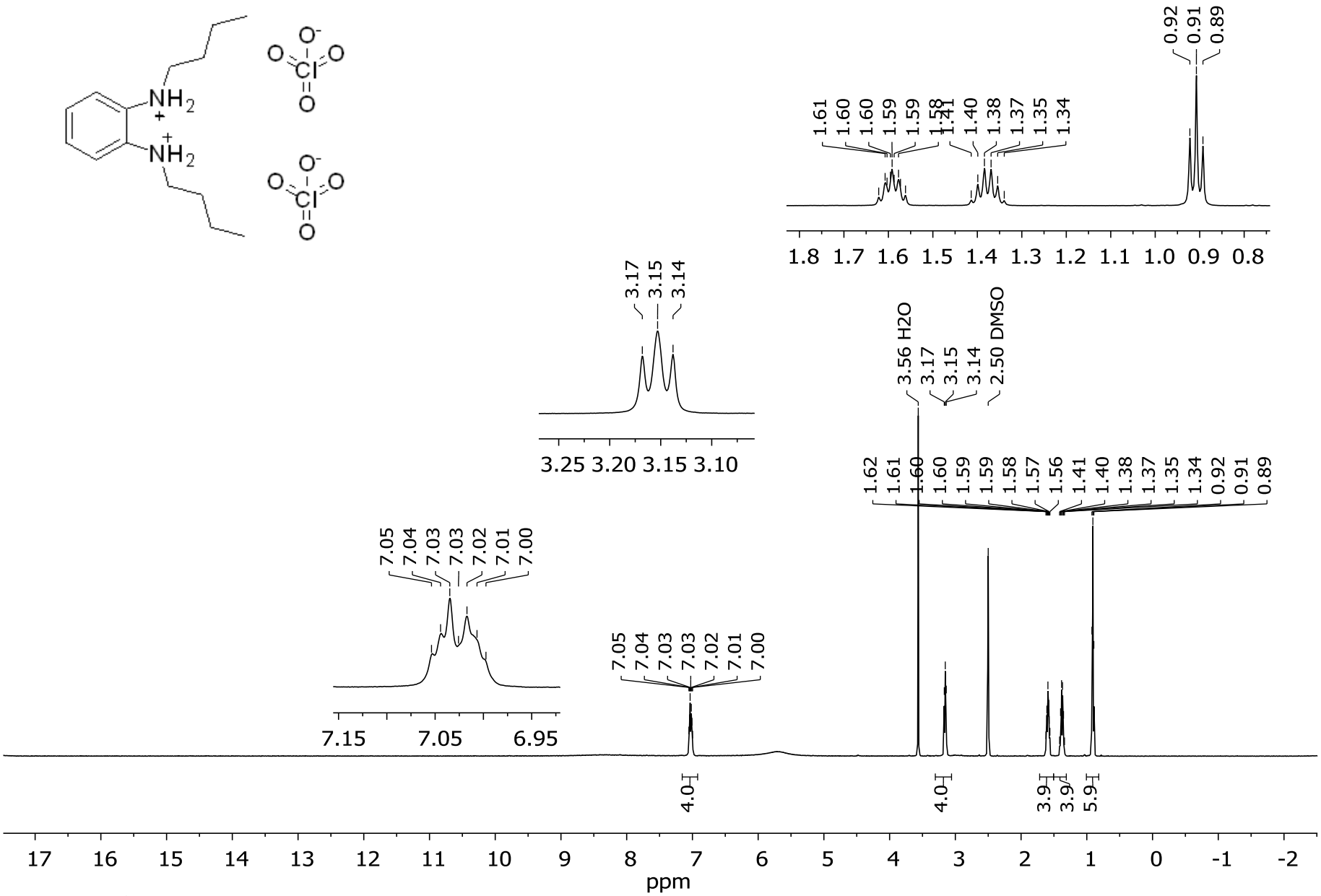

Figure S69. ^{1}H NMR spectrum of diperchlorate of compound **8c×2HClO$_4$** (DMSO-d_6, 500 MHz).

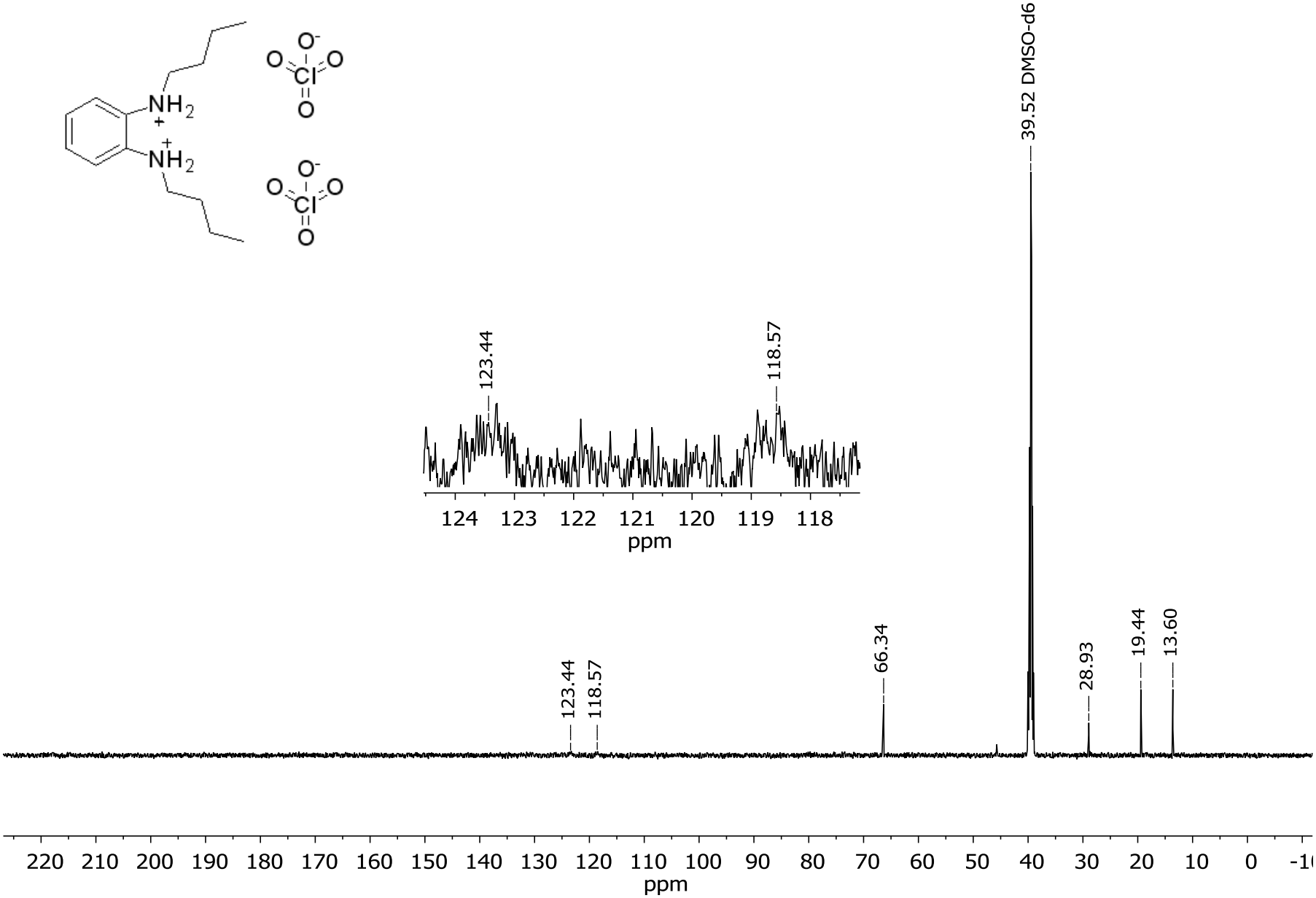

Figure S70. ^{13}C NMR spectrum of diperchlorate of compound **8c×2HClO$_4$** (DMSO-d_6, 125 MHz)

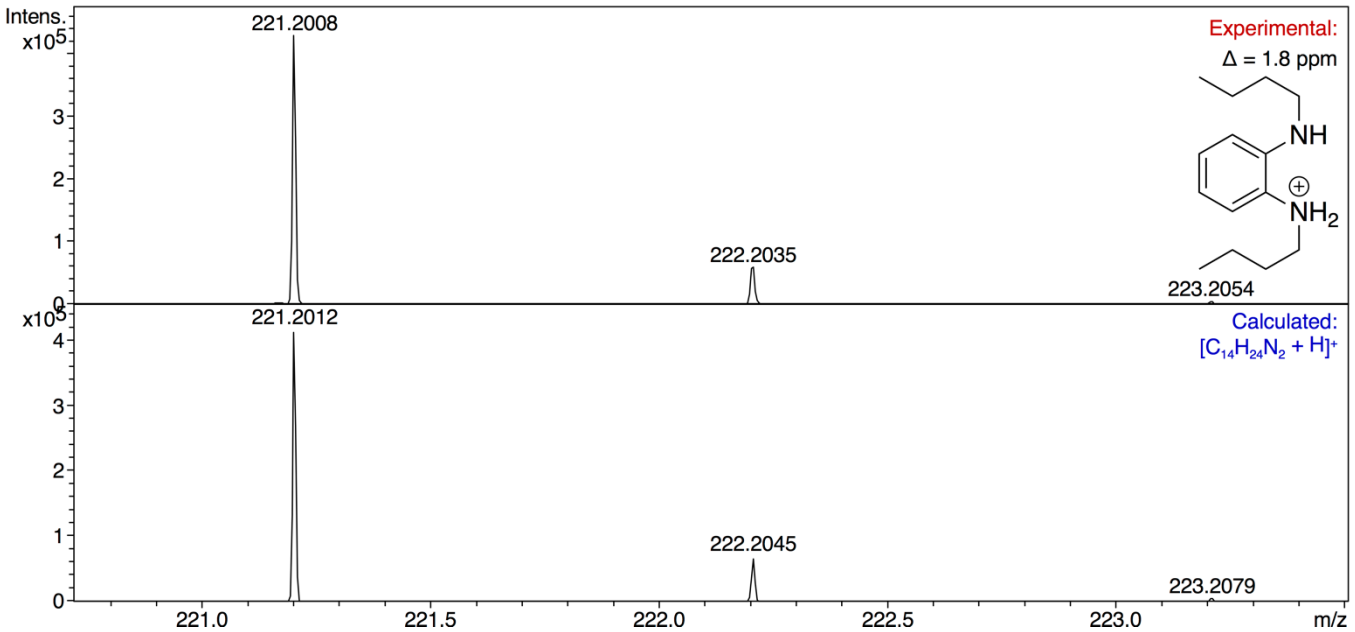

Figure S71. ESI-(+)MS spectrum of the dihydrochloride of compound **8c×2HClO$_4$** in CH_3CN solution expanded to the $[M - HClO_4 - ClO_4]^+$ region.

GC-MS data

GC-MS measurements were carried out using an Agilent 7890A GC system, equipped with an Agilent 5975C mass-selective detector (electron impact, 70 eV) and a HP-5MS column (30 m×0.25 mm × 0.25 μm film) using He as carrier gas at a flow of 1.0 mL/min. The following temperature program was used in all GC-MS measurements: initial temperature 45 °C, hold for 2 min, then 20 °C·min^{-1} to 85 °C and hold for 5 min, then 25 °C·min^{-1} to 185 °C and hold for 1 min, then 10 °C·min^{-1} to 280 °C and hold for 6.5 min. Injector temperature: 290 °C, initial pressure 1.5128 psi. Injection volume: 0.5 μL using the splitless injection mode (splitless time: 0.75 min).

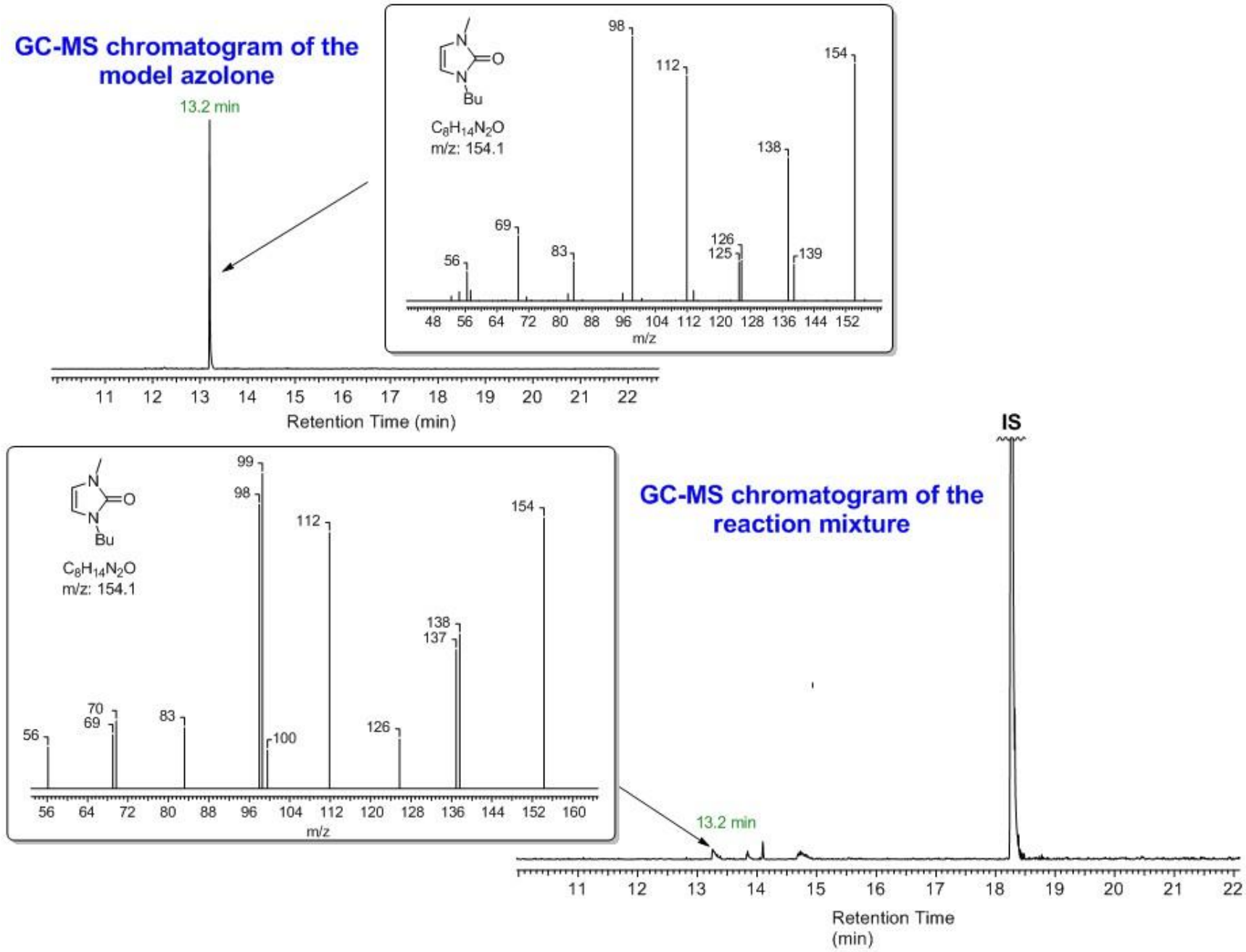

Figure S72. GC-MS chromatogram (TIC) of the authentic sample of azolone **7l** (left) and the reaction mixture (right) after heating compound **2o** with $KOH_{(aq)}$ in 1,4-dioxane (entry 37 in the Table S1).

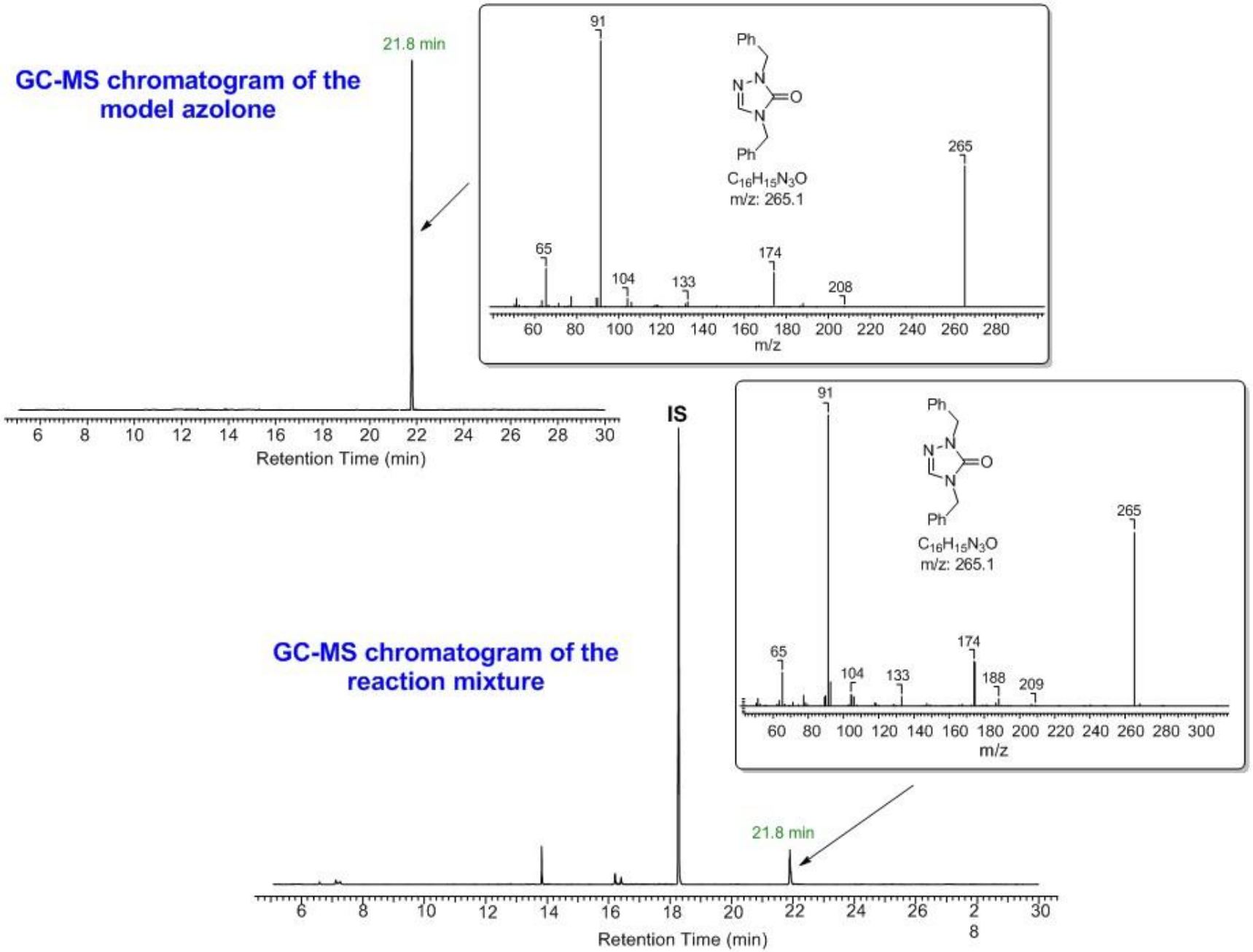

Figure S73. GC-MS chromatogram (TIC) of the authentic sample of azolone **7n** (top) and the reaction mixture after heating compound **2q** with $KOH_{(aq)}$ in 1,4-dioxane (entry 41 in the Table S1) (bottom).

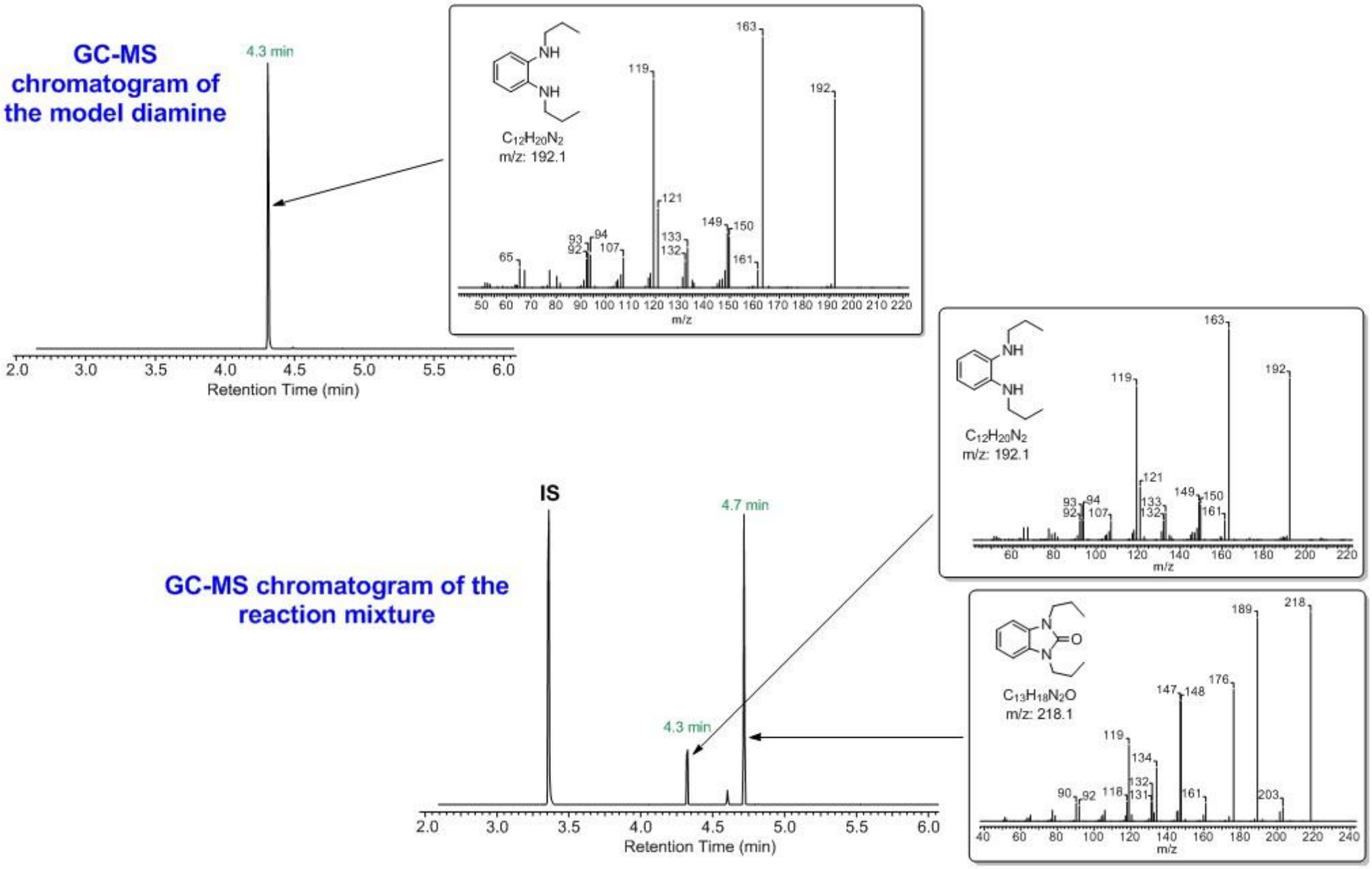

Figure S74. GC-MS chromatogram (TIC) of the authentic sample of diamine **8b** (top) and the reaction mixture after heating compound **4b** with *t*-BuOK in 1,4-dioxane (entry 46 in Table S1) (bottom).

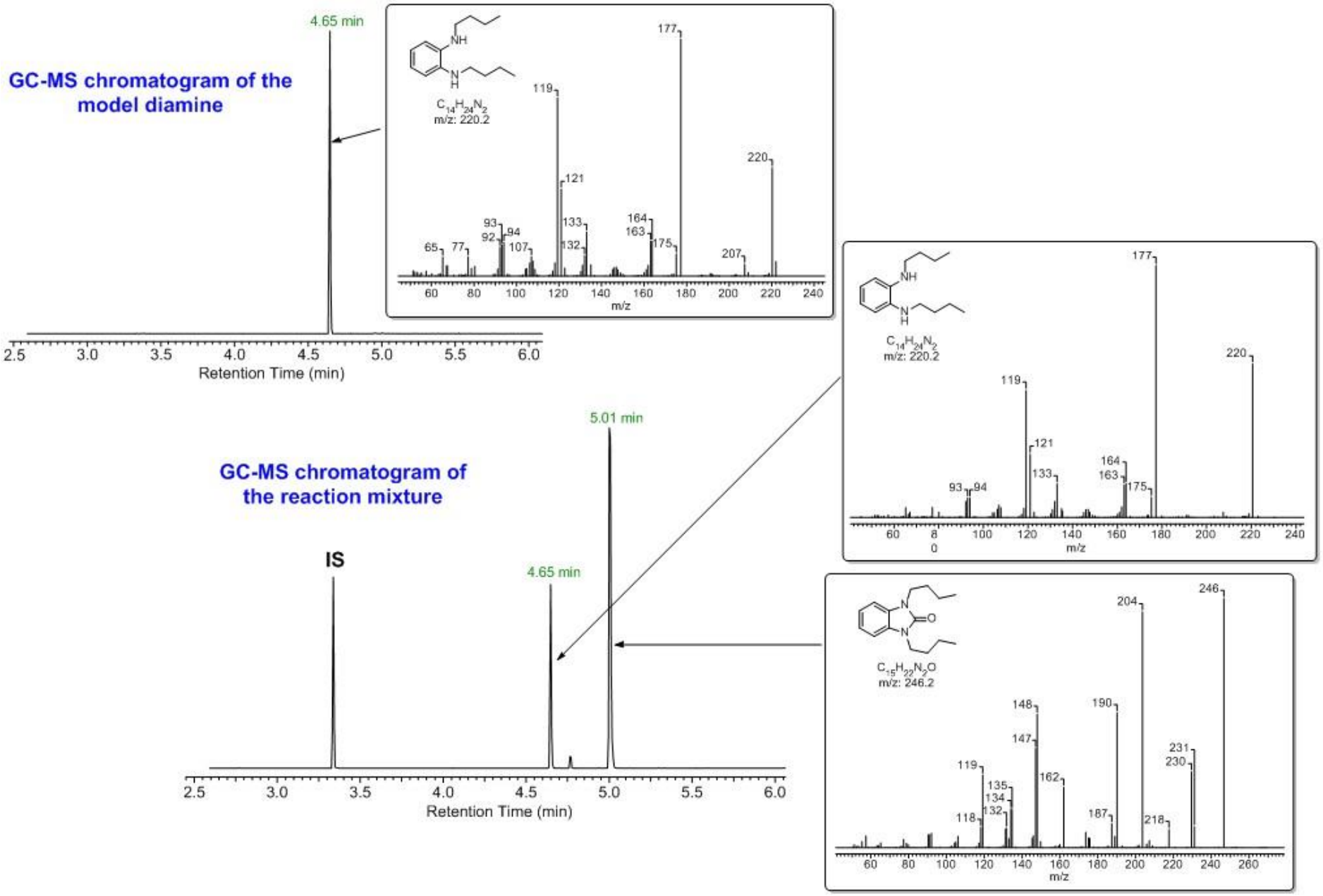

Figure S75. GC-MS chromatogram (TIC) of the authentic sample of diamine **8c** (top) and the reaction mixture after heating compound **6b** with *t*-BuOK in 1,4-dioxane (entry 52 in Table S1) (bottom).

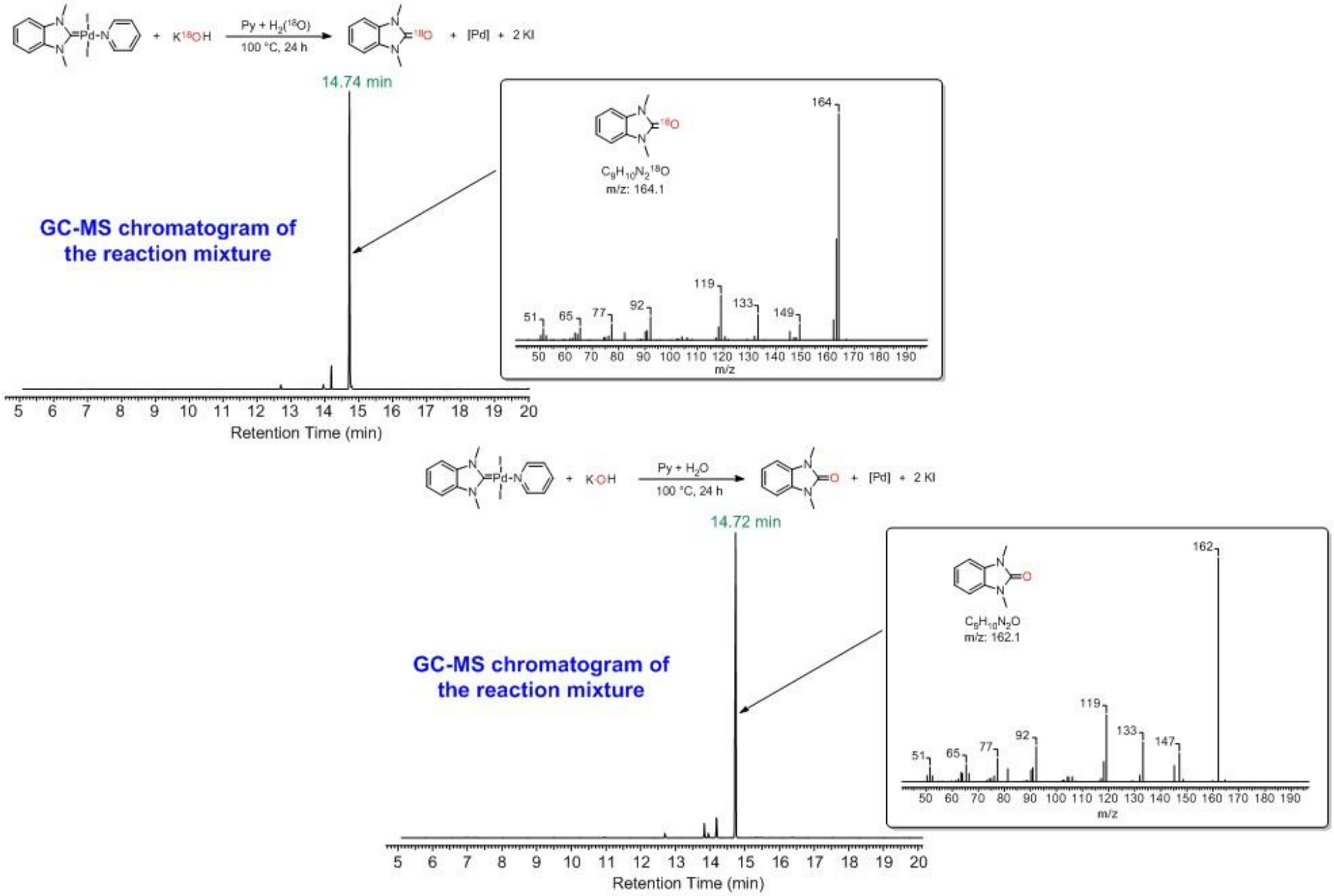

Figure S76. GC-MS chromatogram (TIC) of the compound **7a** obtained by the reaction of **2a** with $K^{18}OH$ (top) and $K^{16}OH$ (bottom) in aqueous pyridine.